TEXAS HIPLEX
INTERIM PROGRESS REPORT

Prepared by:

TEXAS DEPARTMENT OF WATER RESOURCES
POST OFFICE BOX 13087
CAPITOL STATION
AUSTIN, TEXAS 78711

Published October 10, 1978

Interim Progress Report for April 1 - September 30, 1978

Prepared for:

DIVISION OF ATMOSPHERIC WATER RESOURCES MANAGEMENT
BUREAU OF RECLAMATION
BUILDING 67, DENVER FEDERAL CENTER
DENVER, COLORADO 80225

LP-85
JANUARY 1979

TEXAS DEPARTMENT OF WATER RESOURCES
1700 N. Congress Avenue
Austin, Texas

TEXAS WATER DEVELOPMENT BOARD
A. L. Black, Chairman
John H. Garrett, Vice Chairman
Milton T. Potts
George W. McCleskey
Glen E. Roney
W. O. Bankston

Harvey Davis
Executive Director

TEXAS WATER COMMISSION
Felix McDonald, Chairman
Dorsey B. Hardeman
Joe R. Carroll

October 10, 1978

Dr. Archie M. Kahan, Chief
Division of Atmospheric Water
Resources Management
Bureau of Reclamation
Building 67, Denver Federal Center
Denver, Colorado 80225

Dear Dr. Kahan:

In compliance with Amendatory Agreement No. 1 to Contract No. 14-06-D-7587 between the Bureau and the Department, we are herewith submitting twenty (20) copies of the interim progress report on the Texas High Plains Cooperative Program (HIPLEX). The report discloses work performed, all data and information obtained, and all results achieved during the period April 1 - September 30, 1978 and is composed of four sections:

(1) A description of activity in each of the program areas addressed in the 1978 Texas HIPLEX Operations Plan;
(2) A brief statement of work planned for the next 6-month reporting period (October 1, 1978 - March 31, 1979);
(3) A list of personnel involved in the 1978 Texas HIPLEX Program; and,
(4) An appendix which contains a summary report of the Department's forecast support provided for the 1978 Texas HIPLEX season.

If you have any questions concerning the interim progress report or if you need additional details, please do not hesitate to contact us.

Sincerely,

Herbert W. Grubb

Herbert W. Grubb
Director, Planning and
Development Division

Texas HIPLEX Interim Progress Report

April 1, 1978 - September 30, 1978

Prepared by the staff of the

Weather Modification & Technology Section

Texas Department of Water Resources

October 10, 1978

TABLE OF CONTENTS

EXECUTIVE SUMMARY

In 1974 the Bureau of Reclamation (Bureau) Office of Atmospheric Resources Management, entered into a cooperative cost-sharing agreement with the Texas Water Development Board, one of three predecessor water agencies to the Texas Department of Water Resources (TDWR), for the purpose of conducting a long term comprehensive, atmospheric research and weather modification development program known as HIPLEX. The overall goal of the HIPLEX program is "...establishing a verified, working technology and operational management framework capable of producing additional rain from cumulus clouds in the semi-arid Plains States." In order to achieve this goal, three field research sites in the High Plains region were selected by the Bureau. One site was located in Montana, another was located in Kansas, and a third site was located in the Big Spring-Snyder area of Texas. The Texas HIPLEX site has been and continues to be managed by the TDWR under the overall guidance of the Bureau.

To date, the objective of the Texas HIPLEX program has been to better understand the cloud and precipitation processes associated with natural as well as seeded clouds which develop over West Texas. This objective is being accomplished through the cooperative efforts of the following groups:

Bureau of Reclamation
Texas Department of Water Resources
Colorado River Municipal Water District
Texas A&M University
Texas Tech University
Meteorology Research, Incorporated

This report presents the work performed by these groups during the six-month period April 1, 1978 through September 30, 1978.

The report discusses the Texas Department of Water Resources continuing role as manager and administrator of the Texas HIPLEX program. The Department negotiated, awarded, and/or administered eight subcontracts with the various Texas HIPLEX participants. The Department helped develop the 1978 field operations plan and provided staff meteorologists to serve as field program managers.

The services provided by the Colorado River Municipal Water District (CRMWD) are discussed. In brief the CRMWD maintained and operated an extensive network of recording and non-recording raingages, and provided the services of a rawinsonde operator and a radar meteorologist. In addition, the CRMWD also provided the services of two multi-engine aircraft for the purpose of performing cloud seeding and cloud sampling flights.

Texas A&M University's network of surface and upper air meteorological measuring instruments is discussed. These data are needed to study the inter-relationships between cloud development and the environment. Results of previous years' analyses are also presented.

Texas Tech University's work with satellite data is presented. Cloud characteristics derived from satellite imagery and radiance data of Texas HIPLEX clouds are discussed, as well as techniques to extract quantitative cloud information, such as cloud top temperature from the radiance data.

Meteorological radar data collected and analyzed by Meteorology Research, Incorporated during the reporting period are discussed. The analyses of radar data were primarily oriented toward the study of small scale (mesoscale) rainshower patterns and their relationships with environmental conditions.

It is important that these data about West Texas summertime clouds, and their environment, be collected and studied so that a high level of confidence in the cause and effect aspects of cloud behavior, both seeded and unseeded, can be obtained. Only when this level of certainty is reached can the Texas HIPLEX program progress to a point whereby predicted changes of seeded clouds in West Texas and their resulting rainfall behavior can be verified.

SECTION I

WORK PERFORMED DURING THE PERIOD

APRIL 1 - SEPTEMBER 30, 1978

TEXAS DEPARTMENT OF WATER RESOURCES

MANAGEMENT OF THE TEXAS HIPLEX PROGRAM
AND SUPPORT STUDIES

LIST OF TABLES

CONTRACT ADMINISTRATION

During the reporting period of April 1, 1978 through September 30, 1978, the Department negotiated two contracts and administered six other contracts in force as of April 1, 1978 in support of the 1978 Texas HIPLEX program. These contracts are identified in Table 1. In June 1978, Department Contract No. 14-80002 with Texas A&M University (TAMU) was amended to extend the termination date from 8-31-78 to 12-15-78.

Table 1. Contracts Awarded by TDWR in Support of the 1978 Texas HIPLEX Program.

Contract Number	Organization	Period		Purpose
		Begin	End	
14-80002	Texas A&M U.	9-30-77	12-15-78	analyze mesoscale data collected during the 1977 Texas HIPLEX Program
14-80039	Texas A&M U.	2-6-78	8-31-79	provide Chief Scientist and collect/ analyze data during the 1978 Texas HIPLEX Program
14-80004	Texas A&M U.	9-30-77	8-31-78	construct a radar-echo climatology for the Texas HIPLEX area
14-80026	Texas Tech U.	1-16-78	8-31-79	analyze satellite data gathered during the 1977 and 1978 Texas HIPLEX Programs
14-80050	Texas Tech U.	5-19-78	8-31-78	construct detailed climatology of storm occurrence in the Texas HIPLEX area
14-80038	Meteorology Research, Inc.	11-1-77	10-31-78	collect radar data during the 1978 Texas HIPLEX program and analyze and process data collected in 1976 and 1977
14-80040	Colorado River Municipal Water District	2-10-78	12-31-78	perform cloud-seeding operations and collect rainfall and rawinsonde data as part of the 1978 Texas HIPLEX Program
14-80049	Colorado River Municipal Water District	5-1-78	10-31-78	provide Aztec aircraft for cloud-seeding purposes during the 1978 Texas HIPLEX field program

FIELD PROGRAM AND MEETINGS, BIG SPRING MUNICIPAL AIRPORT

The 1978 Texas HIPLEX field program was conducted as planned during the period June 1 through July 31. The "HIPLEX 1978-79 Operations Plan, Big Spring-Snyder, Texas" was prepared by the Chief Scientist in collaboration with the Department staff, reviewed by all HIPLEX participants and approved by the Bureau. This plan was followed daily throughout the mesoscale-day designation, morning briefing of all participants on current and forecast weather conditions, review of equipment status, and seeding strategy and post-flight debriefings when applicable.

A pre-season maintenance and calibration check of the 81 Belfort recording rain gages located throughout the HIPLEX area was performed jointly by Department and Colorado River Municipal Water District (CRMWD) personnel during May.

Department staff meteorologists served as program manager, group coordinator and assisted the Chief Scientist during the two-month operational period. During June, nine cloud-seeding missions were flown on five days,

12 mesoscale days were declared and three cloud-sampling days occurred; while during July, seven cloud-seeding missions were flown on five occasions, seven mesoscale days were declared (including one rapid scan day), and four cloud-sampling days occurred (Table 2). A compilation of the summer HIPLEX data inventory collected by each participant was assembled and transmitted to the Bureau in August.

The Department's resident meteorologist at Big Spring began the daily HIPLEX support duties in May. These duties include the issuance of the 12- and 24-hour terminal forecast; analysis of morning and afternoon regional surface

Table 2. Summary of Texas HIPLEX Operations for June and July (with the number of cloud-seeding missions given in parentheses).

MONTH	DAY	MESO-SCALE DAY		HIPLEX OPERATIONAL DAY			
				Go			No-Go
		Go	No-Go	Seeding Performed	No-Seeding Performed	Sampling Only	
JUNE	1	X			X		
	2	X[2]				X	
	3		X				X
	4	X			X		
	5	X		(3)			
	6	X		(1)			
	7	X		(1)			
	8		X				X
	9		X				X
	10		X				X
	11		X				X
	12		X				X
	13	X		(3)			
	14	X[1]					X
	15		X				X
	16		X				X
	17		X				X
	18		X				X
	19		X				X
	20		X				X
	21		X				X
	22		X				X
	23		X				X
	24		X				X
	25		X				X
	26		X				X
	27	X[2]					X
	28	X[2]				X	
	29	X				X	
	30	X		(1)			
JULY	1	X		(1)			
	2		X			X	
	3		X	(3)			
	4		X				X
	5		X				X
	6		X				X
	7		X				X
	8		X				X
	9		X				X
	10		X				X
	11		X				X
	12		X				X
	13		X				X
	14		X				X
	15		X			X	
	16		X				X
	17	X			X		
	18		X				X
	19		X				X
	20		X	(1)			
	21	X					
	22	X				X	
	23	X		(1)			
	24	X				X	
	25	X[2]					
	26		X	(1)			
	27		X				X
	28		X				X
	29		X				X
	30		X				X
	31		X				X

[1] "Rapid Scan" day

[2] A partial mesoscale day (rawinsondes were launched at 3-hr intervals beginning at 1600 LDT)

charts; collection and storage of daily climatological data, ice nuclei count data and facsimile chart data. These duties were performed through August to expand the data base used for the forecast evaluation study and to refine the local forecast decision tree. The computer data terminal at the facility was used throughout the reporting period to process daily forecasts and rawinsonde data and to transmit these to the Bureau's computer.

Several Texas HIPLEX planning and evaluation meetings were conducted and attended by various members of the program's participants during the field exercise. The Department's Weather Modification Advisory Committee (WMAC) met at the meteorological facility on June 29. A special meeting was arranged on June 26 to demonstrate to officials of the U.S. Air Force Logistics Command the importance and need for retaining the FPS-77 radar for the benefit of both the HIPLEX program and the CRMWD. A HIPLEX planning session was conducted on July 24-25 at Big Spring to establish the immediate direction of the program for next year.

REPORTS

Work continued through the HIPLEX summer season on the Big Spring thunderstorm prediction model and the Big Spring forecast decision tree. A summary report of the performance of the Big Spring Forecast Decision Tree, prepared by William O. Alexander, is contained in the appendix to this interim progress report.

Three reports prepared by Texas HIPLEX participants were received, reviewed, bound and distributed during this reporting period. These reports include "Precipitation Climatology for the HIPLEX Southern Region" written by Dr. Donald R. Haragan of Texas Tech University and distributed to the Bureau on August 1, 1978; "A Radar Echo Climatology for Southern

HIPLEX" written by Dr. Dennis M. Driscoll of Texas A&M University and transmitted to the Bureau on September 6, 1978; and, "Mesoscale Characteristics of the Texas HIPLEX Area During Summer 1976" written by Dr. James R. Scoggins and others of Texas A&M University and distributed to the Bureau on October 26, 1978.

TEXAS DEPARTMENT OF WATER RESOURCES

"TEXAS HIPLEX 1978 FIELD OPERATIONS SUMMARY"

The Department published Technical Report LP-73 "Texas HIPLEX 1978 Field Operations Summary," prepared by Robert F. Riggio and William O. Alexander, to fulfill the responsibility to document the daily HIPLEX operations conducted in the Big Spring-Snyder experimental area during 1978. The field operations summary was transmitted to the Bureau on October 25, 1978.

METEOROLOGY RESEARCH, INC.

"SNYDER RADAR-DATA COLLECTION PROGRAM
AND DATA ANALYSIS"

The following report was prepared by Meteorology Research, Inc. and submitted to the Department as an interim progress report for the period April 1 - September 30, 1978.

The LIST OF TABLES and LIST OF FIGURES provided below is supplemental information to the MRI report added by the Department for ease of reference purposes.

LIST OF TABLES

LIST OF FIGURES

mri **Technical Report**

BIG SPRING - HIPLEX

Interim Report No. 7 for the Period
1 April 1978 to 30 September 1978

MRI 78 IR-1578

Subcontract with
Texas Department of Water Resources
Post Office Box 13087
Capitol Station
Austin, Texas 78711

Bureau of Reclamation Contract
14-06-D-7587 as amended 1 June 1975

Date 6 October 1978

Meteorology Research, Inc.
Box 637, 464 West Woodbury Road
Altadena, California 91001
Telephone (213)791-1901 Telex 675421
A Subsidiary of Cohu, Inc.

TABLE OF CONTENTS

1. Introduction

The following report covers work performed under the subject contract for the period from 1 April 1978 to 30 September 1978.

The objectives of the MRI portion of the Texas Hiplex program have been given as:

a. Acquisition and processing of quantitative radar data

b. Development and interpretation of M-33 radar climatologies

c. Interpretation of M-33 radar data in terms of mesoscale organization characteristics

Processing of the radar data has been plagued with problems related to the digital processor and, earlier, to problems with the wave guide. Editing corrections have now been made in all 1976 and 1977 radar data tapes. The 1978 data were the cleanest tapes so far obtained and initial processing is nearly complete.

Development and interpretation of the M-33 radar climatologies has not been pursued since the radar data tapes were not in the final format which could be used for generation of these climatologies.

Analyses of mesoscale patterns have generally followed a case study approach. Six mesoscale cases have been studied to date.

2. Radar Data Processing

In late September 1977 discussions between Bureau of Reclamation and MRI personnel resulted in an agreement as to the format and content of the processed M-33 radar tapes. Purpose of the processing was to transform the originally recorded data into a format which could be accepted for routine processing by the University of North Dakota. Through the development of extensive error correcting programs the 1976 and 1977 tapes have now been processed into this agreed-to format. Processing of the 1978 tapes will be completed in October 1978.

In the early spring of 1978 a sample of one of the processed tapes was sent to the University of North Dakota to be run through the final processing program (RADPROC). Several unforeseen problems arose as a result of this test:

1. Due to wind loading the rotational speed of the M-33 antenna varies somewhat during one revolution. This variation was not acceptable to the RADPROC program.

2. Also due to wind loading the elevation angle of the M-33 radar antenna varies slightly (few tenths degree) during any given revolution.

3. The nature of the M-33 recording is to record continuously. The Enterprise system does not record, for example, during the portion of the scan cycle in which the antenna elevation is being lowered from maximum elevation to base elevation.

The RADPROC program was unable to accept any of these deviations from the format of the Enterprise records. As a consequence, a further preconditioning of the M-33 tapes must be carried out so that they can be processed into the summary form required for development of radar climatologies. This will require a software development followed by routine processing of all of the 1976-78 tapes.

The radar data have been processed routinely into PPI plots of every other base elevation scan. These plots have formed the basis for the mesoscale case studies and for the development of the pattern climatology which are described in the following sections.

3. Summary of Case Studies

The important characteristics of cases are summarized in Table 1. In most cases the cloud formation was associated with the presence of surface front/trough and upper air trough in the vicinity of the Hiplex area. The preferred location of the trough was in the west or on the site. The convergences of air and moisture associated with the synoptic convergence were essential to the initiation of the cloud system in most cases. However, the case of July 10-11, 1976 was initiated by surface heating.

Table 1

CASE STUDY SUMMARY

	Time[1]	Troughs[2]		Feature[3]	θ_e-Sounding[4]	LOC[5]	Windshear[6]		T.M.[7]
		sfc	Upper Air				(°)	(m sec^{-1})	
1976									
June 22-23	N	W	I	SQ-LN	U-N	P	113	13.2	MESO-DYN
July 10-11	D	W	I	CMPX	U	BS	98	4.2	SFC-HT
1977									
June 9-10	N	I	W	IC, (LN)	U	P	121	9.1	CONV
June 11-12	N	W	W	SQ-LN	U	MAF	160	11.0	MESO-DYN
*June 23-24	D	W	W	CMPX(SQ-LN)	U	BS	98	10.0	MESO-DYN
July 8-9	D	I	I	CMPX	U	RL	215	5.4	L.S. CONV

Key: [1] N-Night, D-Dav

[2] I-In-site, W-West

[3] SQ-LN-Squall-line, CMPX- Complex, IC-Isolated cells

[4] U-Unstable, N-Neutral

[5] LOC-Location of storm: P-Post, BS-Big Spring, RL-Robert Lee, MAF-Midland Air Force Base

[6] Shear is calculated at the observation station closest to echo activities (expressed in vector direction and magnitude, 500-850 mb)

[7] T.M.-Triggering mechanism of cloud formation: MESO-DYN - Mesoscale dynamics
SFC-HT - Surface heating
CONV - Local convergence
L.S. CONV - Large scale convergence

* To be presented in this report.

The θ_e stability was an important measure of the convective potential. The results showed that the formation of nonsquall-line type cells required moist unstable environment, while the squall-line type cell required less instability; the environmental air could be neutral. The less stringent requirement on instability explained that the squall line could happen in both day and nighttime. The selected case study (June 22-23, 1976) showed that the cloud formation, growth and movement of the squall line were controlled by the environmental wind structure (vertical profile and horizontal distribution) as well as the static energy distribution.

The MWS radar summary maps could only depict large echo coverage, and in some instances, no detail mesoscale echo feature could be detected from the maps. The M-33 radar observation was able to reveal the fine detail of the echo organization even in a rather complex mesoscale system such as a squall line. There were three types of echo organizations, namely: isolated cells, complex cells (cluster) and squall line (or cloud line) patterns.

The orientation of echoes was sensitive to the vertical shear of horizontal winds. The individual echoes could line up transverse or parallel to the environmental shear vector measured between the 850 and 500 mb winds. The analyses showed that representative environmental winds should be sufficiently close to the cloud system but not in the immediate neighborhood of the cloud system. The magnitude of shear vector was related to the echo organization scale. The high shear was connected with a large system such as a squall line. The echo movement was closely associated with lower level (700 or 850 mb) winds. However, the lower level winds deviated from the echo translation vector, thus the right- or left-moving echoes were observed. See Section 4 for case study example.

4. Case Study, June 23-24, 1977

4.1 General Synoptic Conditions

A surface trough was situated near the northwest corner of the Texas Panhandle. The funneling condition (shape of 1012 and 1016 mb isobars) favored moisture advection from southern Texas to the Hiplex site at 1800Z. The funneling condition still existed up to 0000Z and the trough intensified at the Texas-Oklahoma border (Figure 1a). The upper air analysis shows a low (trough) was centered in the middle of New Mexico and upper air winds were roughly from a southwesterly direction in the Hiplex site (Figure 1c).

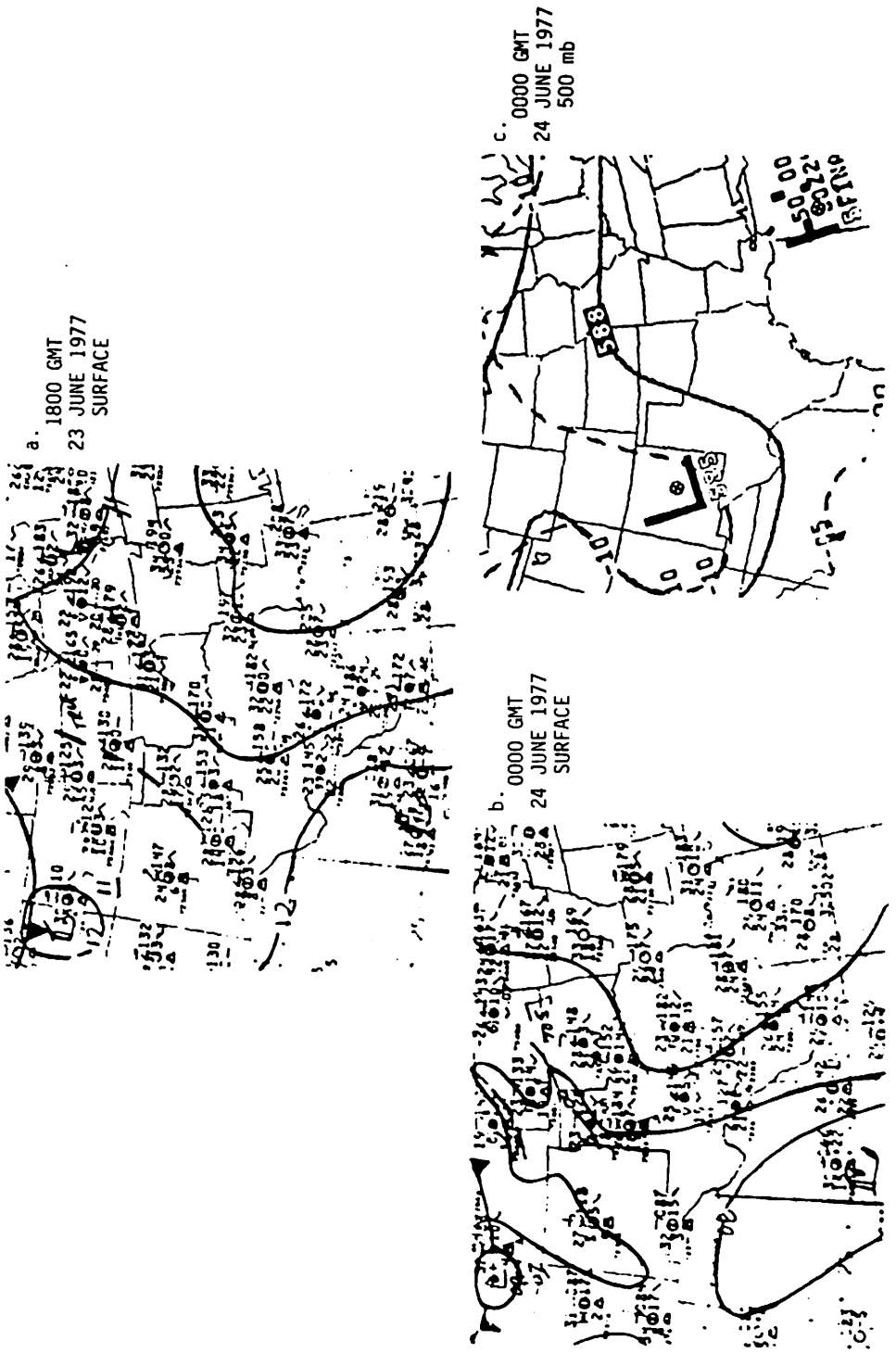

Figure 1. Surface and upper air maps.

The MWS radar summary maps reveal very little echo organizations except at 1835Z, near the northern edge of the Hiplex site, where three was a line oriented in a northeast-southwest direction. The other times show echo activities covered the Hiplex site and at 0035Z a north-south squall line was observed near the Texas-New Mexico border (Figure 2).

The θ_e-soundings at Post show very moist conditions at all levels for the entire day. The air above the boundary layer was near neutral and slightly unstable. The air in the boundary layer was very unstable. This vertical thermal structure is favorable for initiating convective clouds (Figure 3).

The wind directions (shown in Figure 3) were rather uniform at 1500 and 1800Z. They were mostly southwesterly at all levels at Big Spring and Post. From 2100Z and onward, in the layer from the surface to 800 mb, the directional shear increased both at Big Spring and Post. At 0000Z the directional shear layer extended up to 700 mb and the magnitude of winds increased at the surface and 800 mb, but 700 mb winds were weaker than that of 800 mb. At 0300Z the wind shears were not well organized below 600 mb. Winds below 500 mb changed in direction and magnitude at all times.

4.2 Mesoscale Features

Two episodes of cloud line development were observed on the M-33 radar PPI display. In Episode 1, an intense narrow-line development was observed south of Snyder in the Big Spring-Vincent-Garden City area with a line orientation of 70-200°. A few isolated cells formed a northern branch of the line which was located north of Snyder. The northern branch of the line dissipated by 1726 CDT (2226Z). The southern branch remained narrow from 1426 to 1505 CDT (1926-2052Z). There were three convective complexes that formed within the southern branch (Figure 4). Complex A (near Snyder) had the longest lifetime among the three complexes. By 1551 CDT (2051Z) the line contained two active cells of Complex A and the remaining weak echoes of two other complexes. The two active cells dissipated about 1726 CDT (2226Z).

In Episode 2, a line composed of weak echoes formed in the southeast of the line in Episode 1 at 1551 CDT (2051Z). The newly formed line was situated in about the same location as the original line at 1925Z

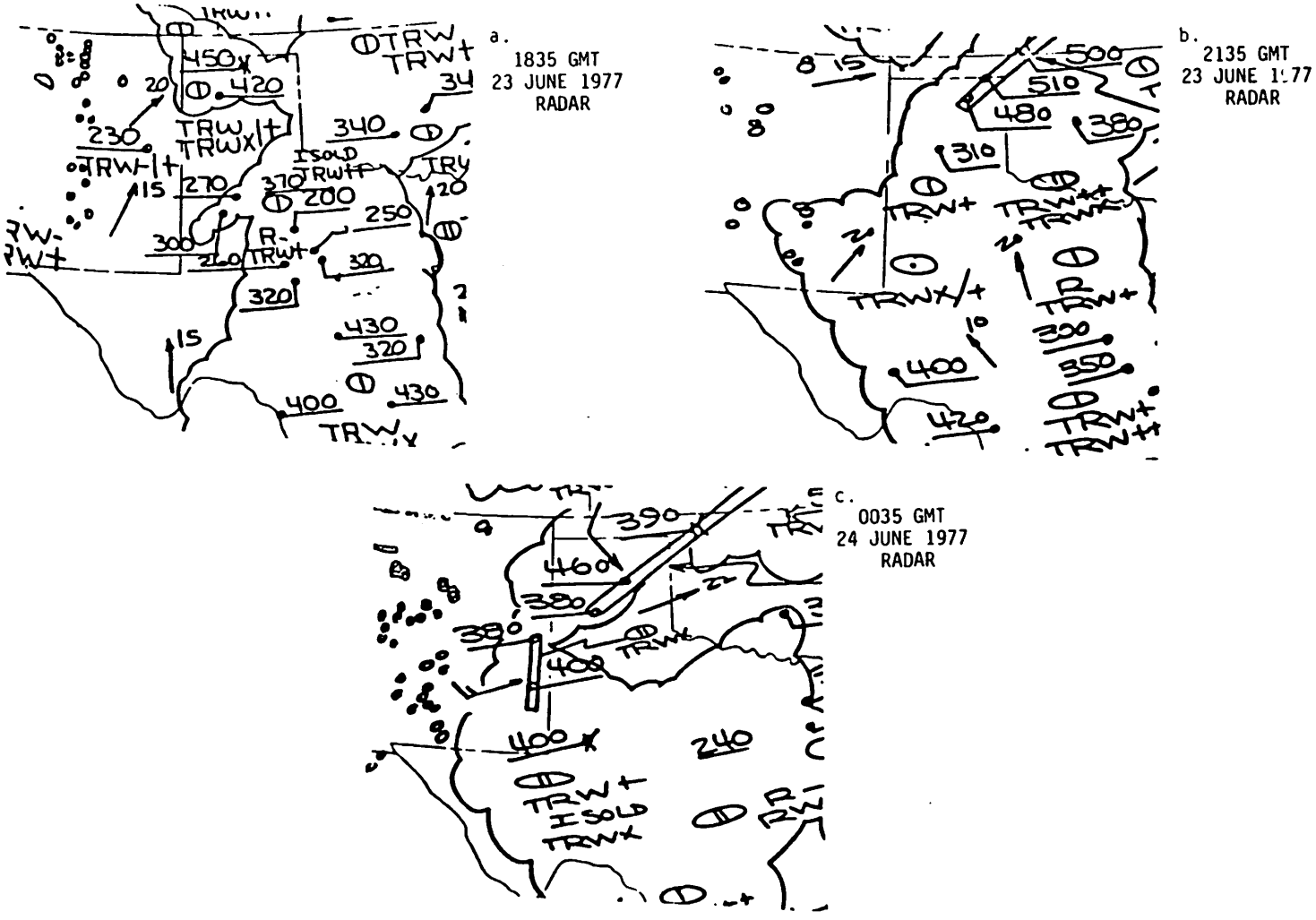

Figure 2. National weather service radar summary maps.

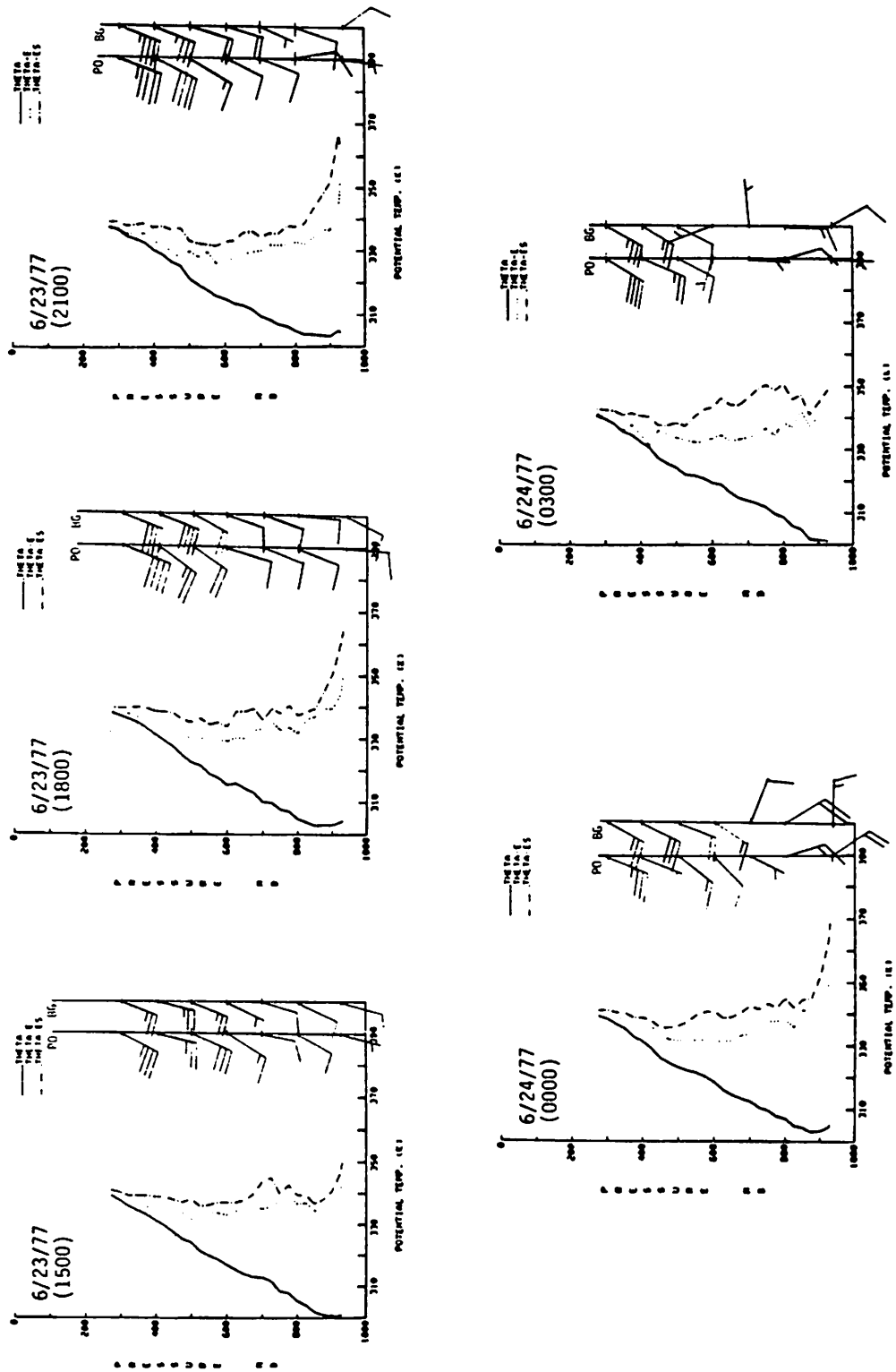

Figure 3. The time display of θ-soundings and horizontal winds at selected levels at Post. The PO line is for Post, and the BS line is for Big Spring. The conventional wind value representation (knots) is used.

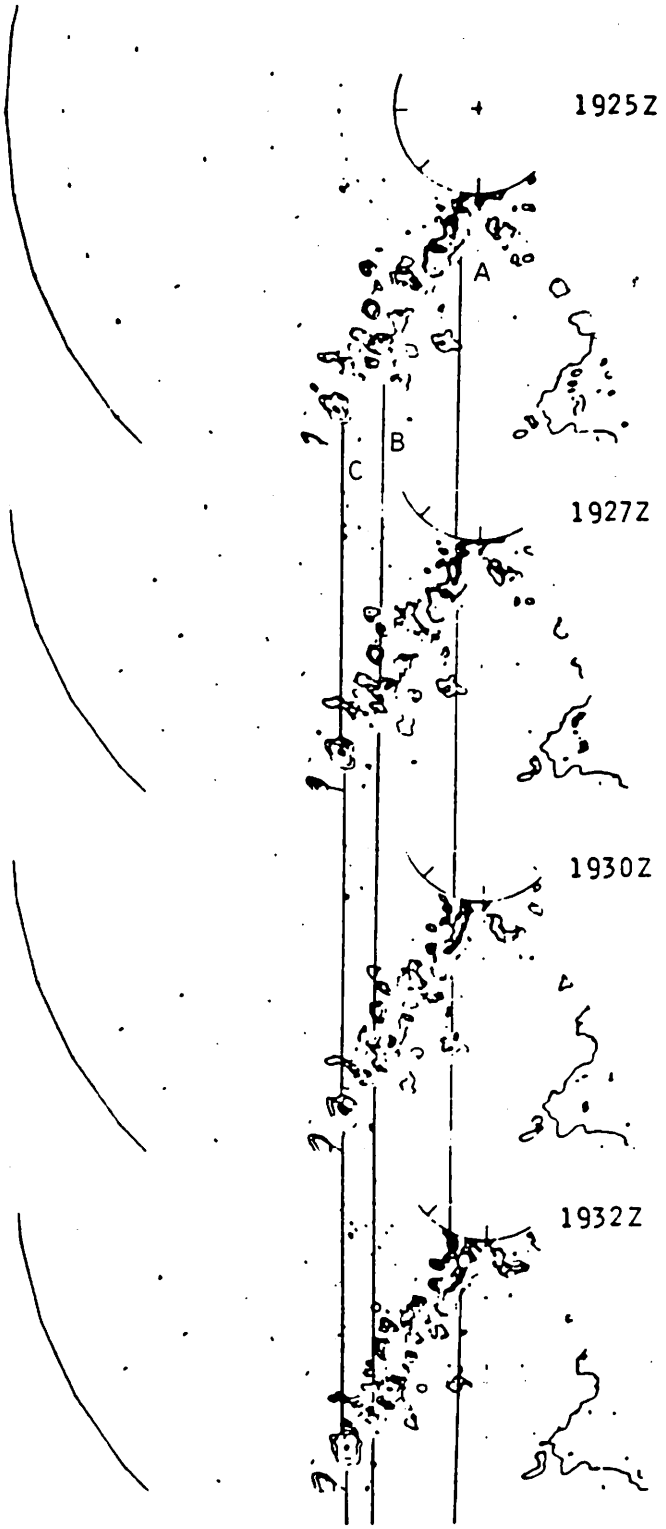

Figure 4a. The echo development in a mesoscale line. The letters A, B, and C and the solid lines mark the approximate locations of echo complexes A, B, and C at designated times.

EPISODE 1. continued

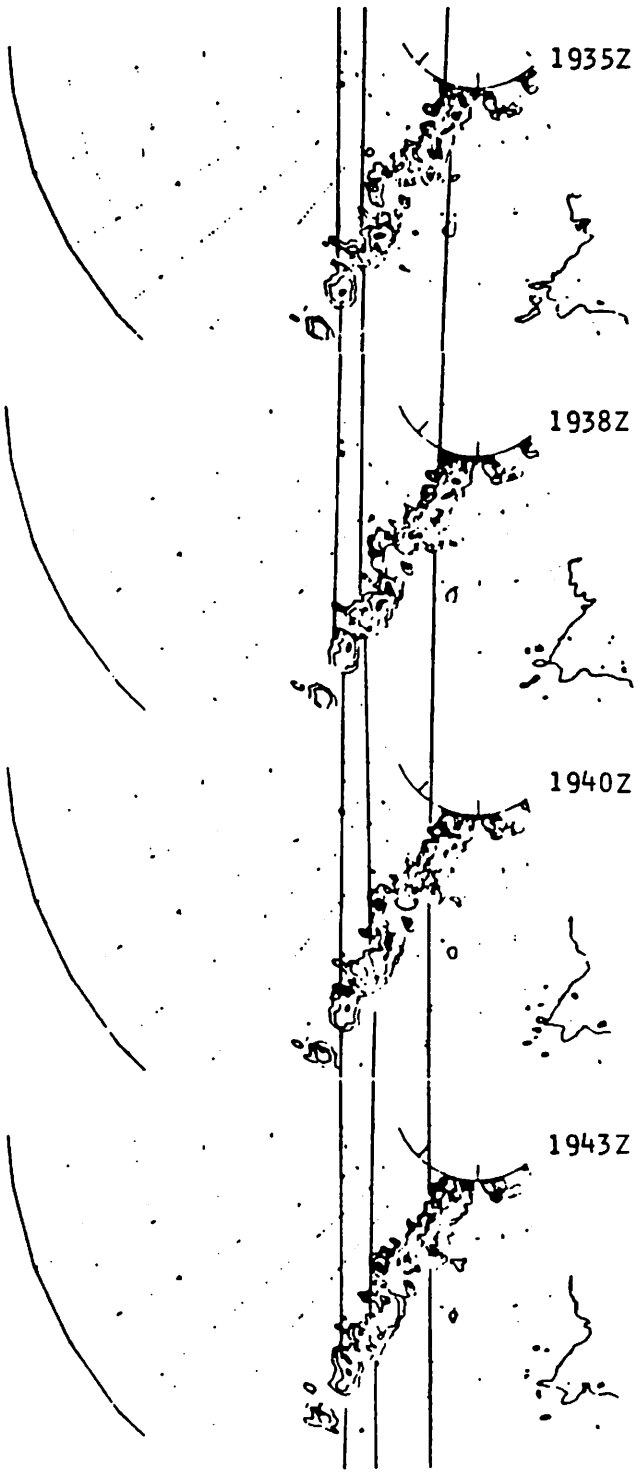

Figure 4b. Same as in Figure 4a.

EPISODE 1, continued

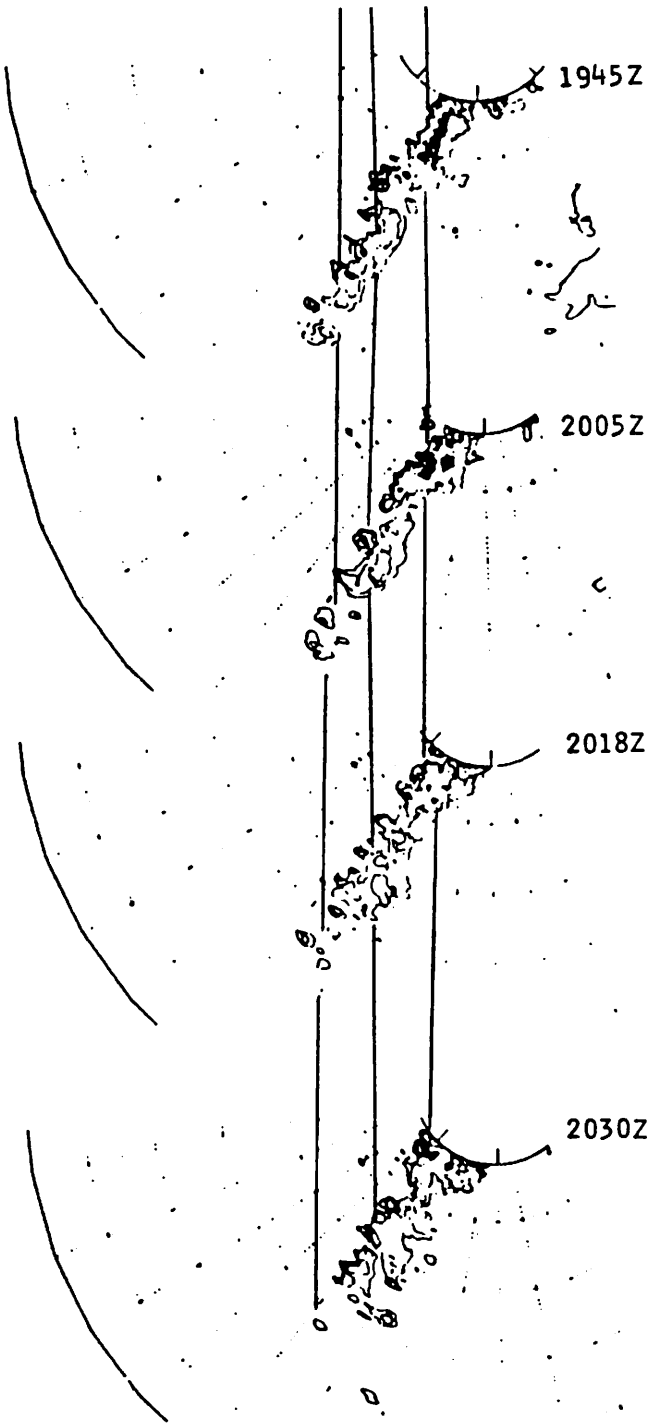

Figure 4c. Same as in Figure 4a.

(Figure 5). The echoes in the line formed three convective complexes. Complex C' (near Midland) was the dominant long-lasting system in the line. The line became quasi-stationary about 1835 CDT (2355Z), but the development of Complex C' and new cells continued westward.

4.2.1 Episode 1

It is postulated that the initiation of the narrow echo line was triggered by mesoscale dynamics - the upward motion induced by the downdraft formation of a decaying broad line near Robert Lee. The gravity wave propogation asserts the location of cloud line (preferred wavelength) and local convective motion set up the individual echoes in the line.

The subsequent development of the line was more or less controlled by the environmental wind structure. The response of line organization to the windshear variation will be examined. The shear analysis in Big Spring at 1425 CDT (1925Z) shows a 96° direction, a rather poor relation to the line orientation (70-200°), but the shear at Midland (86°) shows a 10° angle between the line orientation and shear vector (Figure 6). Since Big Spring was too near the clouds the required environmental shear was not properly represented[1]. Some echoes formed a transverse mode[2] line but the dimension of this line was small (<20 km). A more detailed examination of echo generations will be discussed in Section 4.3.

In the Robert Lee area winds at indicated levels show outflow condition and the environmental winds were restored after the cloud decayed. From the general northward winds at all stations and the synoptic map, the moisture advection was expected from the south.

The echo trajectory is shown in Figure 7. In the Big Spring and Robert Lee areas good correlation of 850 mb winds and the echo movement is shown. This indicates that the echo movement was steered by the lower level winds. The 700 and 500 mb winds did not coincide with the echo movement, but the shear between 850 and 500 mb appeared to be perpendicular to the direction of the echo movement. The tracking also shows that the majority of echoes were right-moving echoes according to the 850 mb winds.

---

[1] The affect of cloud system to the environmental windfield was studied by Kropfli and Miller (1976). The study showed that the winds adjacent to the cloud system are very different from the environmental winds.

[2] The mode of line orientation is defined by the windshear direction and echo organization. In the longitudinal mode the echoes are lined parallel to the windshear vector, and in the transverse mode the echoes are perpendicular to the windshear vector.

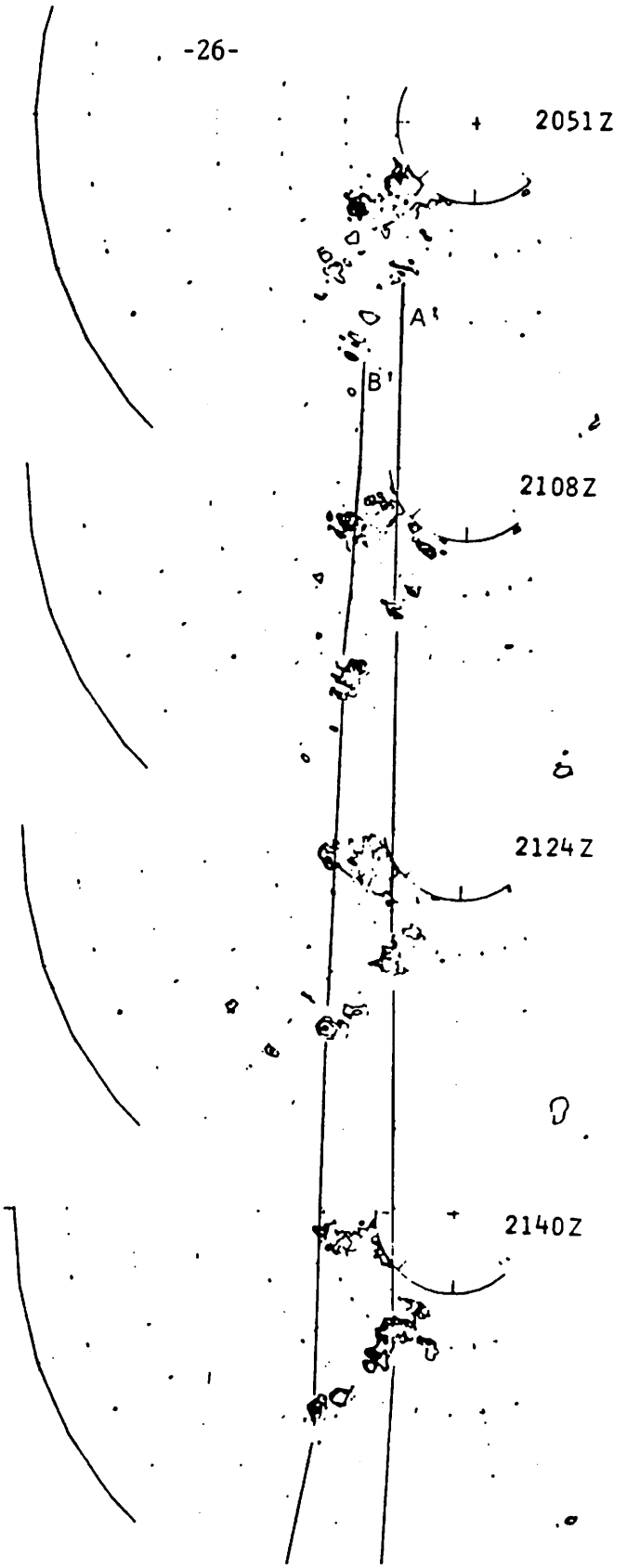

Figure 5a. The echo development in a mesoscale line. The letters and the solid lines mark the approximate locations of echo complexes A' and B' at designated times.

EPISODE 2, continued

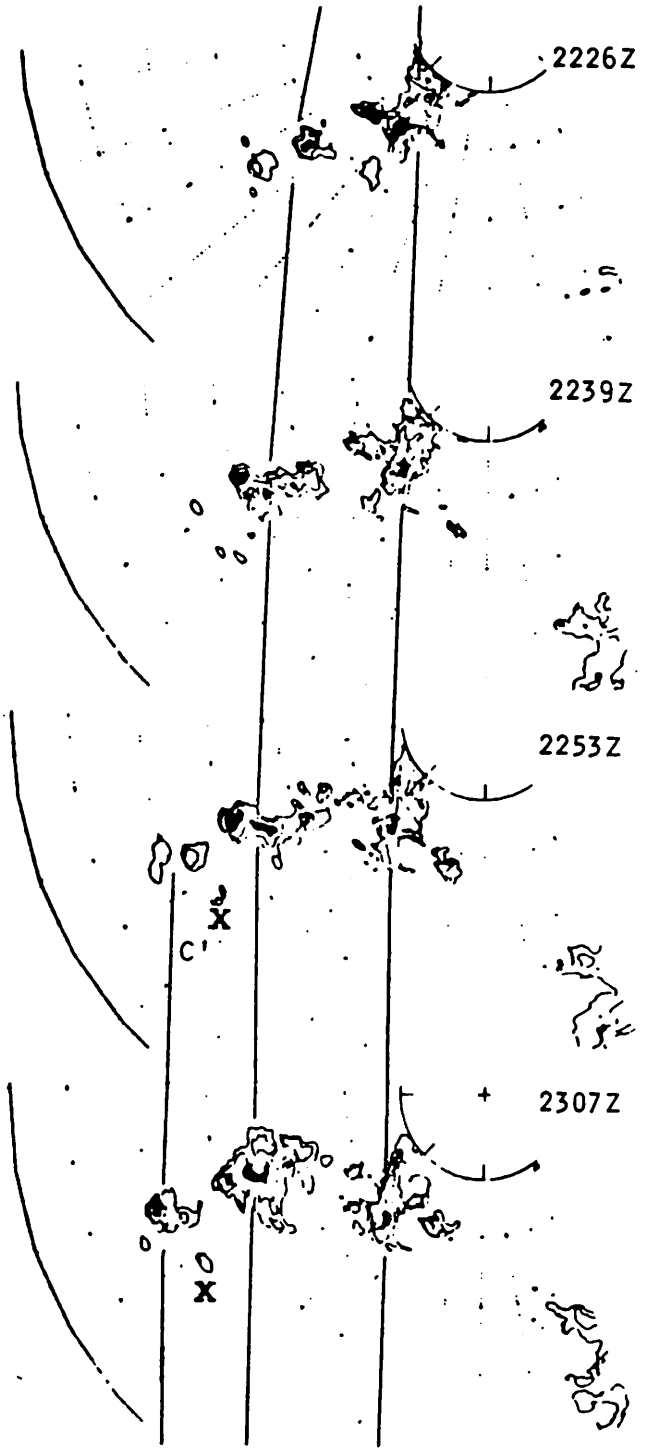

Figure 5b. Same as in Figure 5a except letter C' and the additional line mark the approximate location of echo complex C'. The X mark is a fast-growing echo in complex C'.

EPISODE 2, continued

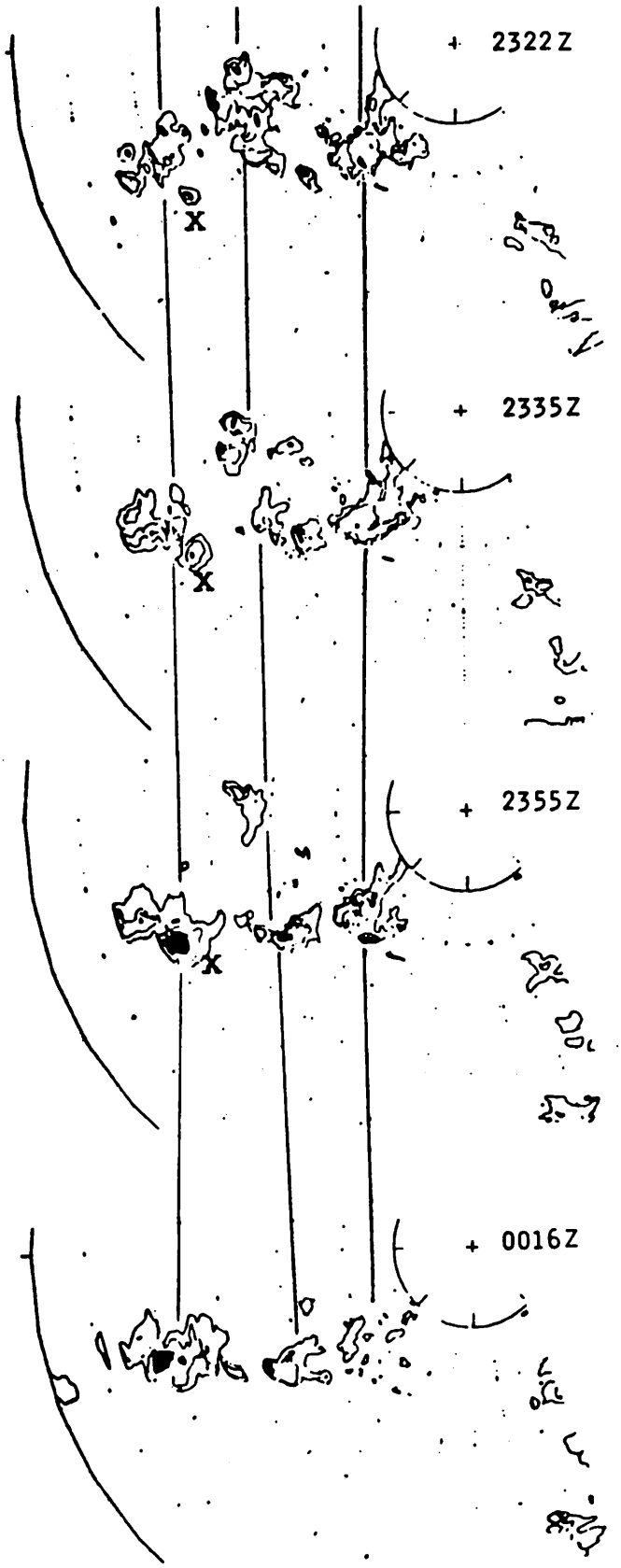

Figure 5c. Same as in Figure 5b.

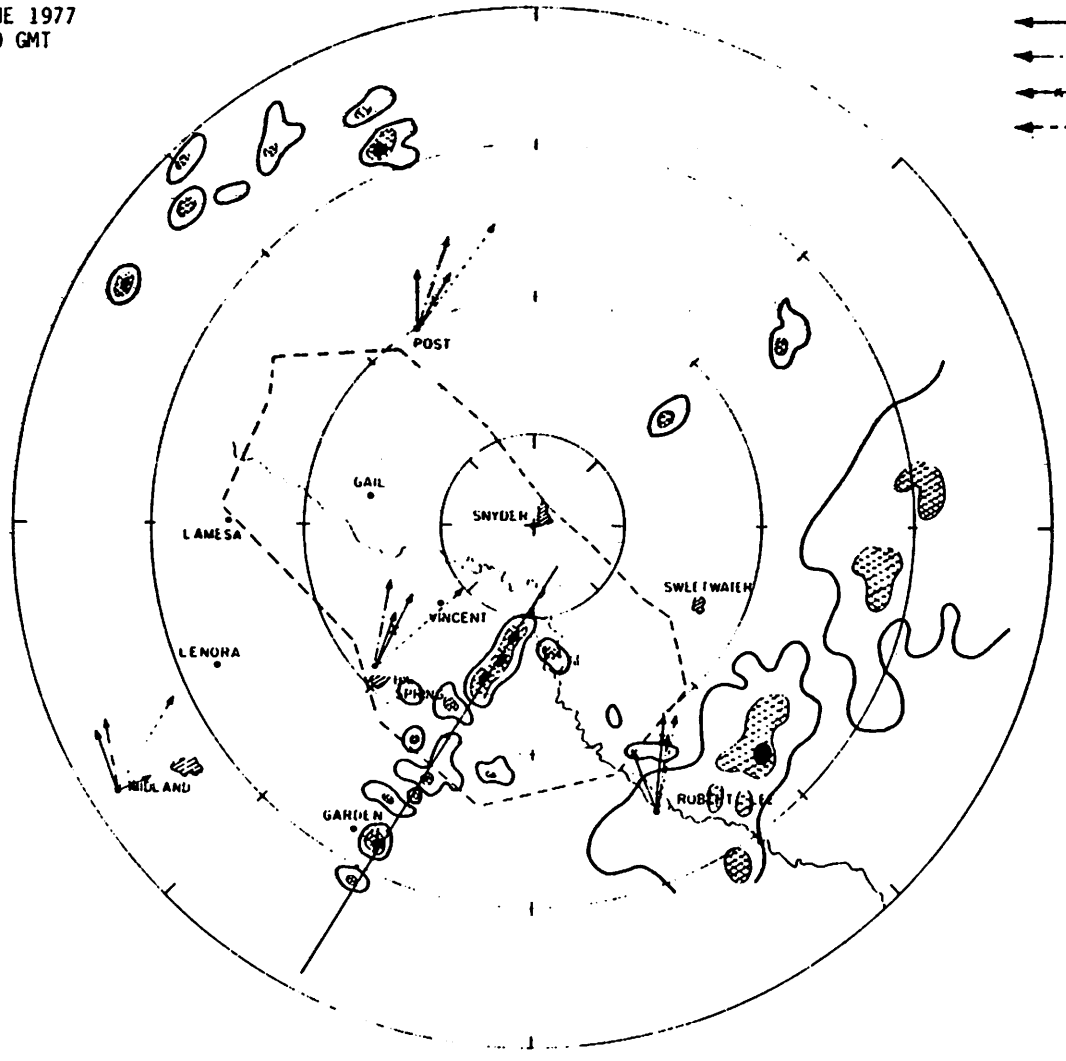

Figure 6. PPI display and winds at 1800Z. The unshaded area contains echo larger than 25 dbZ, the hatched area contains echo larger than 35 dbZ, and the blackened area contains echo larger than 45 dbZ.

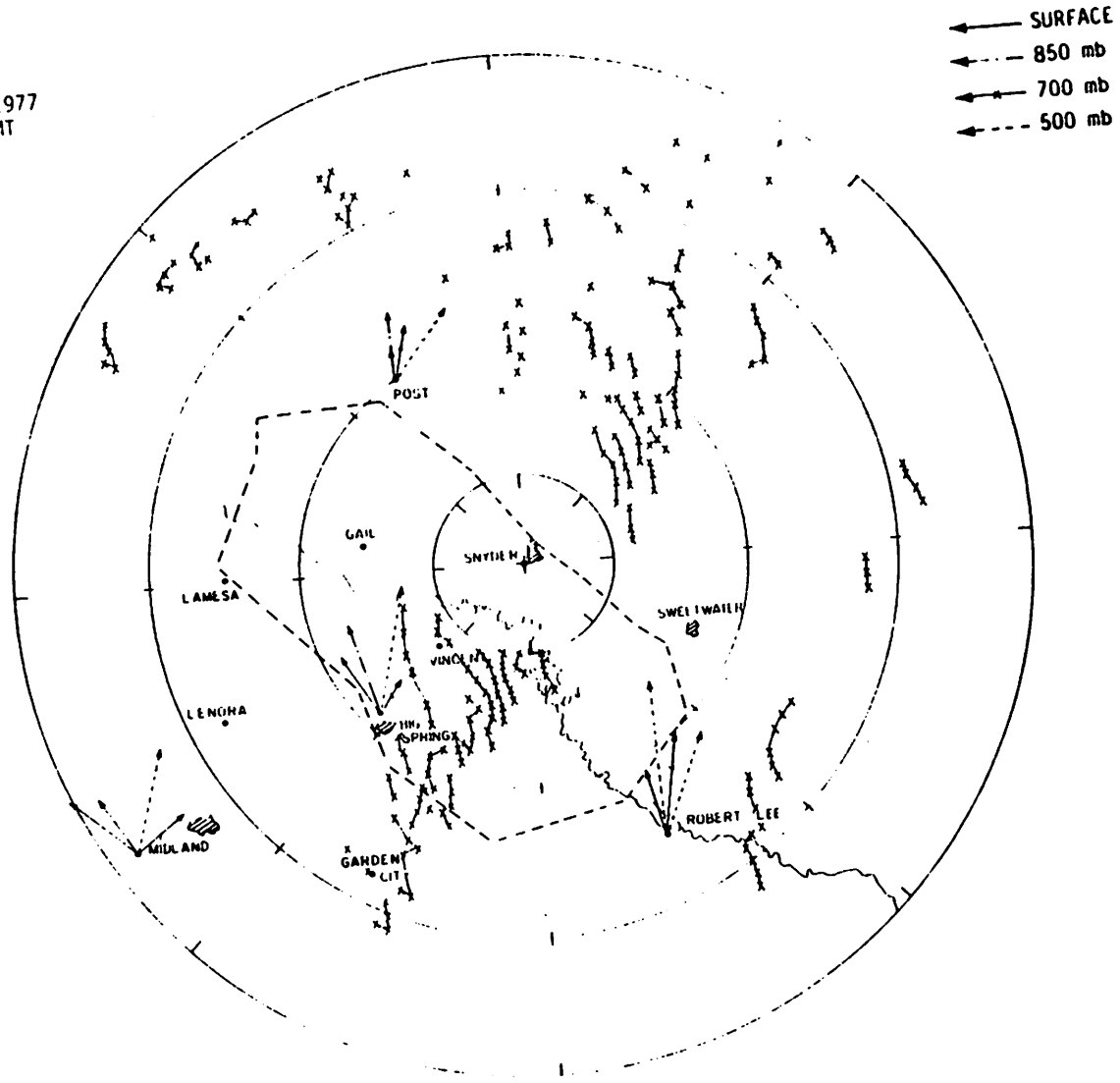

Figure 7. Echo tracking from 1935Z to 2230Z. The track was made in about 5 min intervals. The directions of the echo movements is not indicated, but the general movements are from south to north.

4.2.2 Episode 2

The beginning of Episode 2 was the formation of Line 2 behind the decaying Complex A in Line 1. The line initially formed as a collection of weak echoes in longitude mode at 2051Z (Figure 5). The shear at Big Spring was almost the same as in Midland. In the absence of a strong line development the environmental winds at 2100Z might not have been modified as much as at 1800Z in the Big Spring area. The cloud population in the southern sector at 2100Z was not as large as at 1800Z. The subsequent development of an echo complex in Line 2 will be presented in detail in Section 4.3.

The line orientation was parallel to the windshear at Midland at 0016Z (longitudinal mode) (Figure 8). By this time the line was quasi-stationary. The winds at Big Spring indicated that the cloud system had an inflow condition from the surface to 850 mb and outflow above 500 mb. This wind structure, with strong directional shear in the lower levels and the large magnitude shear in the upper levels, is a common occurrence in a long-lasting cloud system (Barnes, 1978). Downwind (referring to low level winds) echo development was observed in both Complexes B' and C'.

The steering wind of the echo movement appeared to be at 850 mb. Numerous right-moving echoes were observed from 2235 to 0115Z. The echo movement was apparently transverse to the windshear vector at Midland (Figure 9).

4.2.3 Comparisons of Episodes 1 and 2

The early development of echo line was similar in both episodes, but the later development of echo complexes was very different in two episodes. The environmental conditions were examined and the differences are listed in Table 2.

Table 2

ENVIRONMENTAL CONDITIONS

	Windshear ($m\ sec^{-1}$)	Moisture Distribution
Episode 1	5	Less Homogeneous
Episode 2	10	Homogeneous

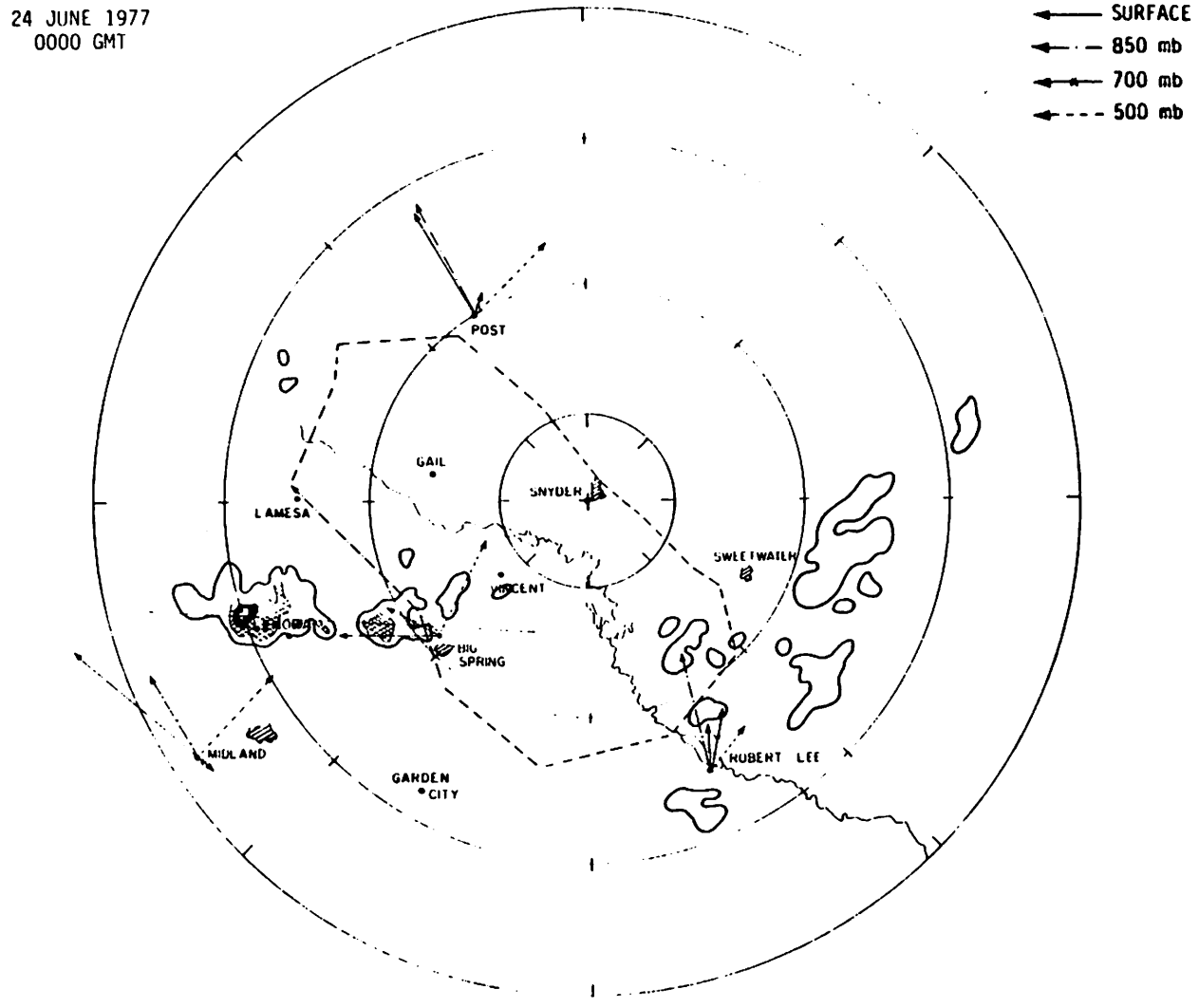

Figure 8. PPI display and winds at 0000 Z. (Same as in Figure 6).

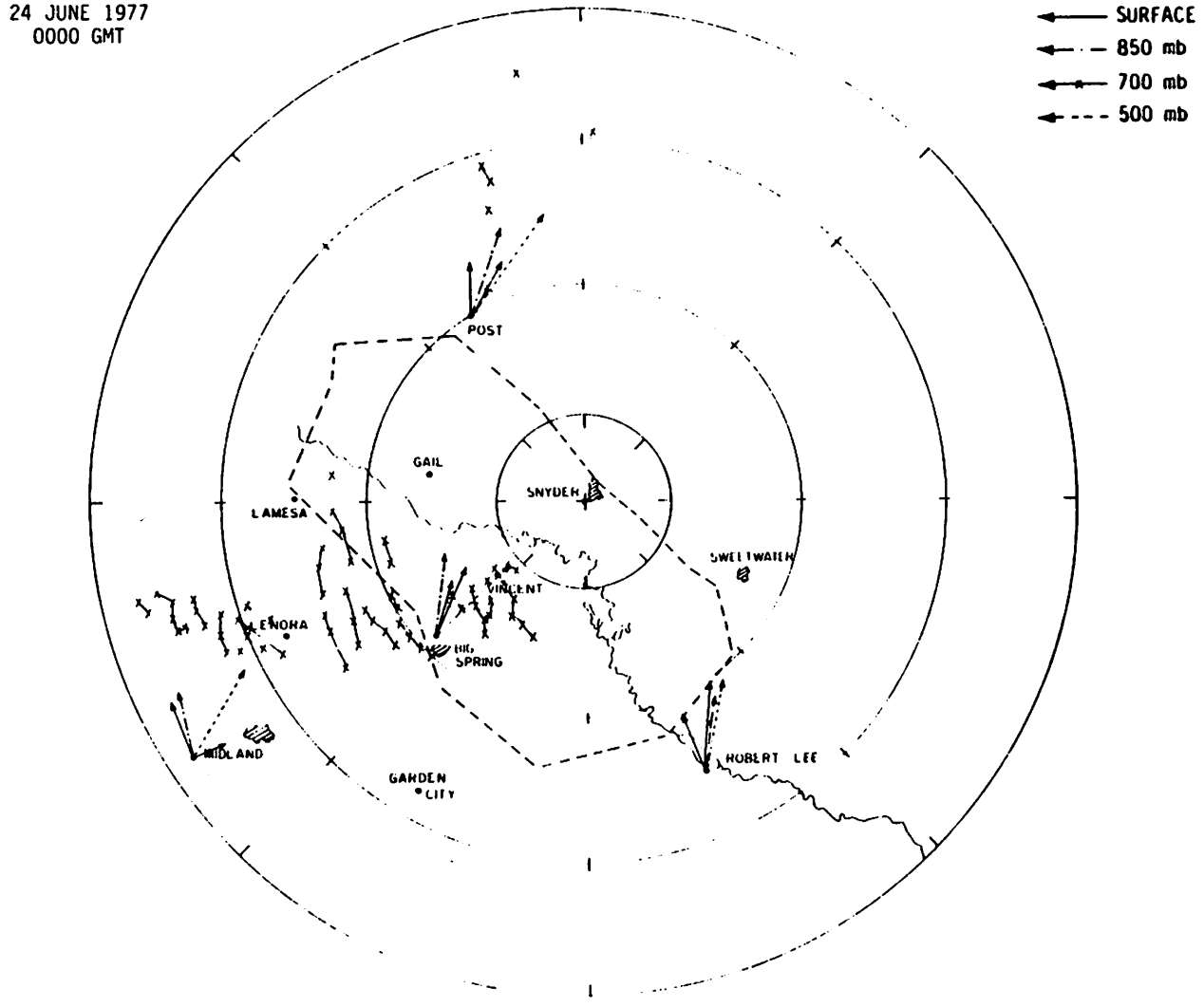

Figure 9. Echo tracking from 2235Z to 0115Z. (Same as in Figure 7).

The surface pressure distribution changed from 1800 to 0000Z (Figure 1a and b). In this period the trough intensified and the pressure gradient increased in the Hiplex area. The increases of surface and 850 mb winds were observed in this time period. Therefore, the shear value at 0000Z was more than the value at 1800Z. In the beginning stage of Episode 1 the moisture distribution was not homogeneous in the southwest quadrant of the Hiplex area. The narrow line formed due to the long gravity wave induced by the cloud system at Robert Lee. The line swept across the southwest region and the moisture advected from the south. The combined effect made the moisture distribution more even in the end period of Episode 1 than in the beginning. The line in Episode 2 formed by short gravity wave of the line in the end period of Episode 1. The line developed in a moist and highly sheared environment. Therefore, the echo features in the two episodes were different.

4.3 Echo Complex Evolution

4.3.1 Complex A (Colorado City)

At 1425 CDT (1925Z) (Figure 10), two modes of development were observed in Complex A. One mode was along the major axis - an echo area consisting of four high intensity echoes was observed. The other mode was perpendicular to the major axis - two large satellite echoes (>35 dbZ) aligned in a transverse mode. A few small satellite echoes surrounded the major echoes. The echoes did not align with the shear vector at Big Spring (96°), but somewhat aligned with the shear at Midland (86°) (arrow on Figure 10). This discrepancy is expected because the wind observation was at 1800Z.

The four echoes (contained in an area) decayed and merged within a narrow strip about 20 km long from 1925 to 1935Z. From 1938 to 1943Z, 35 dbZ echoes were broken into more than two areas. At 1945Z a narrow high dbZ zone appeared. The major echo area merged with the southern satellite at 1940Z and the satellite maintained identity until 2018Z. The east side satellite did not merge into the major echo area nor develop into a big complex. It decayed around 1945Z. The complex became broader as time progressed. In the decaying stage (2018Z) the major axis began to change from northeast-southwest to northwest-southeast. At 2051Z the windshear analysis shows a good agreement between shear direction and cell orientation. Two major cells lined up in longitudinal mode and the satellite echoes were in transverse mode. However, the satellite echoes did not grow to a big sized complex.

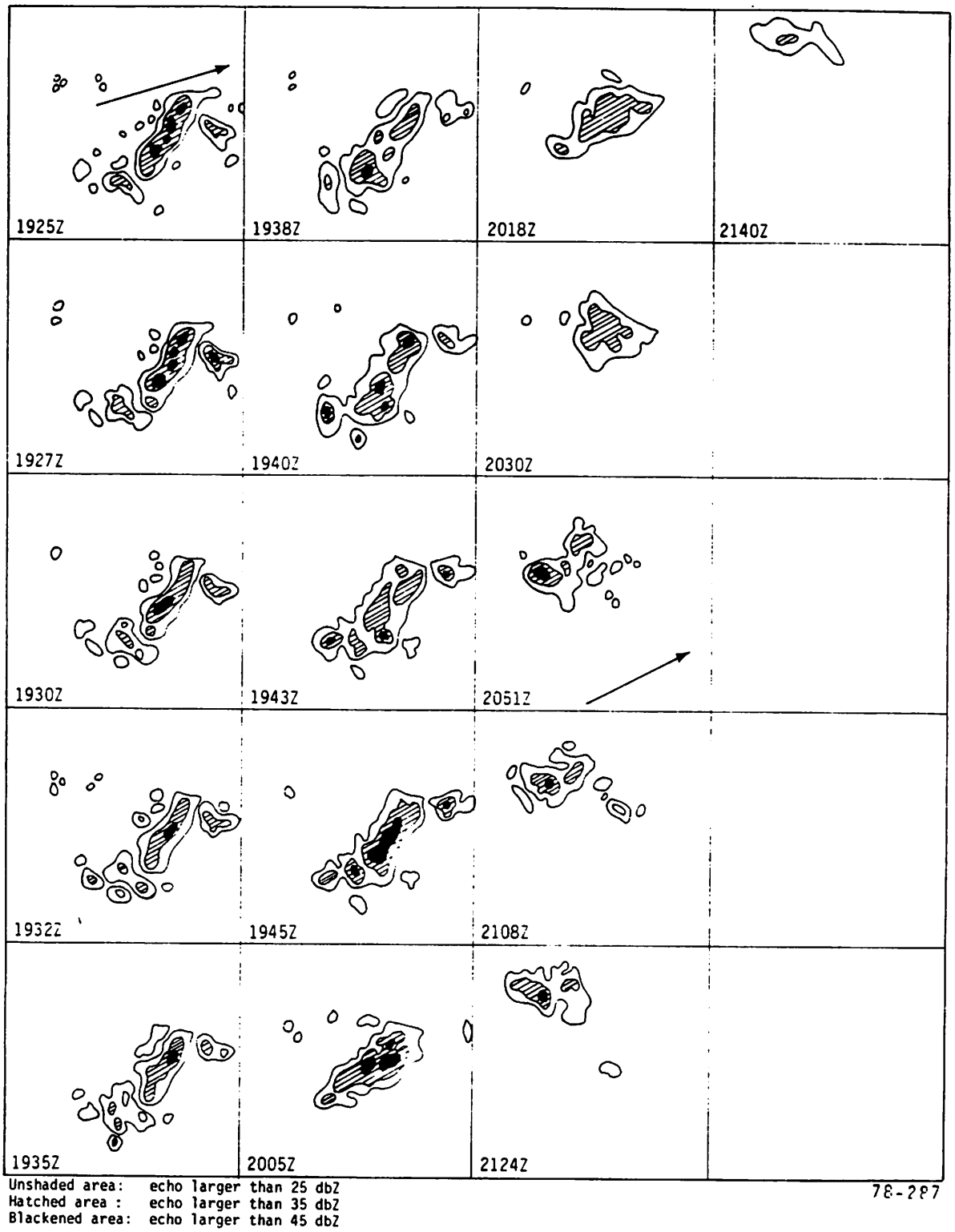

Figure 10. The evolution of echo patterns of complex A in Episode 1. The arrow at 1725Z is the windshear vector at Midland at 1800Z. The arrow at 2051Z is the windshear vector at Big Spring at 2100Z.

4.3.2 Complex B (Big Spring)

This complex was not so well organized as Complex A in the beginning of the observation. However, transverse organization was recognizable. As time progressed the longitudinal mode became obvious. The cells merged about 1932Z and reached peak activity around 1938Z, thereafter decaying was observed. The complex aligned well with shear vector in the dissipating stage. By 2051Z two weak echo lines were parallel to the windshear.

4.3.3 Complex C (Garden City)

Most of the echoes in this complex remained isolated. The transverse mode was observed in the decaying stage (2030Z). By 2051Z only a line of weak echoes remained in longitudinal mode.

4.3.4 Complex A' (Colorado City)

A few weak echoes behind Complex A grew and merged to form Complex A'. At the beginning of Episode 2 the longitudinal mode was barely observable. As time progressed echoes became well organized. By 2226Z two modes of growth were visible. By 2239Z satellites had formed in longitudinal mode. (Windshear interpolation shows the shear direction is east-west at 2230Z.) One of the satellites merged with the major echo area at 2253Z. By 2322Z the cell line showed that the shear direction was deflecting southward and the system became a collection of small echoes. This complex had the shortest lifetime among the three complexes in Episode 2.

4.3.5 Complex B' (Big Spring)

The formation of Complex B' was similar to that of Complex A'. The echo orientation also rotated to confirm the change of shear direction. By 2239Z the complex had about a 30 km major axis and high dbZ echoes were developed at 2253Z. By 2307Z the echo was decaying and two modes of organizations were obvious. The major axis became a minor axis by 2322Z and at 2335Z the echo complex split into two systems. The northern one soon decayed (2335Z) and the southern one remained active (in longitudinal mode) until 0041Z.

4.3.6 Complex C' (Garden City-Midland)

Complex C' was possibly initiated by a gravity wave by Complex B' at 2239Z. The weak echo organization showed longitudinal mode (Figure 11).

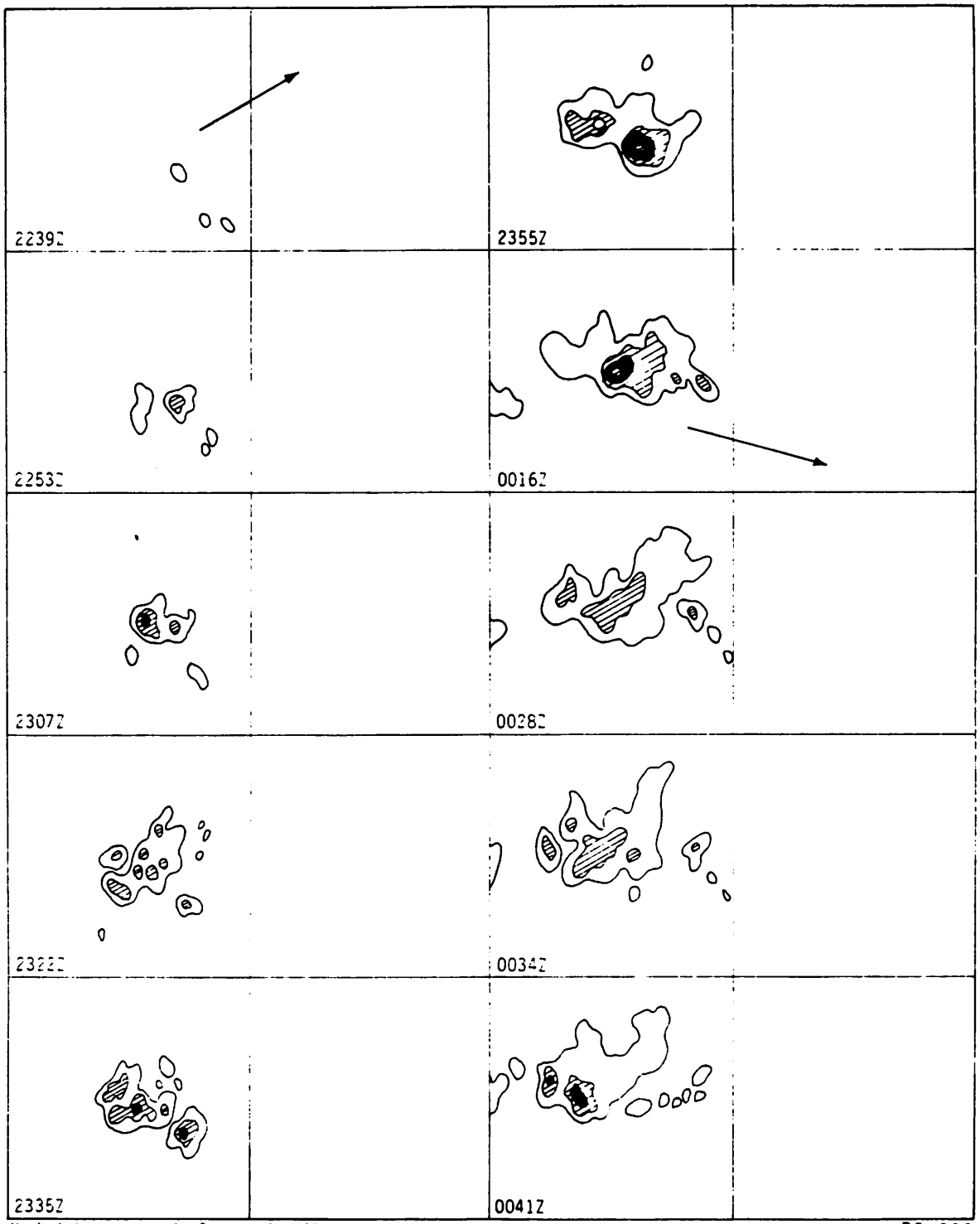

Figure 11. The evolution of echo patterns of complex C' in Episode 2. The arrow at 2239Z is windshear vector at Big Spring at 2100Z. The arrow at 0016Z is the windshear at Big Spring at 0000Z.

A pair of echoes grew rapidly and formed a complex about 2322Z, and an echo southeast of the complex grew very rapidly. This fast growing echo became dominant in this complex. At 0028Z some echo satellites formed, apparently from gravity wave generation, but they did not grow to a big system. However, the western branch of the complex continued to grow and merge with the new echoes. This was a very long lasting echo complex system.

4.4 Summary

1. Echo organization and development was mostly in longitudinal mode and the echo movement coincided with the 850 mb winds.

2. Winds too close to clouds could not be used in shear-line orientation analysis.

3. Windshear variation responded to the change of echo line orientation.

4. Cloud line could form at the same location within three hours.

5. Evolution of Cloud Population

In the cumulus ensemble theory of Arakawa and Schubert (1974), the cloud size distribution function was used to relate to the properties of environmental air. The cloud size distribution function used in this work was defined as a continuous spectrum of cumulus clouds that were distinguished by their entrainment rates. The basic assumption was that a tall cloud has a small entrainment rate and vice versa. Ogura and Cho (1973), developed a model which was similar to the Arakawa and Schubert model to determine the cumulus cloud populations from observed large scale variables. Lewis (1975), used the model to study the interaction between a squall line and its environment. The observed and theoretical distributions of clouds compared favorably on the relative frequency of a tall cloud and the total areal coverage by clouds.

Since the cloud population and large scale (environmental) variables are closely related, the change of cloud population may reflect the change of large scale variables. In the following analysis, the time history of echo

size distributions with respect to equivalent echo diameter were studied. The energetics were not analyzed. The graphic display of size distributions are shown in Figure 12. (The case studied was June 23-24, 1977, included in this report.)

In Figure 12 the vertical axes are the number of echoes and the equivalent area in a designated 5 km size interval. The horizontal axis is the equivalent diameter of an echo defined by a 35 dbZ contour area reduced to a circular area. The assumption is made that the relationship between the equivalent diameter and the entrainment parameter (λ in Arakawa and Schubert's notation) is an inverse relationship. The present analysis thus is related to the conventional expression of cloud distribution by reverting the horizontal axis.

Figure 12 shows that from 1500 to 1700Z, the echo population was confined in sizes less than and equal to 15 km diameter. At 1730Z, a noticeable change of echo distribution was observed; a second mode was located about 30 km in diameter. The area coverage distribution (hatched area) shows that the echo area coverage contributed by the 25 to 35 km size range was nearly equal to the echo area coverage by the 5 to 20 km size range. At 1800Z, the number of echoes in the size range 0 to 10 km increased and large size echoes (40-45 km) were observed. The area distribution showed that echoes larger than 30 km had more contribution than small size echoes (0-15 km). At 1831Z, the distribution was about continuous from the 0 to 35 km size range. The peak of the area distribution was in the 20-25 km range. At 1900Z, bimodal distributions were observed for the number and area distribution. At 1930Z the distributions showed nearly continuously in the size range 0-50 km with holes in the distributions, and the majority of area coverages were larger than 20 km diameter. At 2000Z, two separate size ranges, 0-25 km and 40-45 km, were observed. The major contribution of area coverage was in the 40-45 km range. This major contribution of area coverage persisted until 2100Z. At 2030Z, the peak of area coverage moved to the 25-30 km range and at 2100Z, 30-35 km. After 2100Z, the echoes reduced in number, area coverage, and sizes. At 2130Z, the distributions were similar to that at 1730Z. By 2200Z only a few echoes were observed at the 10-15 km range.

In the case study moist instability was identified from 1500Z to 0000Z and at 1800Z a very pronounced unstable layer existed below 800 mb (Figure 3). It was expected from the θ_e-sounding analysis that the convective potential was maximum around 1800Z. The present analysis showed that from 1730Z to 2100Z the echo distribution changed rapidly

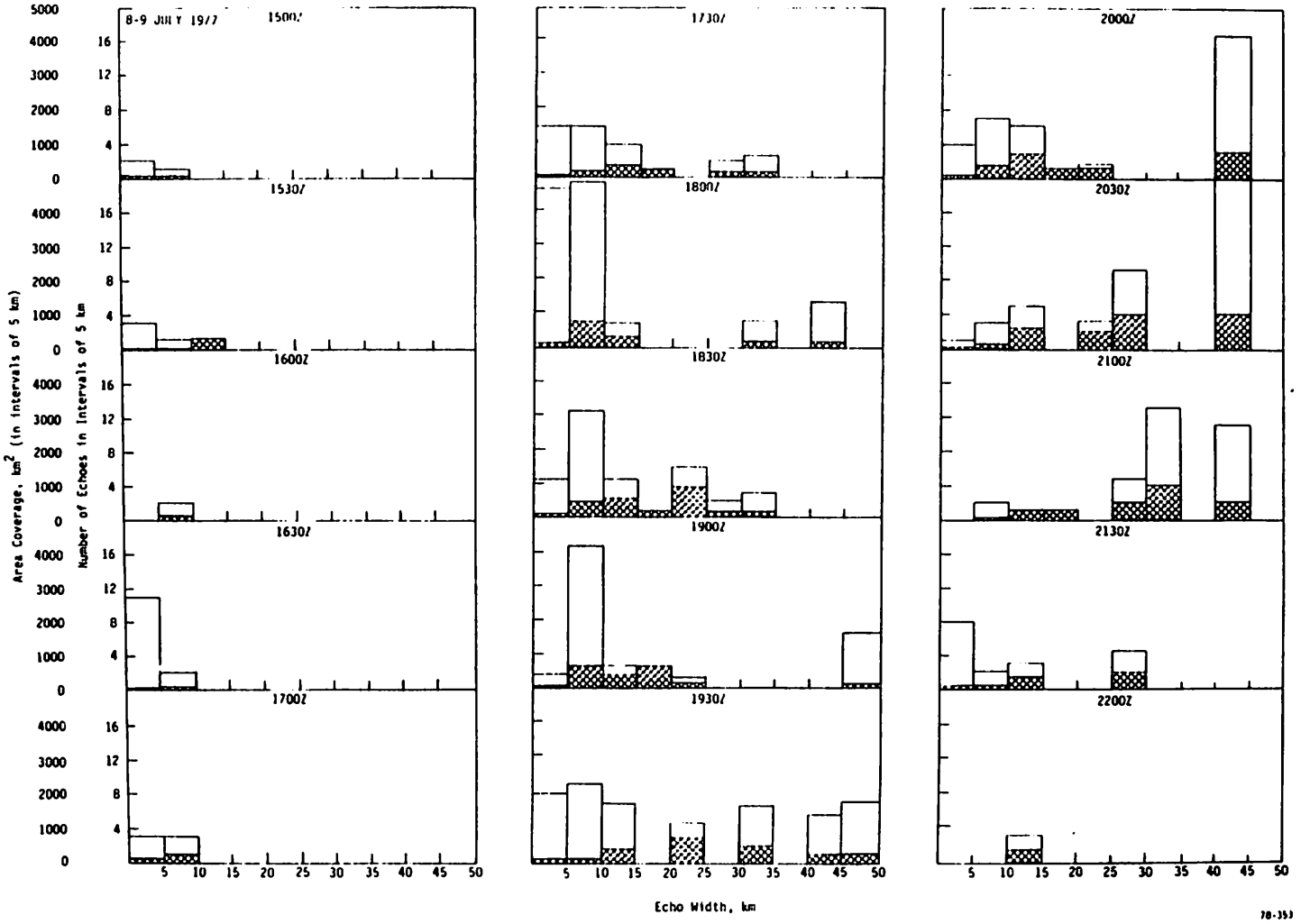

Figure 12. The evolutions of echo number density distribution (non-hatched) and echo area coverage distribution (hatched). (Observed on June 23-24, 1977.)

in a 30 minute interval and the major areal contribution of echoes changed continuously from small size echoes to large size echoes. The previous analysis also showed that the merging of echoes was frequent, and very large echo complexes (~40 km) existed for a long time. The echo distribution reflected this phenomenon from 1900 to 2100Z.

Two conclusions can be drawn from the above analysis:

1. The environmental static stability (large scale variables) controlled the echo population.

2. The merging of echoes changed the echo size distribution.

The exact reasons for the echo to merge are not clear at this time. However, the reasons will be known if the approach of Lewis (1975) is used to calculate the theoretical echo population and analyze the different mechanisms in the cloud and environmental interactions. The application of the "cloud ensemble model" to study seeding effect on a mesoscale cloud population would be very valuable. For example, from the large scale variables the theoretical cloud distribution function can be obtained. This distribution could be considered as the natural background cloud population. In the seeded case, the observed echo population will be analyzed and compared with the theoretical cloud distribution. If a substantial difference is observed between the theoretical and the observed cloud distributions, the seeding effect can be determined. The seedability and nonseedability can also be determined from the calculation of mesoscale, the contribution terms in static, dynamic and feed back processes. There are many more applications of the cumulus ensemble theory, especially in energetic analysis.

6. Mesoscale Radar Echo Climatology

The description of cloud processes, including their development, maturation, and dissipation, is an important part of the Texas Hiplex program. Knowing how these clouds respond to and modify their environment requires an adequate description of the ongoing mesoscale processes. The Skywater radar data collected during the 1976 and 1977 Texas Hiplex operational seasons provide the valuable information needed to identify mesoscale systems. The Hiplex radar data, in conjunction with WSR-57 radar data obtained from the National Weather Service (NWS) allow two scales of radar echoes to be resolved, the meso-α scale and the meso-β scale.

The meso-α scale has a spatial dimension of about 700 km and spans about 15 hours. Meso-α radar patterns are a composite of many radars and are usually associated with familiar mesosynoptic features such as fronts, troughs, and vorticity centers.

The meso-β scale has a spatial dimension of about 150 km and time frame of five hours and is considerably smaller than the meso-α scale. The meso-β radar echoes are resolved exclusively by the Hiplex radar. Radar displays on the meso-β scale resolve squall lines, convective complexes, and isolated cells.

All radar data available from the Texas Hiplex program were classified on both the meso-α and meso-β scales. Radar echo climatologies, interactions between radar scales, as well as inferences concerning individual mesoscale system circulations were possible after analysis of the classification data. This section briefly outlines the results of the above work with a complete technical report to follow shortly.

6.1 Meso-α Echo Classification

Of foremost importance in the approach to classification of both meso-α and meso-β echo patterns is complete objectivity in the screening of each system. National Weather Service (NWS) radar summary displays were examined for each hour for each day during the periods of 1 June to 17 July 1976 and 1 June and 10 July 1977. During this meso-α examination, no reference was made to any other information or analyses, such as synoptic maps or satellite displays. While the NWS radar summaries are subjective to some extent in outlining of the echo area, it is felt that the large scale echo features are adequately represented. Also, since considerable data were missing from the 1976 Snyder radar, the NWS analysis proved to be the only data routinely available for that year. Each day, 1000 CDT to 1000, was cataloged as either:

1. An event day where radar echoes persisted for at least one hour and were within 140 km radially from Snyder, Texas.

2. A vicinity day where radar echoes were outside the Snyder radar coverage but within 280 km radially from Snyder.

3. A no-echo day where no echoes were observed within 280 km of Snyder.

A plastic overlay was constructed and used as a guide for classification when placed over the NWS output. This insured complete objectivity and eliminated bias by the observer. In addition, radar echoes must have persisted for at least one hour to be classified. Operationally this was accomplished by requiring that echoes be observed on two consecutive radar summary displays.

A total of 86 days were finally cataloged with: 54 days classified as event days (62.8 percent), 21 days classified as vicinity days (24.4 percent), and 11 days classified as no-echo days (12.8 percent). The radar echo patterns for each event and vicinity day were then classified according to: area and time of echo formation, subsequent growth and development, line orientation and movement, cell movement, and time of echo dissipation. Analysis of these data tabulations indicated four major echo systems could be identified. Synoptic conditions common to each type of echo system were then examined. Synoptic features surveyed at each level include:

Surface - Pressure patterns, temperatures, dew points, wind flow, and frontal locations

850 mb - Pressure patterns, temperatures, dew points. and wind flow

500 mb - Same as 850 mb but including vorticity

Significant and consistent synoptic patterns that were unique to each type of echo system were found.

6.2 Meso-β Echo Classification

All event and vicinity days, where Snyder radar was available, during the periods of 1 June 1976 to 17 July 1976 and 1 June 1977 to 10 July 1977, were examined and classified for meso-β echo patterns. To insure complete objectivity and eliminate bias, no reference was made to

any other information such as NWS radar summaries, synoptic maps, satellite displays, or previous meso-α classification. As an initial classification, each Snyder PPI hardcopy display was characterized as containing either a mesoscale isolated system (Type I) or a mesoscale line system (Type L). After examining a few days, it became apparent that both isolated and line systems occurred on the same day with enough frequency to justify further subclassification. A mesoscale episode was defined as an occurrence of either an isolated system or a line system. A mesoscale day was classified by the predominate mesoscale episode. A mesoscale day, as in the meso-α classification, was from 1000 CDT to 1000 CDT inclusive.

A total of 12 days were finally cataloged with: 6 days classified as mesoscale isolated systems (50 percent) and 6 days classified as mesoscale line systems (50 percent). A total of 19 events could be identified with: 10 events classified as mesoscale isolated systems (52.6 percent) and 9 events classified as mesoscale line systems (47.4 percent). The I or L letter designation is called the mesoscale character for each day or event. Each mesoscale day and event were subclassified according to echo character as shown below.

Echo Character	Description
1	Isolated cells without orientation
2	Isolated cells with orientation
3	Cell complex without internal line organization
4	Cell complex with internal line organization

Important relationships between wind shear, static stability, and echo orientation and organization resulted from the analysis of the classification results.

6.3 Meso-α Radar Echo Classification

An in-depth analysis of the data that resulted from the itemization and organization reviewed in section 6.1 revealed that all echo systems observed in the 1976 and 1977 Texas Hiplex operational seasons could be represented by four major categories. These categories are Type A, Type B, Type C, and Type D. After identifying in which category an echo system could be associated, further subclassification was made depending on duration and intensity of convection, upper air wind flow regimes, and system orientation with respect to synoptic environmental features. The first two categories, Type A and Type B, are not associated with frontal systems and probably rely on surface heating and/or orographic lifting as

the convective trigger mechanism. The latter two categories are associated with frontal activity and differ only in frontal orientation and its subsequent effects.

6.3.1 Echo System Type A

The Type A echo classification is the most common and recurring echo system in the Texas Hiplex region and will be discussed in the greatest detail. During the 1976 and 1977 operational seasons, 48 percent of the echo events were Type A. This type is characterized by initial formation of radar echoes on the lee side of the Rocky Mountains and/or Sierra Madre Orientals near 1200 CDT. Both echo number and echo intensity increases rapidly along the eastern slopes and forms a line oriented north - south along the Texas - New Mexico border with activity often extending northward into Colorado. Echoes develop as a result of the release of convective instability generated aloft by the juxtaposition of hot, dry desert air to the west and southwest over the warm, moist air from the Gulf of Mexico to the east and southeast. Initial vertical parcel accelerations are provided by rapid surface temperature increases as a result of intense heating. Upslope motion may also be a factor as mentioned earlier. Figure 13 shows the radar echo history for 2 - 3 June 1976, a Type A example.

Two different types of echo/line dissipation in the Type A category facilitate a further subclassification. In most cases, the line becomes stationary over or near the Hiplex area and dissipates by 0500 CDT. This is classified as Subtype 1 or A_1. Occasionally, however, instability can be maintained after surface temperatures have decreased through favorable moisture convergence patterns and upper air temperatures. In this case, echo activity may persist well into the day after formation. This is termed Subtype 2 or A_2. Some evidence also shows that echoes of Type A_2 are further distinguishable from those of A_1 in that they form slightly away from the eastern mountain slopes and closer to the Texas High Plains area.

In order to further classify each A_1 and A_2 system, the 850- and 500-mb wind direction at Midland, Texas, at 1900 CDT was tabulated for each event day for both echo patterns. The 1900 CDT (0000 GMT) sounding was selected because of its proximity in time to the peak growth period for both echo regimes. The 850-mb wind direction was between 105° and 185° for 92 percent of the event days. Eighty-five percent of the event days experienced 850-mb winds from 130° to 185°. After examining the tabulations for the 500-mb winds, two distinct ranges were evident. Those events with 500-mb winds between 305° and 010° were classified as north cases and those events with winds between 220° and 295° were

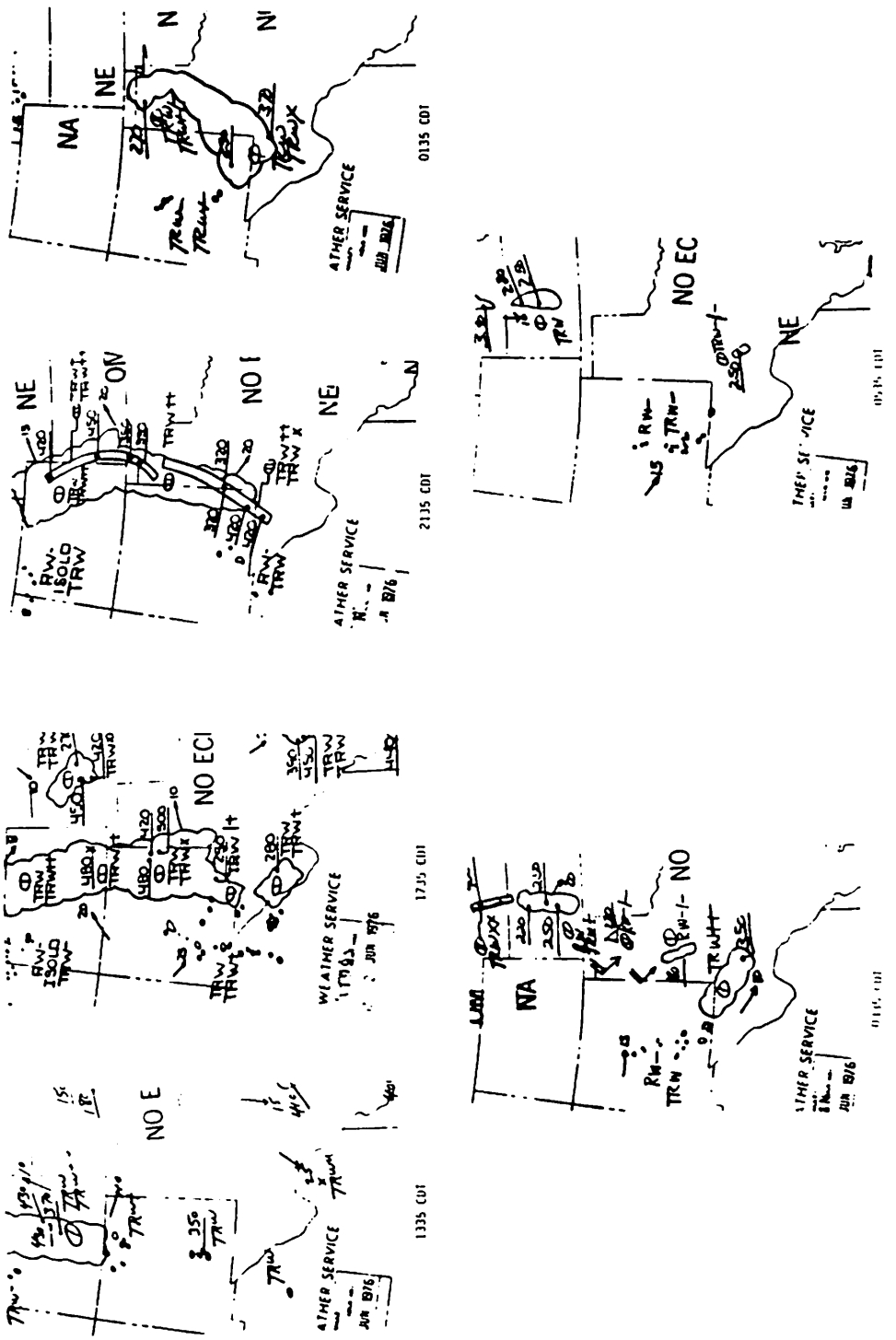

Figure 13. Echo System Type A - June 2-3, 1976

labeled as south cases. A total of four subclassifications constitute the total A category: A_1N, A_1S, A_2N, and A_2S.

6.3.2 Echo System Type B

The Type B echo classification is the other category of echo systems not associated with frontal activity. During the 1976 operational period 19 percent of the total events were classified as Type B. No Type B events are documented for the 1977 operational season. This echo system type is associated with strong moisture advection from the Gulf of Mexico at all levels in the lower troposphere. The characteristic echo pattern associated with this type of system is diurnal in its development and growth but on occasion will persist into the late night and early morning hours. Persistent systems are usually associated with positive vorticity advection at 500 mb. The Type B system is easily recognizable by the large areal coverage of radar echoes.

Further delineation of the Type B system can be accomplished by defining the position of the Hiplex region relative to the orientation and echo motion. Subtype 1 (B_1), Subtype 2 (B_2), and Subtype 3 (B_3) represent echo motion from the southwest, south, and southeast, respectively. Each subtype is merely a reflection of the relative positions of the subtropical high pressure system and the Texas High Plains.

6.3.3 Echo System Type C

The Type C echo system is the smallest of the two categories of frontally induced or enhanced convective systems. The other group is a Type D system discussed in section 5.3.4. Type C systems accounted for about eight percent of the total event days. These systems are associated with surface cold or stationary fronts with an east to west orientation. Radar activity was observed to form in lines parallel to the frontal surface. Most east to west fronts remained well north of the Hiplex region and most echo activity was also north of the area.

Three subclassifications of Type C events became apparent after examining the data tabulations. The Subtype C_1 includes all echo events associated with prefrontal cold or stationary fronts located to the north of the Hiplex region. The Subtype C_2 includes prefrontal cold or stationary fronts undergoing frontolysis or changing into northeast advancing warm fronts. The Subtype C_3 includes postfrontal echo events following frontal passage or postfrontal echo clusters in cyclonic northerly flow accompanying advancing cold fronts or stationary fronts to the south of the Hiplex region.

6.3.4 Echo System Type D

Type D echo systems are associated with advancing cold fronts moving into and through the Hiplex region and oriented northeast to southwest. Type D systems accounted for 29 percent of the echo event days and 78 percent of echo event days associated with frontal systems. The advancing frontal echo systems are often preceded by a Type A echo regime which usually dissipates before the Type D system occurs.

As in Type C echo system, the Type D regime has three subclassifications: D_1, D_2, and D_3. Again, each subtype refers to prefrontal, frontolytic, and postfrontal echo formation, respectively. Again, Types D_1 and D_2 represent activity ahead of and behind the front, but Type D_2 needs some further description. Type D_2 is associated with a northeast-southwest stationary front. Frontolysis can occur when east to easterly flow at 700 mb and 500 mb advects cooler air ahead of the stationary surface system. As the stationary front dissipates leaving a trough of low pressure, another front "appears" to form further north. Analysis at the NWS includes two fronts on the surface map. The existence of two fronts is doubtful, but the analysis represents the only routinely available product and thus the basis for classification.

A summary of all days classified in the meso-α scale is given in Table 3.

6.4 Meso-β Radar Echo Classification

An analysis of the mesoscale classification showed that all mesoscale echoes observed in the 1976 and 1977 Texas Hiplex operational seasons were either isolated (Type I) or line (Type L) systems. Further subclassification in each of these mesoscale character groups resulted in identification of two echo character groups. These echo groups are isolated cell conditions or echo complex conditions. Furthermore, the isolated cell conditions could be subclassified as either having some orientation or not having orientation. In addition, the cell complexes could be subclassified as to whether their component cells had line organization or not. Figure 14 illustrates, in block diagram form, the possibilities for one meso-α type. The arrows indicate the classification path for an echo system associated with an east - west front (Type C) that consisted of line formation of echo complexes with line organized internal cells. The days classified under the meso-β scheme are given in Table 4.

Table 3

MESO-α ECHO TYPE CLASSIFICATIONS

Operational Day	Day 1000-1000 (CDT)	Event Day	Vicinity Day	No Echo Day	Event Occurrence			Event Duration (Hours)	Event Beginning Hour (CDT)
					Daytime 1000-2200 (CDT)	Night 2200-1000 (CDT)	Day and Night		
Yes	1-2	C_3			X			2	1000
	2-3		A_1S					-	-
	3-4		A_1S					-	-
	4-5			NE				-	-
	5-6			NE				-	-
	6-7		C_2					-	-
	7-8		B_3					-	-
Yes	8-9		B_1					-	-
Yes	9-10	A_1S					X	11	1600
Yes	10-11	A_1N			X			6	1700
Yes	11-12	A_1S-D_1					X	15	1700
Yes	12-13		D_1-D_3					-	-
Yes	13-14	D_3				X		5	2200
Yes	14-15		A_1N					-	-
	15-16			NE				-	-
	16-17			NE				-	-
	17-18			NE				-	-
	18-19		D_2					-	-
	19-20		D_2					-	-
Yes	20-21	A_1S					X	10	2100
Yes	21-22	A_2S					X	19	1500
Yes	22-23	A_2S					X	24	1000
Yes	23-24	A_2S					X	18	1000
Yes	24-25	A_2S-D_2					X	20	1000
Yes	25-26	D_1					X	15	1000
Yes	26-27	A_2N			X			6	1600
Yes	27-28	A_2N					X	8	1600
Yes	28-29	D_2				X		3	2300
	29-30		D_2					-	-
Yes	30-1	D_2					X	13	1500

Table 3

MESO-α ECHO TYPE CLASSIFICATIONS
(Continued)

Operational Day	Day 1000-1000 (CDT)	Event Day	Vicinity Day	No Echo Day	Event Occurrence: Daytime 1000-2200 (CDT)	Event Occurrence: Night 2200-1000 (CDT)	Event Occurrence: Day and Night	Event Duration (Hours)	Event Beginning Hour (CDT)
	1-2	D_2			X			3	1500
	2-3	A_1S			X			3	1500
	3-4		A_1S					-	-
	4-5		A_1S					-	-
	5-6		A_1S					-	-
	6-7		D_1					-	-
Yes	7-8	D_2			X			4	1600
Yes	8-9	D_2-D_3					X	17	1000
Yes	9-10	D_3-D_2			X			8	1300

Table 3

MESO-α ECHO TYPE CLASSIFICATIONS
(Continued)

Operational Day	Day 1000-1000 (CDT)	Event Day	Vicinity Day	No Echo Day	Event Occurrence			Event Duration (Hours)	Event Beginning Hour (CDT)
					Daytime 1000-2200 (CDT)	Night 2200-1000 (CDT)	Day and Night		
Yes	1-2		C_2					-	-
	2-3	A_1S-D_1					X	18	1600
Yes	3-4	D_1-D_3			X			11	1000
	4-5	D_3					X	10	1500
	5-6	D_3			X			13	1000
	6-7			NE				-	-
	7-8			NE				-	-
Yes	8-9	B_2				X		3	0700
	9-10	B_2-B_3					X	23	1000
Yes	10-11	B_3-B_2					X	24	1000
Yes	11-12	B_2-B_1					X	24	1000
Yes	12-13	B_1					X	18	1000
	13-14	B_1					X	24	1000
	14-15	B_1					X	24	1000
	15-16	B_1-C_1					X	23	1000
	16-17	C_1-C_2					X	14	1000

Table 3

MESO-α ECHO TYPE CLASSIFICATIONS (Continued)

Operational Day	Day 1000-1000 (CDT)	Event Day	Vicinity Day	No Echo Day	Event Occurrence: Daytime 1000-2200 (CDT)	Event Occurrence: Night 2200-1000 (CDT)	Event Occurrence: Day and Night	Event Duration (Hours)	Event Beginning Hour (CDT)
	1-2			NE					
	2-3	A_1N				X		7	2200
Yes	3-4	A_2N					X	8	1600
	4-5	A_2N					X	24	1000
	5-6	A_2N			X			12	1000
	6-7	A_2N			X			7	1200
	7-8	A_2N-A_1S			X			9	1200
	8-9	A_2N			X			6	1300
Yes	9-10		A_1S					-	-
	10-11		A_1S					-	-
Yes	11-12	A_1S			X			5	1600
	12-13			NE				-	-
	13-14	A_1S			X			7	1500
	14-15			NE				-	-
Yes	15-16		D_3					-	-
	16-17			NE				-	-
	17-18	A_1S-D_1					X	12	1300
	18-19		D_3					-	-
	19-20		D_3						
	20-21	A_2N					X	2	0800
	21-22	A_2N					X	16	1000
Yes	22-23	A_2N-A_1S-D_1					X	22	1000
Yes	23-24	D_1					X	15	1000
	24-25	D_3					X	7	1700
Yes	25-26	A_1S					X	7	1900
	26-27	B_2					X	5	2100
	27-28	B_2			X			8	1400
Yes	28-29		C_1					-	-
	29-30	C_2				X		8	2300
	30-1	C_2					X	10	1500

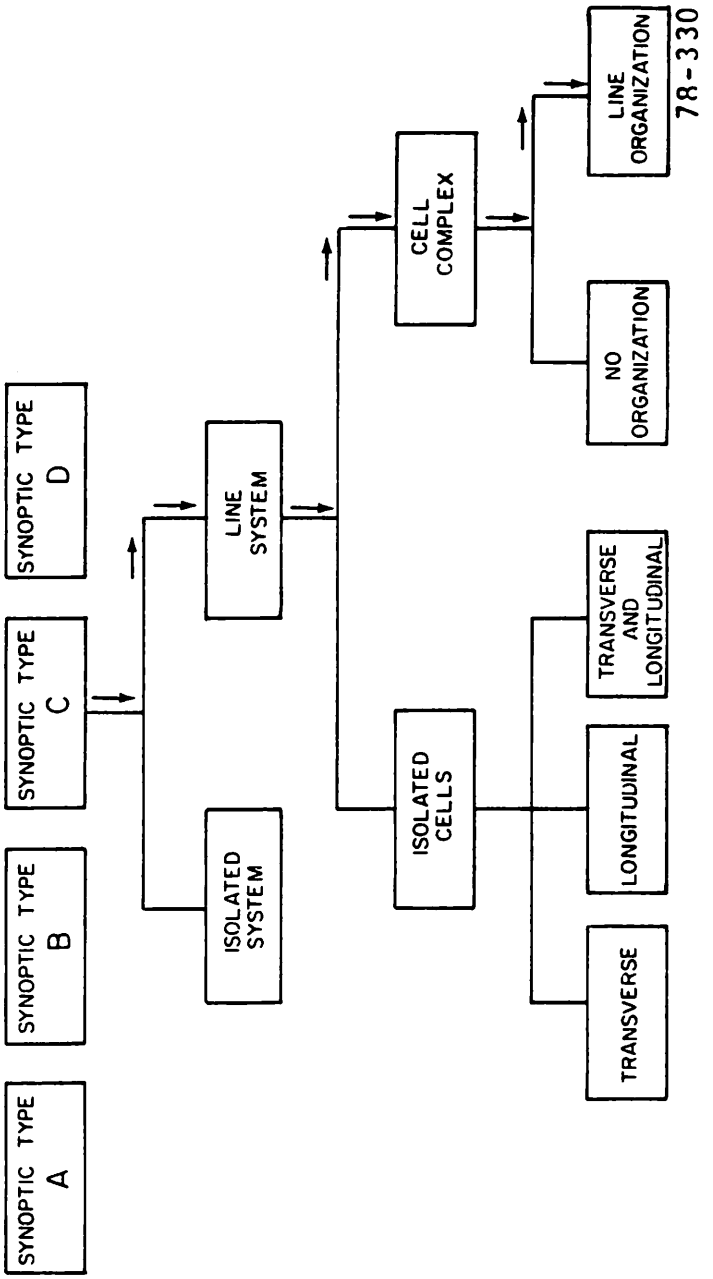

Figure 14. One possible route to classify a mesoscale radar echo system

Table 4

MESO-β ECHO TYPE CLASSIFICATIONS

Date	Echo Type	Beginning Hour (CDT)	Ending Hour (CDT)	Mesoscale Character	Echo Character	MAF 850-500 Wind Shear From (°)	MAF 850-500 Wind Shear Speed (mps)	MAF Stability $\Delta\theta_e$ 850-500
1976								
June 3-4	A_2N	1600	0000	I	2	298.3	7.7	15.0
June 4-5	A_2N	1000	1000	I	2	321.2	10.1	NA
July 10-11	B_3, B_2	1000	1000	L	2	310.4	4.5	11.3
July 10-11	B_3, B_2	1000	1000	L	4	310.4	4.5	
1977								
June 1-2	C_3	1000	1200	L	3	159.2	5.6	12.8
June 9-10	A_2S	1600	0300	I	2	348.7	5.32	5.8
June 9-10	A_2S	1600	0300	I	3	348.7	5.32	
June 11-12	A_2S, D_1	1700	0800	L	4	304.5	5.37	14.2
June 20-21	A_2S	2100	0700	L	3	306.8	8.85	NA
June 21-22	A_2S	1500	1000	I	2	037.6	0.73	9.2
June 22-23	A_2S	1000	1000	I	2	256.7	3.28	4.1
June 22-23	A_2S	1000	1000	I	3	256.7	3.28	
June 23-24	A_2S	1000	0400	L	4	273.1	5.34	
June 23-24	A_2S	1000	0400	L	3	273.1	5.34	13.0
June 23-24	A_2S	1000	0400	I	2	273.1	5.34	
July 8-9	D_2, D_3	1000	0300	L	4			0.4
July 8-9	D_2, D_3	1000	0300	L	2			
July 9-10	D_3, D_2	1300	2100	I	2			16.5
July 9-10	D_3, D_2	1300	2100	I	4			

6.4.1 Mesoscale Isolated System (Type I)

Half of the total number of days involved in the meso-β classification were Type I days and slightly over half of the total number of meso-β events were Type I events. Most of these isolated systems were not associated with well defined synoptic features (e.g. fronts) and thus were classified as meso-α Type A or Type B days.

Four distinct cloud-scale echo characters are possible in a mesoscale isolated system. They are:

1. Isolated cells with no orientation with respect to environmental (850 - 500 mb) wind shear.

2. Isolated cells with orientation with respect to environmental wind shear.

3. Cell complexes without line organization of internal cells.

4. Cell complexes with line organization of internal cells.

Further subclassification of Type 2 echo characters is possible. Two modes of orientation, denoted 'a' and 'b' are given as follows:

a. Transverse - Individual cells are aligned along a line normal to the vector 850 - 500 mb wind shear.

b. Longitudinal - Individual cells are aligned along a line parallel to the vector 850 - 500 mb wind shear.

Figure 15 illustrates a portion of a typical PPI echo display for each echo character.

6.4.2 Mesoscale Line System (Type L)

Half the total number of days involved in the meso-β classification were also Type L days. A little less than half of the total number of meso-β events were Type L events. Most Type L days and events were associated with well defined synoptic features, although there were notable exceptions. The cloud-scale echo characters and isolated cell orientations that formed the subclassifications of the Type I systems were also evident in the Type L systems. The results of both Type I and Type L climatologies are given in Table 5.

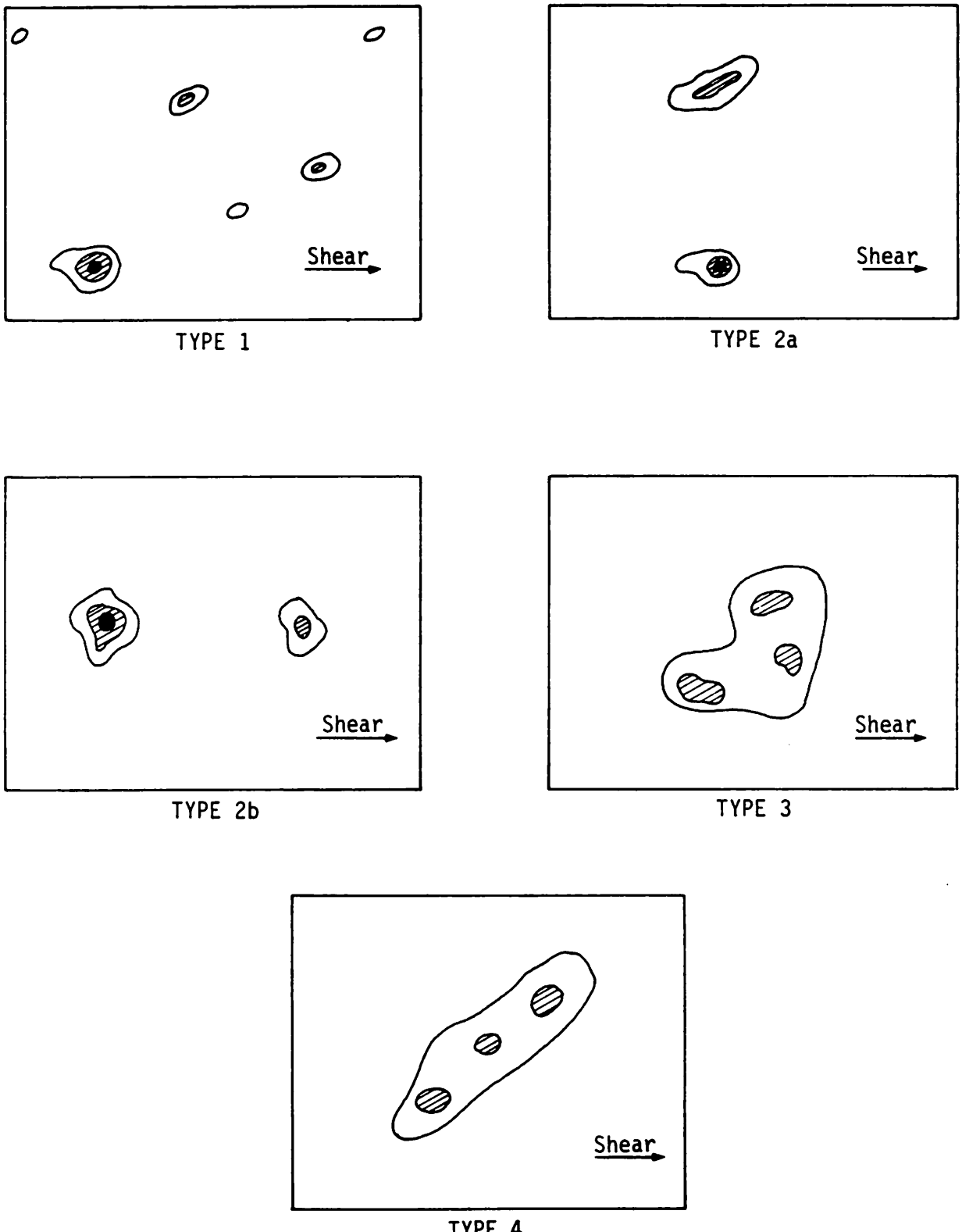

Figure 15. Meso-β echo types

Table 5

MESO-β ECHO CLIMATOLOGY

Mesoscale Character	Echo Character	No. Days	Total Days (%)	No. Events	Total Events (%)
I		6	50	10	53
	1	0	0	0	0
	2	6	50	7	37.1
	3	0	0	2	10.6
	4	0	0	1	5.3
L		6	50	9	47
	1	0	0	0	0
	2	1	8.5	2	10.3
	3	2	16.5	3	15.5
	4	3	25.0	4	21.2

Code Key:

I - Mesoscale Isolated System

L - Mesoscale Line System

1 - Isolated cells (no orientation)

2 - Isolated cells (transverse & longitudinal)

3 - Cell complex without line organization

4 - Cell complex with line organization

A considerable amount of analysis and detail already completed has not been presented in this report in an effort to be brief. A complete discussion of the following is included in the technical report now in preparation:

1. Literature review.

2. Detail of each meso-α and meso-β subclassification.

3. Relationships between the meso-α, meso-β, and cloud scales.

4. Relationships between meso-α systems and synoptic features.

5. Relationships between meso-β systems and the mesoscale vertical wind shear and convective instability.

6. Suggested future work.

REFERENCES

Arakawa, A., and W. H. Schubert, 1974: Interaction of a cumulus cloud ensemble with the large scale environment, Part I. J. Atmos. Sci., 31, 674-701

Barnes, S. L., 1978: Oklahoma thunderstorms on 29-30 April 1970. Part I: Morphology of a tornadic storm. Mon. Weather Rev., 106, 673-684.

Lewis, J. M., 1975: Test of the Ogura-Cho model on a prefrontal squall line case. Mon. Weather Rev., 103, 764-778.

Kropfli, R. A., and L. J. Miller, 1976: Kinematic structure and flux quantities in a convective storm from dual-Doppler radar observations. J. Atmos. Sci., 33, 520-529.

Ogura, Y., and H. R. Cho, 1973: Diagnostic determination of cumulus cloud populations from observed large-scale variables. J. Atmos. Sci., 30, 1276-1286.

TEXAS A&M UNIVERSITY

"MESOSCALE FIELD PROGRAM AND DATA ANALYSIS"

The following report was prepared by Dr. James R. Scoggins, Chief Scientist of the Texas HIPLEX Program, and submitted to the Department as an interim progress report for the period April 1 - September 30, 1978.

The TABLE OF CONTENTS provided below is supplemental information to the report added by the Department for ease of reference purposes.

TABLE OF CONTENTS

LIST OF TABLES

LIST OF FIGURES

SEMI-ANNUAL PROGRESS REPORT

TDWR Contract Nos. 14-80039 and 14-80002

Period: April 1 - September 30, 1978

Prepared for
Texas Department of Water Resources
Austin, Texas

Funded by
Department of the Interior, Bureau of Reclamation, and
the State of Texas through the Texas Department
of Water Resources

James R. Scoggins, Principal Investigator
Department of Meteorology
College of Geosciences
Texas A&M University
College Station, Texas 77843

October 5, 1978

1. CONDUCT OF FIELD PROGRAM

Preparations for the mesoscale field program had begun prior to the report period and continued to the day we left for the field. During April and May, five instrument shelters were made, microbarographs and hygrothermographs cleaned, repaired, and calibrated under field conditions, all instrument shelters (15) painted, all equipment (Army rawinsonde, TAMU rawinsonde, instrument shelters, microbarographs, hygrothermographs, and other miscellaneous items) transported to the field, setup, and checked out, personnel trained and transported to their duty stations, a room built and air conditioned at both Post and Robert Lee to house rawinsonde equipment, arrangements made for living quarters, and supplies obtained. All personnel and equipment were ready for the start of the mesoscale field program on June 1st.

During the mesoscale field program (June 1 - July 27), data (except wind) were collected from sixteen surface stations (15 special stations plus Big Spring), coded, logged, and sent to TAMU for further processing. Wind records from the MRI automatic weather stations were given to MRI personnel for processing. The locations and elevation of the special surface stations are shown in Table 1.1. Measurements at each station consisted of temperature, relative humidity, pressure, wind speed, and wind direction. The inventory of missing surface thermodynamic data for the entire mesoscale period is given in Table 1.2. During the mesoscale field program, Texas A&M University personnel also manned rawinsonde sites at Post and Robert Lee, obtained soundings from the National Weather Service station at Midland, maintained and repaired surface instrumentation and rawinsonde units at Post and Robert Lee, coded soundings from all four sounding stations (Post, Robert Lee, Midland, and Big Spring), and mailed coded data to TAMU for further processing. An inventory of all soundings made as part of the mesoscale program is given in Table 1.3 in coded form, and in Table 1.4 in more graphical form. A series of color slides was made of weather stations, airplanes, clouds, rawinsonde station operations, and other items of interest for documentation and briefing purposes. Unfortunately, opportunities were few to photograph convective clouds that were developing and/or had been seeded. Time lapse movies were made on three occasions, but the targets of opportunity were of limited interest.

Table 1.1. Location and elevation of special surface stations used in Texas HIPLEX mesoscale program during Summer 1978.

Location	Elevation* (m)
Andrews (Airport)	969
Big Spring (USDA Agricultural Extension Station)	763
Clairemont	653
Gail (Borden County High School)	781
Garden City (Garden City School Yard)	816
Lamesa	904
Lenorah	867
Post (Post-Garza County Airport)	771
Robert Lee	589
Rotan (Airfield)	592
Seminole (Airfield)	1030
Snyder (Airport)	740
Sweetwater (Airport)	728
Tahoka (Airport)	950
Vincent	724
Walsh-Watts	718

* includes instrument shelter height

Table 1.2. Inventory of missing surface data by station during the Summer of 1978 for the Texas HIPLEX area for the period June 1 through July 26.

Station	Data Missing		
	Temperature	Relative Humidity	Pressure
Seminole	None	None	6/1-6/2*: 01-11* 6/14-6/16: 03-12
Andrews	None	None	None
Lamesa	None	None	6/1-6/7: 01-11
Tahoka	6/1: 01-14	6/1: 01-14	6/1: 01-14 7/1-7/4: 12-11
Lenorah	6/1: 01-19	6/1: 01-19	6/1: 01-19
Post	None	None	None
Gail	None	6/2-6/5: 15-14	None
Garden City	None	None	6/1-6/3: 22-11
Vincent	6/1: 01-09	6/1: 01-09	6/1: 01-09 7/15-7/17: 13-13
Walsh Watts	None	None	None
Clairemont	None	None	None
Snyder	7/26: 11-24	6/1: 01-11 7/26: 11-24	6/1: 01-11 7/26: 11-24
Rotan	None	None	None
Sweetwater	None	None	None
Robert Lee	6/29-6/30: 17-11	6/29-6/30: 17-11	6/29-6/30: 21-11
Big Spring	None	None	None

*Inclusive dates and times (CDT).

Table 1.3. Coded inventory of rawinsonde soundings for Texas HIPLEX mesoscale program during Summer 1978.

	RL	PO	MA	BG
June 28-29	78062821	78062821	78062821	78062821
	78062900	78062900	78062900	78062900
	78062903	78062903	78062903	78062903
June 29-30	78062921	78062921	78062921	78062921
	78063000	78063000	78063000	78063000
	78063003	78063003	78063003	78063003
June 30-01	78063015	78063015	78063015	78063015
	78063018	78063018	78063018	78063018
	78063021	78063021	78063021	78063021
	78070100	78070100	78070100	78070100
	78070103	78070103	78070103	78070103
July 1-2	78070115	78070115	78070115	78070115
	78070118	78070118	78070118	78070118
	78070121	78070121	78070121	78070121
	78070200	78070200	78070200	78070200
	78070203	78070203	78070203	78070203
July 17-18	78071715	78071715	78071715	78071715
	78071718	78071718	78071718	78071718
	78071721	78071721	78071721	78071721
	78071800	78071800	78071800	78071800
	78071803	78071803	78071803	78071803
July 21-22	78072115	78072115	78072115	78072115
	78072118	78072118	78072118	78072118
	78072121	78072121	78072121	78072121
	78072200	78072200	78072200	78072200
	78072203	78072203	78072203	78072203
July 22-23	78072221	78072221	78072221	78072221
	78072300	78072300	78072300	78072300
	78072303	78072303	78072303	78072303
July 23-24	78072315	78072315	78072315	78072315
	78072318	78072318	78072318	78072318
		78072321	78072321	78072321
		78072400	78072400	78072400
		78072403	78072403	78072403
July 24-25		78072418	78072418	78072418
		78072421	78072421	78072421
		78072500	78072500	78072500
		78072503	78072503	78072503
July 25-26		78072515	78072515	78072515
		78072518	78072518	78072518
	78072521	78072521	78072521	78072521
	78072600	78072600	78072600	78072600
	78072603	78072603	78072603	78072603

Table 1.3. (Continued)

	RL	PO	MA	BG
June 1-2	78060115	78060115	78060115	78060115
	78060118		78060118	78060118
	78060121		78060121	78060121
	78060200	78060200	78060200	78060200
	78060203	78060203	78060203	78060203
June 2-3		78060218		
		78060221		
		78060300		
		78060303		
June 4-5	78060415	78060415	78060415	78060415
	78060418	78060418	78060418	78060418
	78060421	78060421	78060421	78060421
	78060500	78060500	78060500	78060500
	78060503	78060503	78060503	78060503
June 5-6	78060515	78060515	78060515	78060515
	78060518	78060518	78060518	78060518
	78060521	78060521	78060521	78060521
	78060600	78060600	78060600	78060600
	78060603	78060603	78060603	78060603
June 6-7	78060615	78060615	78060615	78060615
	78060618	78060618	78060618	78060618
	78060621	78060621	78060621	78060621
	78060700	78060700	78060700	78060700
	78060703		78060703	78060703
June 7-8	78060715	78060715	78060715	78060715
	78060718	78060718	78060718	78060718
	78060721	78060721	78060721	78060721
	78060800	78060800	78060800	78060800
	78060803	78060803	78060803	78060803
June 13-14	78061315	78061315	78061315	78061315
	78061318	78061318	78061318	78061318
	78061321	78061321	78061321	78061321
	78061400	78061400	78061400	78061400
	78061403	78061403	78061403	78061403
June 14-15	78061415	78061415	78061415	78061415
	78061418	78061418	78061418	78061418
	78061421	78061421	78061421	78061421
	78061500	78061500	78061500	78061500
	78061503	78061503	78061503	78061503
June 27-28	78062721	78062721	78062721	78062721
	78062800	78062800	78062800	78062800
	78062803	78062803	78062803	78062803

Table 1.4. Graphical inventory of rawinsonde soundings for Texas HIPLEX mesoscale program during Summer 1978.

	RL					PO					MA					BG				
	15	18	21	00	03	15	18	21	00	03	15	18	21	00	03	15	18	21	00	03
June 1-2	✓	✓	✓	✓	✓	✓			✓	✓	✓	✓	✓	✓	✓	✓	✓	✓	✓	✓
June 2-3							✓	✓	✓	✓										
June 4-5	✓	✓	✓	✓	✓	✓	✓	✓	✓	✓	✓	✓	✓	✓	✓	✓	✓	✓	✓	✓
June 5-6	✓	✓	✓	✓	✓	✓	✓	✓	✓	✓	✓	✓	✓	✓	✓	✓	✓	✓	✓	✓
June 6-7	✓	✓	✓	✓	✓	✓	✓	✓	✓		✓	✓	✓	✓	✓	✓	✓	✓	✓	✓
June 7-8	✓	✓	✓	✓	✓	✓	✓	✓	✓	✓	✓	✓	✓	✓	✓	✓	✓	✓	✓	✓
June 13-14	✓	✓	✓	✓	✓	✓	✓	✓	✓	✓	✓	✓	✓	✓	✓	✓	✓	✓	✓	✓
June 14-15	✓	✓	✓	✓	✓	✓	✓	✓	✓	✓	✓	✓	✓	✓	✓	✓	✓	✓	✓	✓
June 27-28			✓	✓	✓			✓	✓	✓			✓	✓	✓			✓	✓	✓
June 28-29			✓	✓	✓			✓	✓	✓			✓	✓	✓			✓	✓	✓
June 29-30			✓	✓	✓			✓	✓	✓			✓	✓	✓			✓	✓	✓
June 30-01	✓	✓	✓	✓	✓	✓	✓	✓	✓	✓	✓	✓	✓	✓	✓	✓	✓	✓	✓	✓
July 1-2	✓	✓	✓	✓	✓	✓	✓	✓	✓	✓	✓	✓	✓	✓	✓	✓	✓	✓	✓	✓
July 17-18	✓	✓	✓	✓	✓	✓	✓	✓	✓	✓	✓	✓	✓	✓	✓	✓	✓	✓	✓	✓
July 21-22	✓	✓	✓	✓	✓	✓	✓	✓	✓	✓	✓	✓	✓	✓	✓	✓	✓	✓	✓	✓
July 22-23			✓	✓	✓			✓	✓	✓			✓	✓	✓			✓	✓	✓
July 23-24	✓	✓				✓	✓	✓	✓	✓	✓	✓	✓	✓	✓	✓	✓	✓	✓	✓
July 24-25							✓	✓	✓	✓		✓	✓	✓	✓		✓	✓	✓	✓
July 25-26			✓	✓	✓	✓	✓	✓	✓	✓	✓	✓	✓	✓	✓	✓	✓	✓	✓	✓

The Chief Scientist served in Big Spring as Project Director for field operations during most of June. His duties consisted primarily of planning aircraft seeding and sampling missions, participation in flight briefings and debriefings, assisting in making forecasts for mesoscale operations, and coordinating activities of all field personnel. The Chief Scientist was assisted in all these duties by personnel of the Texas Department of Water Resources who assumed full responsibility for them during July.

Following termination of the mesoscale field program on July 27, all field equipment for which TAMU was responsible was returned to appropriate locations. The 10 microbarographs on loan were returned to Texas Tech University, the Army's rawinsonde unit was returned to White Sands Missile Range, New Mexico, and all other equipment was returned to Texas A&M University.

2. PROCESSING OF MESOSCALE SURFACE AND RAWINSONDE SOUNDING DATA

Considerable time was spent during this report period on the processing of field data. This is an important task which requires much skill, expertise, diligence, and perseverance on the part of those performing this task. Yet, not much is usually reported to give an appreciation for the magnitude and importance of this task. A brief description is given in this section of the procedures followed at Texas A&M to produce the well-edited surface and rawinsonde sounding data sets that are used in various analyses.

This year marked the beginning of a new approach to handling the vast amount of data created in the combined HIPLEX upper air and surface networks. An interactive computer system was utilized which allowed access, retrieval, and use of any portion of the data set in a matter of minutes. This procedure improved the overall efficiency and quality of the rawinsonde data reduction by allowing more confident identification and correction of errors. The computer terminal provided by the Bureau of Reclamation made this procedure possible.

On each operational day the rawinsonde operators coded the soundings on a form for keypunching, and the data were sent to Texas A&M. The data were then logged-in so that a complete inventory was kept by both the field coordinators and the data specialists at Texas A&M. The data were then punched into computer cards which were labelled and stored to facilitate easy access. At this point, the data were also stored on disk to allow access by an interactive computer terminal.

Error checking of the raw data was begun before the operators returned from the field. The original ordinate and angle data were checked with a computer program that called attention to discontinuous values. This procedure helped to locate keypunching and coding errors. The next step of the error checking procedure was to compute the soundings and obtain actual values of temperature, dewpoint, wind, etc.

Checking the computed soundings consisted of three additional tests. The first of these was very much like that applied to the raw data. A computer program which isolates discontinuous values of temperature, dewpoint, wind direction, and wind speed was run. This program identified reading errors that passed undetected through the first phase.

The second step isolated soundings that were not spatially consistent. Constant pressure maps were plotted for 850, 700, 600, 500, 400, 300, and 200 mb using data from the four HIPLEX rawinsonde stations. Values of temperature, dew-point depression, geopotential height, wind speed, and wind direction were plotted for every sounding time and analyzed to find inconsistencies.

The third check was an analysis of the time continuity of the HIPLEX soundings. Time cross-sections of each station and each operational day were analyzed for the same values plotted on the constant pressure maps. The computer was used to put the data in the proper format for both the constant pressure and time cross-section analyses.

Fortunately, the last three steps described were carried out with the help of the rawinsonde operators. Their knowledge of meteorology and their field experience was imperative in this stage of the error checking.

At this point, final corrections were made to the upper-air data set. Throughout the procedure, the computer cards were also corrected so that they would serve as a backup for the disk data set. Data tapes consisting of ordinate, computed soundings for each pressure contact, and soundings interpolated for 25-mb intervals were prepared. This was the last step in the rawinsonde data reduction process.

Data from the HIPLEX surface network was checked using a program similar to the one used on computed values of upper air data. Discontinuous values were identified and checked by the surface network operators. This data set is now in card form until final compilation on magnetic tape can be accomplished. Numerous corrections were made in surface pressures because of errors in the aneroid used to calibrate the microbarographs.

3. ANALYSIS OF 1977 SURFACE DATA

Data from the special surface and other stations were analyzed for 1977 in the same manner as was done for the 1976 data. Computer-analyzed charts were prepared at 1-hr intervals from 1500 to 0300 GMT for each day on which convective activity of any intensity was observed. Parameters included in this analysis are velocity divergence, moisture divergence, mixing ratio, vertical flux of moisture, vorticity, terrain-induced and planetary boundary layer vertical motion, surface pressure and pressure change, equivalent potential temperature, and temperature. The pressure and pressure change charts were added to the analysis of the 1977 data. It was not possible to perform these analyses on the 1976 data because of errors in the data.

Contingency tables and relative frequency distributions of the various parameters were prepared as function of convective activity. The data were grouped into categories of clear, organized and unorganized echoes, lines, etc. Time histories of the magnitude of selected parameters were prepared and related to the intensity of convective activity as indicated by echo height (values coded as in 1976 analysis).

Results from the analysis of the 1977 data are somewhat different from those of the 1976 data. Specifically, critical values of the parameters which distinguish between convective regimes of various intensities are different in 1977 from those found in 1976. The frequency distributions prepared from 1977 data do not show pronounced peaks as was the case for the 1976 data. The differences appear to be related to the intensity of the convective systems. Our analysis continues on this task.

4. ANALYSIS OF UPPER-LEVEL KINEMATIC PARAMETERS

4.1 Introduction and Data Analysis

The 1976 Texas HIPLEX rawinsonde data, obtained from 14 operational days during June and July, were used to calculate various kinematic parameters aloft from 850 mb to 100 mb at 50 mb intervals. These results were used in the individual case studies to investigate the interactions between convective clouds and their environment for the purpose of determining factors responsible for the initiation, growth, maintenance, and dissipation of convective activity. In summarizing the results of the case studies, average vertical profiles of the kinematic parameters were calculated for those time periods with and without thunderstorms over the network. In 1976, the mesoscale kinematics of the atmosphere were clearly different, at various levels and times, for those periods with and without convective activity. These results indicated that the mesoscale environment exerted a strong controlling influence over thunderstorm development through its three-dimensional circulation.

Similar calculations have been made for the 1977 Texas HIPLEX rawinsonde data. In 1977, vertical profiles of vertical velocity (μbars s^{-1}), horizontal moisture divergence (10^{-7} s^{-1}), and horizontal mass divergence (10^{-8} g cm^{-3} s^{-1}) were computed for the layer from 850 mb to 100 mb at 50 mb intervals for each time period of the 16 operational days when sounding data were available. Days in 1977 for which calculations have been made include June 1, 7, 9, 11, 13, 21, 22, 23, 24, 25, 27, and 30 and July 7, 8, 9, and 10. The data analysis procedures used for the 1977 data are somewhat different from those used in 1976 but the end product is the same. The final result for the upper-level kinematic calculations is still a single vertical profile of a given parameter representing the average environmental conditions over the network bounded by the triangle from Midland (MAF) to Post (PO) to Robert Lee (RL).

For a given time period and pressure surface, the horizontal velocity divergence was computed by use of the expression

$$\vec{\nabla}_p \cdot \vec{V}_2 = \frac{1}{A}\frac{dA}{dt} \simeq \frac{1}{\bar{A}}\frac{\Delta A}{\Delta t}$$

where A is the horizontal triangular area determined from the three rawinsonde balloon locations (MAF, PO, and RL) projected onto a constant pressure surface,

$\overline{A}$ is the average area of the triangle between two pressure surfaces 50 mb apart, and ΔA is the change of triangular area that occurs as the balloons move through a pressure layer 50 mb thick in time Δt.

Horizontal moisture and mass divergence were determined using the vector identity

$$\vec{\nabla}_p \cdot C\vec{V}_2 = \vec{V}_2 \cdot \vec{\nabla}_p C + C\vec{\nabla}_p \cdot \vec{V}_2$$
$$(1) \qquad (2) \qquad (3)$$

where C is any scalar. For moisture and mass divergence, q (mixing ratio) and ρ (air density) were used in place of C. Then term 2 was computed by the centered finite difference formula

$$\vec{V}_2 \cdot \vec{\nabla}_p C = u\frac{\partial C}{\partial x} + v\frac{\partial c}{\partial y} \simeq \overline{u}\frac{(C_2 - C_1)}{\Delta x} + \overline{v}\frac{(C_2 - C_1)}{\Delta y}$$

where $\overline{u}$ and $\overline{v}$ are the average wind components over the network along a pressure surface and $\frac{C_2 - C_1}{\Delta x}$ and $\frac{C_2 - C_1}{\Delta y}$ are the horizontal vector components of the gradient of C in the "x" and "y" directions, respectively. Term 3 was calculated by multiplying C (an average for the pressure surface) by the horizontal velocity divergence computed previously. Since the velocity divergence represents a 50-mb layer mean value, term 2 was actually computed as a mean horizontal advection by averaging data from three 25-mb data levels constituting the 50-mb layer used in the velocity divergence calculation.

Vertical motion was computed on constant pressure surfaces using the formula

$$(\omega_p)_k = \omega_s + \sum^{k} \overline{(\vec{\nabla}_p \cdot \vec{V}_2)}_k (\Delta p)$$

where $(\omega_p)_k$ is vertical velocity on a constant pressure surface k, ω_s is the vertical velocity at the ground (set to "0"), $\overline{(\vec{\nabla}_p \cdot \vec{V}_2)}_k$ is the 50-mb layer mean divergence below layer k, and Δp = 50 mb.

Test comparisons between kinematic calculations made on 1976 data using both data analysis techniques showed only negligible differences.

4.2 Average Conditions of Kinematic Parameters during Times With and Without Convective Activity

In 1977, there were 70 time periods that contained the necessary data for kinematic calculations aloft. These time periods were classified as either

"convective" or "nonconvective" depending upon whether thunderstorms were present over the network bounded by the PO-RL-MAF triangle. If a radar echo in excess of 6.1 km (20,000 ft) was observed ±1 hour surrounding a sounding time, the period was termed convective. All other cases were termed nonconvective except when balloons were suspected of entering thunderstorms. These cases were considered as not representative of the mesoscale environment in which thunderstorms were present and were excluded from averages presented here. Using this classification, there were 15 and 55 time periods with and without convective activity, respectively.

Figures 4.1-4.3 show the 1977 average vertical profiles of vertical velocity, mass divergence, and moisture divergence, respectively, for both the convective and nonconvective cases. For comparison, the 1976 profiles are also included in each figure.

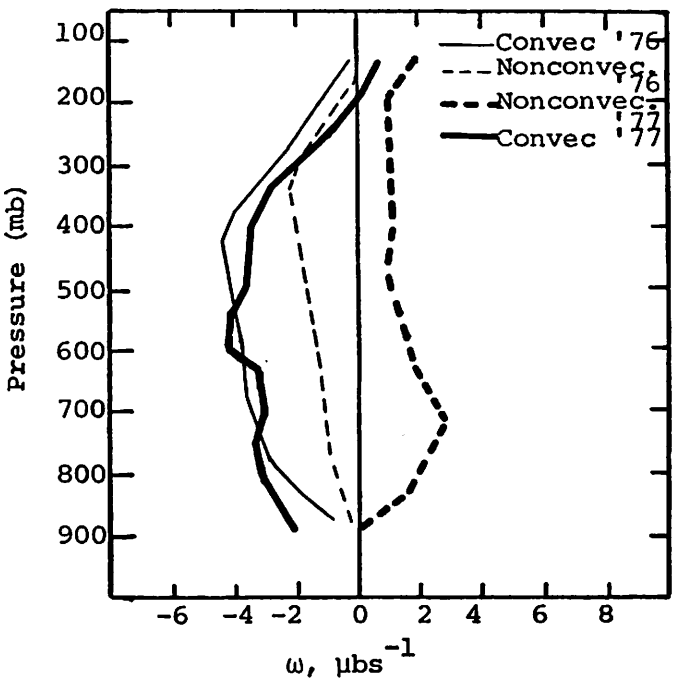

Fig. 4.1. Vertical profiles of vertical motion for Texas HIPLEX area averaged for times of convection and nonconvection for 1976 and 1977.

In Fig. 4.1, average vertical velocities in 1977 were upward (negative) in the convective case at all levels below 200 mb with maximum upward motion of -4 μbars s^{-1} occurring at 600 mb. This profile is almost identical to the 1976 results differing less than 1 μbar s^{-1} at all levels. Subsidence was

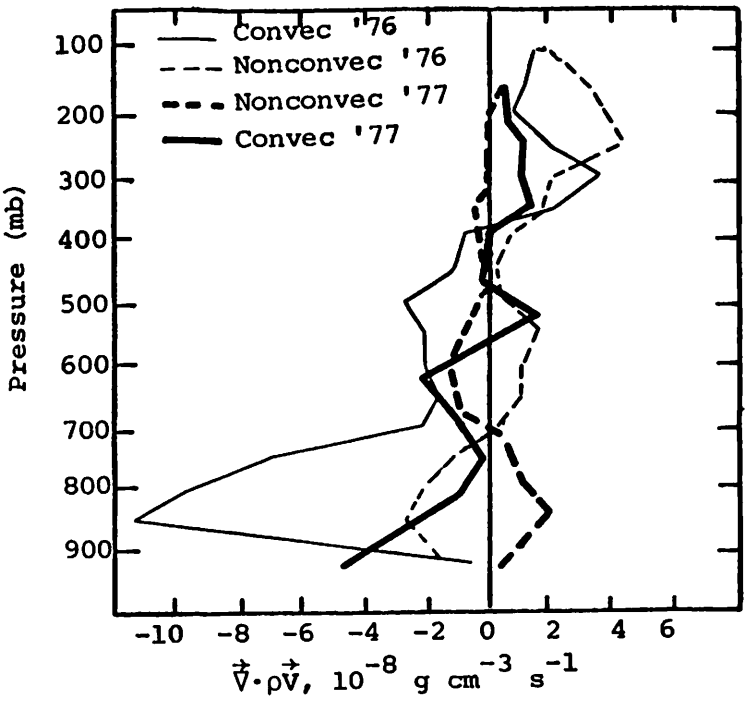

Fig. 4.2. Vertical profiles of mass divergence for Texas HIPLEX area averaged for times of convection and nonconvection for 1976 and 1977.

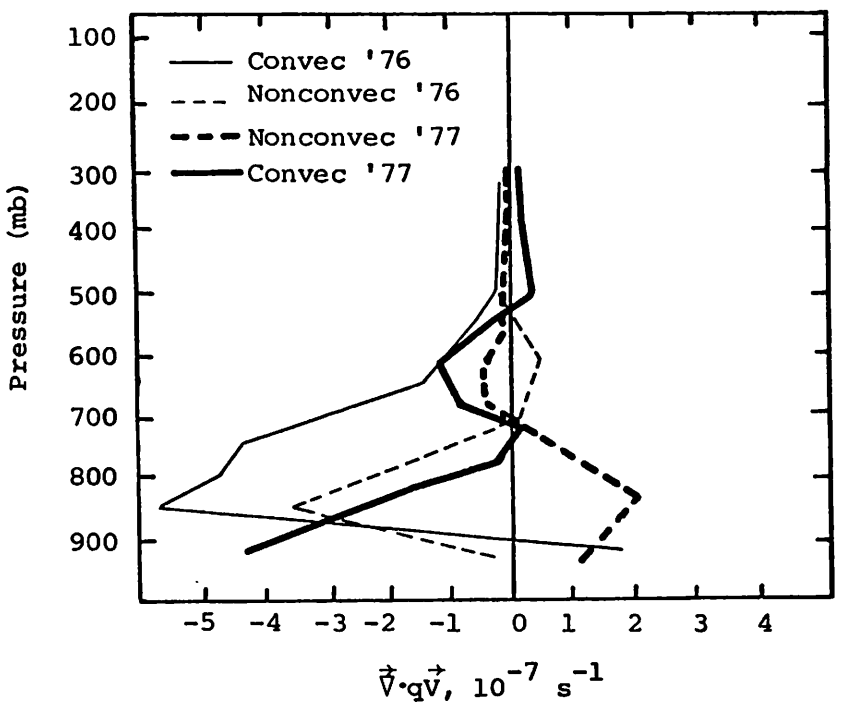

Fig. 4.3. Vertical profiles of moisture divergence for Texas HIPLEX area averaged for times of convection and nonconvection for 1976 and 1977.

present at all levels in the 1977 nonconvective case and largest near 700 mb (3 μbars s^{-1}). In contrast, the 1976 nonconvective profile showed upward motion at all levels.

The horizontal mass divergence profiles in Fig. 4.2 reveal similar vertical distributions of mass divergence in both years for the convective case with mass convergence present below 600 mb and divergence occurring above 400 mb. However, magnitudes of convergence were clearly smaller in 1977 above 900 mb, especially between 850 and 700 mb where 1976 mass convergence values were at least twice as large as the 1977 values. The nonconvective profiles are almost mirror images of each other up to 500 mb where the 1977 results showed mass divergence up to 700 mb and mass convergence above to 500 mb. In 1976, mass divergence was large above 400 mb but near zero in 1977.

The horizontal moisture divergence profiles in Fig. 4.3 also reveal similar vertical distributions of moisture divergence in both years for the convective case with significant moisture convergence present below 500 mb and near zero divergence above. Magnitudes of convergence were also smaller in 1977 above 900 mb, especially between 850 and 700 mb. As with mass divergence, the moisture divergence profiles in nonconvective areas are mirror images of each other up to 500 mb and almost identical above. In 1977, moisture divergence occurred between the surface and 700 mb and moisture convergence was present between 700 mb and 500 mb.

Another significant difference in both the moisture and mass divergence profiles between 1976 and 1977 was the occurrence in 1977 of increasingly larger values of moisture and mass convergence below 700 mb that extended down to the surface.

5. ANALYSIS OF THE MOISTURE BUDGET

The equation for the continuity of water substance can be expressed in the form:

$$\underset{(1)}{\int_v \frac{\partial(q\rho_a)}{\partial t}\,dV} + \underset{(2)}{\int_s (q\rho_a \vec{V}_2)_n\,dS} + \underset{(3)}{\int_s (q\rho_a w)\,dA} = \underset{(4)}{R} \qquad (5.1)$$

where:

q = mixing ratio

ρ_a = density of the air

$\vec{V}_2$ = horizontal wind velocity

w = vertical velocity

n = normal component

v = volume

This equation represents a balance of the total water budget at any particular time expressed in units of (gm/sec). The terms in the equation have the following interpretation: (1) The local rate-of-change or the net gain or loss of water vapor within the volume; (2) Transport of water vapor through lateral boundaries; (3) Transport of water vapor through vertical boundaries; and (4) The sources and sinks of moisture (evaporation, condensation, precipitation, and turbulent flux of moisture through the boundaries).

A triangle was formed over the Texas HIPLEX area by the vertices of three rawinsonde stations (Robert Lee, Post, and Midland), encompassing an area of approximately 8.31×10^9 m^2. Since the effect of balloon drift on area was determined to be negligible, this area was assumed to remain constant with height. The volume for which this analysis was performed is this area times the vertical distance between 850 and 300 mb.

Equation 5.1 was evaluated for 10 days during the summer of 1977, over 50-mb layers using sounding data taken at 3-h intervals from 1500 to 0600 GMT, over the Texas HIPLEX area. These results and a summary for each day will appear in a subsequent report on the analysis of 1977 data. The format of these results, including time profiles of water vapor budget terms and subsequent discussion, will be presented in a similar manner to the Technical Report concerning the analysis of 1976 data. A preliminary analysis of the water vapor budget for 1977 data agree with results previously obtained using 1976 data.

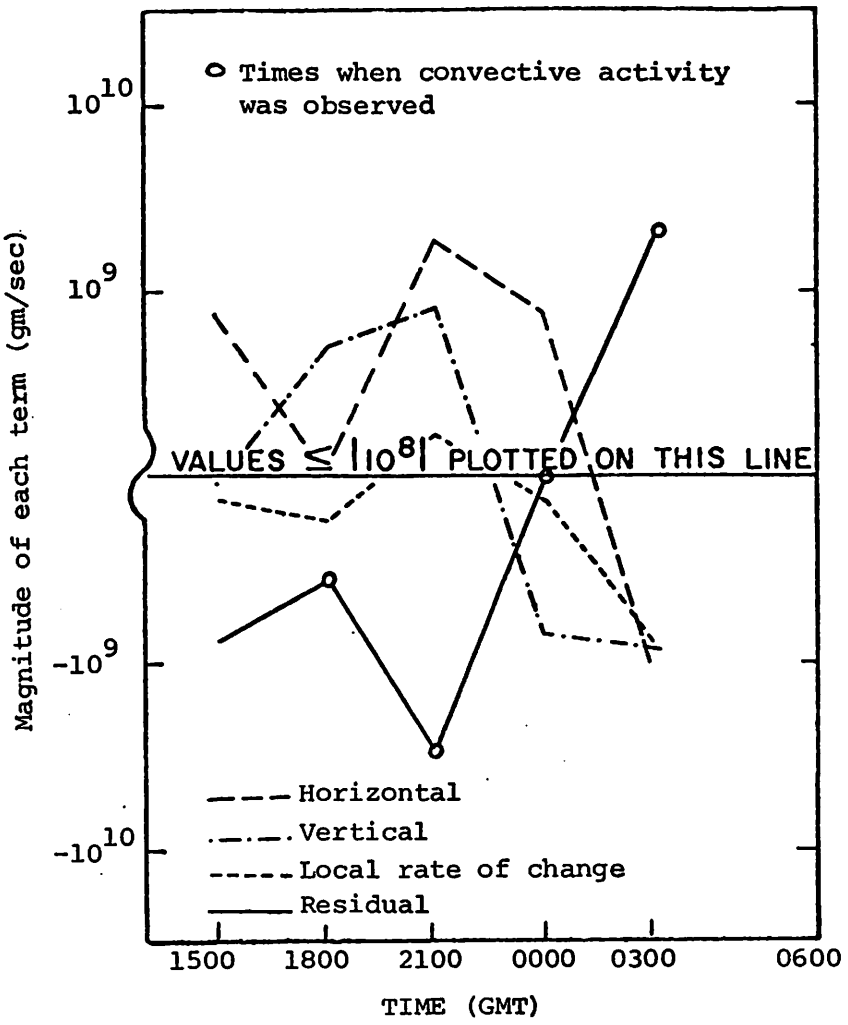

Fig. 5.1. Comparison of terms in the water budget equation for 23-24 June 1977.

An analysis of the complete water budget has been completed for 10 days during the summer of 1977 over the Texas HIPLEX area. Evaluation of the total moisture budget was accomplished by integrating Eq. 5.1 between 850 and 300 mb, for each time sounding data were available. A comparison of the terms in Eq. 5.1 was made for each of the 10 days studied. Figure 5.1 represents a sample comparison of the terms in the water budget equation for sounding times on 23-24 June 1977. Radar maps for this time period indicate the development and movement of a line with associated isolated cells over the Texas HIPLEX area. Intensification and movement of convective activity were observed between 1500 and 0000 GMT, followed by dissipation at 0300 GMT. Specific times when convective activity was observed within the area are indicated on Fig. 5.1.

Horizontal moisture convergence into the Texas HIPLEX area prior to convective activity is shown to be the primary moisture source. This net horizontal convergence reaches a maximum at 2100 GMT, the time when convective activity within the area reached a maximum. Vertical moisture transport also tends to "store" water prior to activity. The local rate-of-change term remains nearly constant, showing a small net gain at 2100 GMT. This may be attributed to the air being nearly saturated at all times throughout the day. Also, at all times during intensification and development, a loss in the residual term is observed, especially at 2100 GMT.

The total mass of water vapor present, defined as the total precipitable water within the volume, PW, can be represented in the form:

$$PW = \int_V (q\rho_a)dV \tag{5.2}$$

where:

q = mixing ratio

ρ_a = density of the air

V = volume

PW expressed in grams was computed for 10 days during the summer of 1977, over the Texas HIPLEX area. These results are shown in Figs. 5.2 and 5.3 for June and July 1977, respectively. Specific times when convective activity was observed from radar maps are shown on these figures. Average values of the total mass of water vapor for each day were obtained from these figures. The results indicate that a "threshold" value in water vapor of about 1.9×10^{14} gm is needed over the Texas HIPLEX area for sustained convective activity and precipitation to occur. These results agree quite favorably with those of 1976, where a "threshold" value of 2.0×10^{14} gm was determined.

The distribution of precipitable water with height was analyzed for 10 days during the summer of 1977, and for 9 days during the summer of 1976. Figure 5.4 represents a sample time cross section of the total mass of water vapor over the Texas HIPLEX area for 13-14 June 1977. Again, specific times when convective activity occurred over the Texas HIPLEX area are shown on this figure. The distribution of precipitable water with height is shown in three layers (850-700 mb, 700-500 mb, and 500-300 mb), including an integrated total amount. A percentage of the total integrated amount in

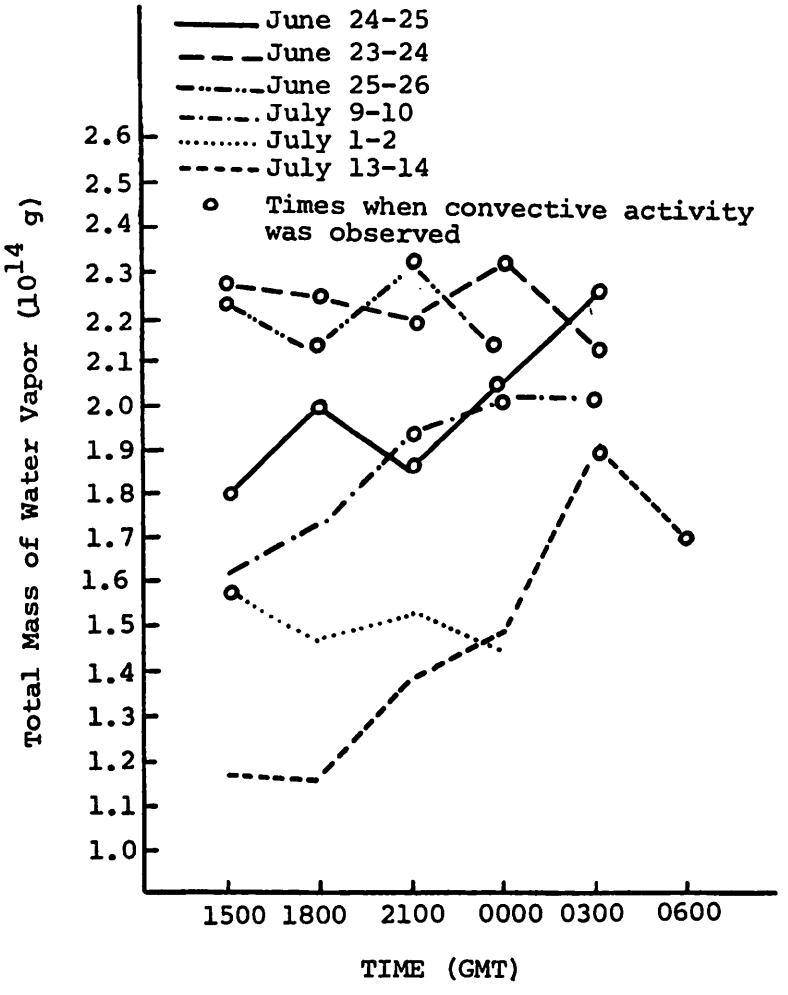

Fig. 5.2. Precipitable water on days during June 1977.

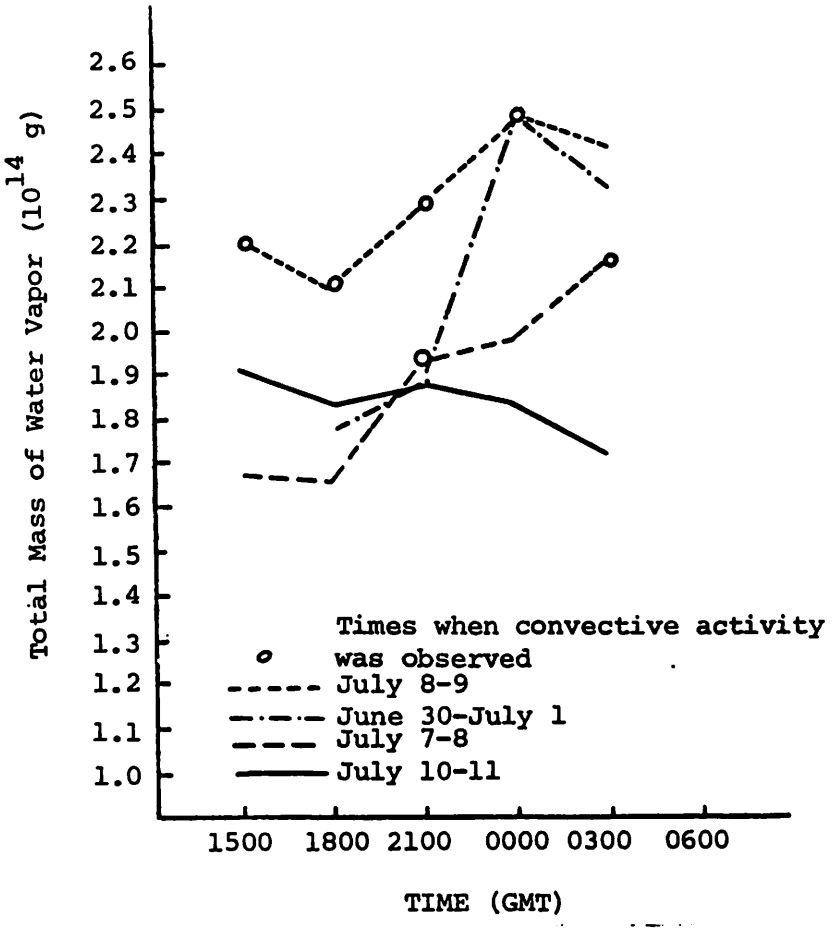

Fig. 5.3. Precipitable water on days during July 1977.

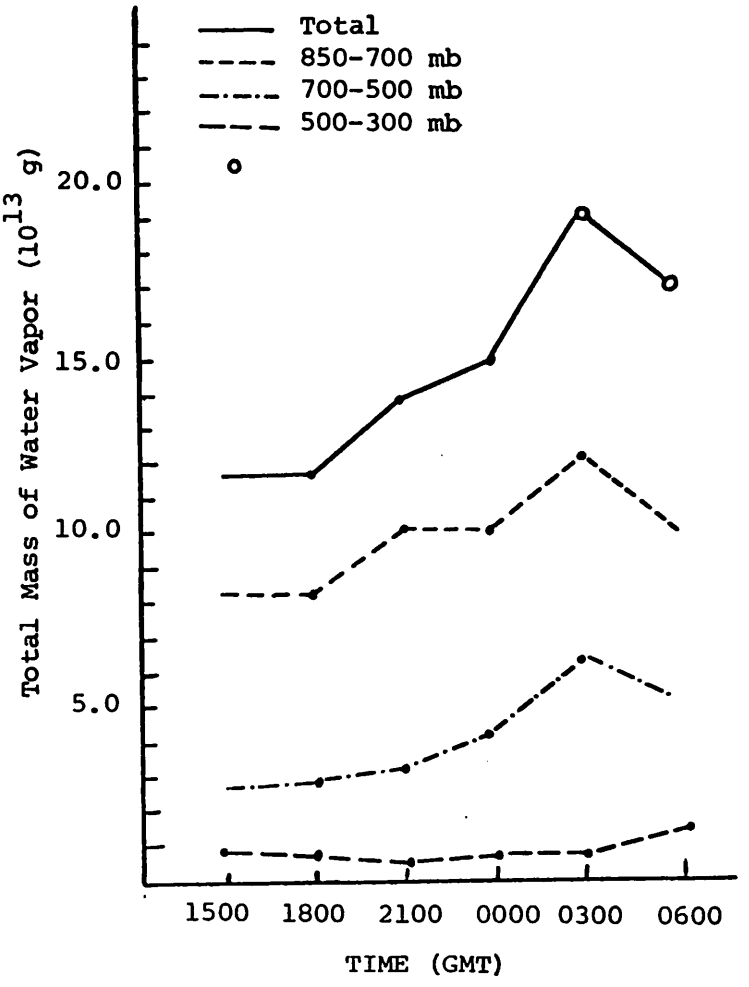

Fig. 5.4. Precipitable water within layers and the total versus time on 13-14 June 1977.

each layer is also noted for each time sounding data were available. Radar summaries indicate the development of several isolated echoes north of the Texas HIPLEX area at 0300 GMT on 14 June 1977, followed by movement and dissipation over the Texas HIPLEX area by 0600 GMT 14 June 1977.

Figure 5.4 shows that the greatest amount of water vapor is between 850-700 mb, averaging 68% of the integrated total. Once convective activity approaches the Texas HIPLEX area, the exchange of moisture aloft increases. This is due to the upward vertical motion and large vertical transports observed in lower layers. These results also agree with earlier results that vertical and horizontal transports tend to "store" water vapor in upper layers prior to convection. The contributions of moisture above 500 mb is small (i.e. less than 10% of the integrated total), and remains nearly constant at all sounding times throughout the day. Once dissipation occurs at 0600 GMT, a gain of moisture is observed only in this layer, due to upward vertical motion and vertical transports aloft.

It has been shown that the magnitude of each term in Eq. 5.1 affects the magnitude of the residual term. A comparison of each term with the residual term shows the relative importance of each term for cases of convection and nonconvection. A ratio of each term to the residual term provides a relative percent of that term comprising the residual term. These ratios were computed for 9 days during the summer of 1976 over the Texas HIPLEX area. The nine days analyzed were divided into two groups: (1) Days when no activity occurred within the network at any time (Table 5.1); and (2) days when activity occurred within the network (Table 5.2). Comparison of Tables 5.1 and 5.2 show that the horizontal transport term is the dominant term of the budget especially during days with convective activity. In cases of sustained convection and precipitation, which were observed on 10-11 July and 11-12 July 1976, the horizontal transport term becomes larger in magnitude than the residual term. Surface observations for 8-9 July 1976 report stratus overcast throughout the day, and might explain such a large ratio of the horizontal transport term. The vertical transport term ratio remains nearly constant for both convective and nonconvective cases, comprising only about 10% of the residual term. The local rate-of-change term ratio decreases significantly during days containing convection, and this might be attributed to the saturation of the air, especially on days of sustained convection and precipitation. These results reinforce the importance of horizontal moisture convergence as a source term for the formation and maintenance of convective activity.

Table 5.1. Ratio of water budget terms to the residual for days during summer 1976 containing no activity over the Texas HIPLEX area.

Date	$\int_S \frac{(q\rho_a \vec{V}_2)_n \, dS}{R} \times 100$	$\int_S \frac{(q\rho_a w)\, dA}{R} \times 100$	$\int_V \frac{\partial}{\partial t} \frac{(q\rho_a)}{R} \, dv \times 100$
JN 25-26	53%	31%	16%
JN 28-29	52%	-14%	62%
JL 1-2	30%	33%	37%
JL 8-9	99%	-23%	24%
Total	58%	7%	35%

Table 5.2. Average ratio of water budget terms to the residual for "activity days" during summer 1976 over the Texas HIPLEX area.

Date	$\int_S \frac{(q\rho_a \vec{V}_2)_n \, dS}{R} \times 100$	$\int_S \frac{(q\rho_a w)\, dA}{R} \times 100$	$\int_V \frac{\partial}{\partial t} \frac{(q\rho_a)}{R} dv \times 100$
JN 22-23	54%	33%	13%
JN 23-24	103%	12%	-15%
JL 3-4	78%	1%	21%
JL 10-11	108%	6%	-14%
JL 11-12	105%	-1%	-4%
TOTAL	90%	11%	-1%

The preliminary results obtained using 1977 data are encouraging and support the validity of the results obtained using 1976 data. Work is still in progress toward evaluating the water budget in three layers (850-700, 700-500, and 500-300 mb) for all the terms in Eq. 5.1 to determine the relative importance of each of these layers during various stages of convection. It is hoped that this analysis will help determine the level at which precipitation originates, and the factors affecting precipitation formation.

The validity of the moisture budget has been shown by a comparison of the actual precipitation recorded to the precipitation computed from the residual term of Eq. 5.1 for two days during the summer of 1976. These results were presented in a progress report for February 1978. Further work is planned using rainfall data on selected days during the summer of 1977.

It has been shown that the terms of Eq. 5.1 vary depending upon the conditions which exist. By determining average values for each of the water budget terms during convective and nonconvective conditions a comparison should reveal any "characteristics" associated with these terms. It is planned to utilize both 1976 and 1977 data to compute these average values and construct average profiles for each respective case. Such a study should determine any significant differences between conditions of convection and nonconvection.

The complete water budget has been evaluated and summarized on a daily basis, indicating results observed during each day. Comparison of days with

similar conditions might reveal certain common characteristics. Using 1976 and 1977 data, it is planned to classify each day as follows: (1) Nonconvective--days when no significant activity was observed over the Texas HIPLEX area; (2) Line--days involving the development and/or movement of a line of convective activity over the Texas HIPLEX area; (3) Isolated cell--Days involving the development and/or movement of scattered isolated convective cells over the Texas HIPLEX area; and (4) Sustained convection--Days involving persistent patterns of strong convection and precipitation observed at most sounding times over the Texas HIPLEX area. After classification, each category will be compared and analyzed further to determine any similarities for the several types of convective activity. It is hoped that such a study might reveal the moisture sources, and therefore the energy sources associated with each case, so a better understanding of convective activity will be achieved.

6. DEVELOPMENT OF ENTRAINMENT MODEL

A model for entrainment into cumulus clouds is nearing completion but not yet ready to be scrutinized by the scientific community. The model is based on the concept that entrainment accounts for differences between the mass budgets of convective storms and their mesoscale environment. Equations have been developed for these mass budgets. The derivation of an equation for entrainment requires some assumptions regarding the interaction of the clouds with their environment. These assumptions and conditions necessary to write the model in equation form are being investigated. As soon as the equations are finalized they will be evaluated by computer to establish their apparent validity.

7. PREPARATION OF RADAR ECHO CHARTS FROM MIDLAND RADAR DATA

PPI radar overlays were obtained from the Midland NWS station, coded on a grid as was done for the 1976 data, keypunched, and contour charts of the coded data prepared by computer. The data were coded at 1-hr intervals for every hour of the day and for all days on which convective activity occurred during the mesoscale experiment period. These charts will be included in the 1978 mesoscale data report between 1500 and 0300 GMT for each day on which convective activity occurred.

TEXAS A&M UNIVERSITY

"A RADAR-ECHO CLIMATOLOGY FOR SOUTHERN HIPLEX"

The final report "A Radar-Echo Climatology for Southern HIPLEX," prepared by Dr. Dennis M. Driscoll, was submitted to the Department during this reporting period and concludes the work performed under HIPLEX contracts 14-70032 and 14-80004. The Department published the study as Technical Report LP-64 and transmitted thirty (30) copies to the Bureau on September 6, 1978.

TEXAS TECH UNIVERSITY

"SATELLITE STUDIES IN THE

TEXAS HIPLEX AREA"

The following report was prepared by Dr. Jerry Jurica and submitted to the Department as the interim progress report on the Texas HIPLEX satellite studies for the reporting period 1 April - 30 September 1978.

SATELLITE STUDIES

IN THE

TEXAS HIPLEX AREA

An Interim Report
for the Period April - September 1978

Jerry Jurica
Atmospheric Science Group
Texas Tech University
Lubbock, Texas 79409

Published October 1978

Report prepared under
TDWR Contract No. 14-06-D-7587 IAC(78-79) 1055

Prepared for
Texas Department of Water Resources
Austin, Texas
and
Bureau of Reclamation, U. S. Dept. of Interior
Denver, Colorado

TABLE OF CONTENTS

LIST OF TABLES

LIST OF FIGURES

1. INTRODUCTION

The following comprises an interim progress report for Interagency Contract IAC(78-79) 1055, covering the period April-September 1978. The report is divided into three sections which follow. The first section reports on results obtained during the report period. Two subsections are included, corresponding to Tasks 1 and 2 described in the contract. The first subsection presents samples of results produced in the analysis of GOES photographic imagery for the 1977 Texas HIPLEX summer field period. The second section presents selections of analysis products derived from a detailed case study of GOES digital radiance measurements for 22 June 1976. Detailed reports covering the two projects briefly described here are in preparation and will be published soon. The second section to follow describes work to be performed during the next contract period. The third section to follow lists personnel employed on the project during this report period.

2. RESULTS OBTAINED DURING THE REPORT PERIOD

2.1 Cloud Characteristics from GOES Imagery

One of the objectives of the Texas HIPLEX satellite studies is to develop information on overall cloud characteristics for the operational area. Of interest are diurnal and spatial variations of cloud cover, numbers of clouds of different types, and cloud movement. The acquisition of data has been accomplished with the assistance of National Weather Service personnel at th Lubbock forecast office.

The project was initiated in the summer of 1976. Every available GOES photograph received at the NWS Lubbock office during the period 1 June-15 July was obtained for analysis. The area of interest is a 315 x 315 km region centered at Big Spring, Texas, as seen in Figure 1. The study area has been divided into 9 sub-areas to investigate possible spatial variations within the area. The results of the 1976 imagery analysis have been reported in an earlier report. The analysis in 1976 was restricted to the period from 1200GMT to 2400GMT (7 a.m. to 7 p.m. CDT). This was done because the infrared imagery available during nighttime hours was judged unsuitable for the derivation of quantitative information. Infrared imagery available at that time was continuous grey-scale, not of an enhanced nature.

During the 1977 Texas HIPLEX summer field period, 1 June-15 July, all available GOES imagery was again obtained from the Lubbock NWS forecast office. By this time, enhanced infra-

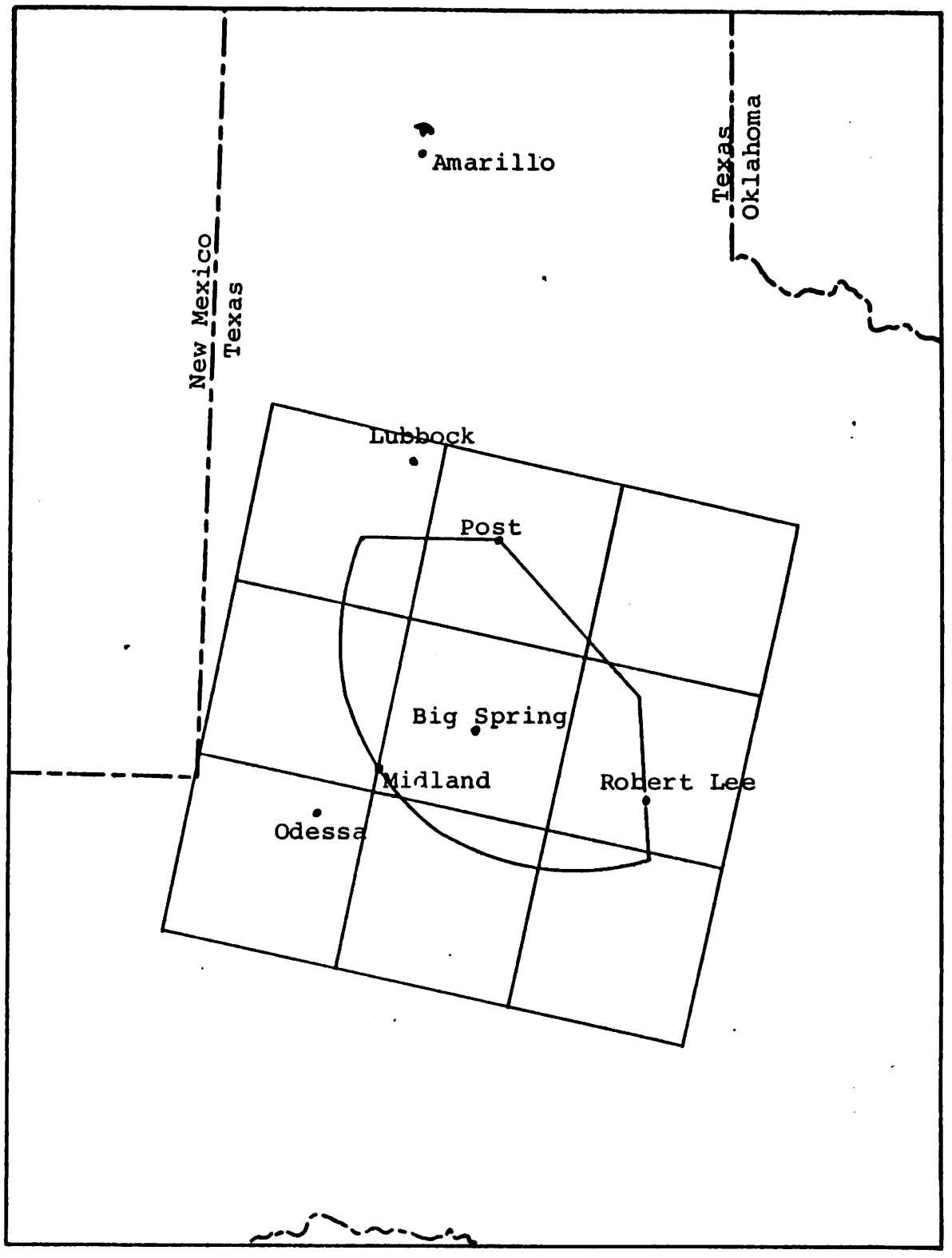

Figure 1. The area of study. The sector at the center is the Texas HIPLEX study region.

red imagery had been made available and was judged to be suitable for analysis. The infrared imagery was used to obtain cloud-top temperatures in addition to supporting some aspects of the visible imagery analysis. Further, cloud characteristics could now be obtained on a 24-hour basis. The data for 1977 have been processed and are undergoing analysis at this time. Samples of the results are presented and briefly discussed below. For purposes of comparison of 1976 to 1977 results, only the time period 1200 to 2400 GMT is treated here.

The daytime variations of percent cloud cover in the study area during June and July are shown in Figures 2 and 3, respectively. The diurnal variation during June is similar in 1976 and 1977, as seen in Figure 2. The maximum cloud cover occurs in the morning, decreases to a minimum at mid-afternoon and then increases again as evening approaches. The overall cloud cover during June was somewhat greater in 1976, averaging 28% for the 12-hour period compared to a 1977 average value of 17%.

Cloud cover in July differed greatly from June. We see in Figure 3 large percentage cloud cover in 1976, averaging 54%. The July 1977 average daytime value is only 11%. In addition, the July diurnal variation differs significantly from that of June.

Figures 4 and 5 display the diurnal variation for June and July, respectively, of the frequency of occurrence of clear skies in the Texas HIPLEX study area. The differences

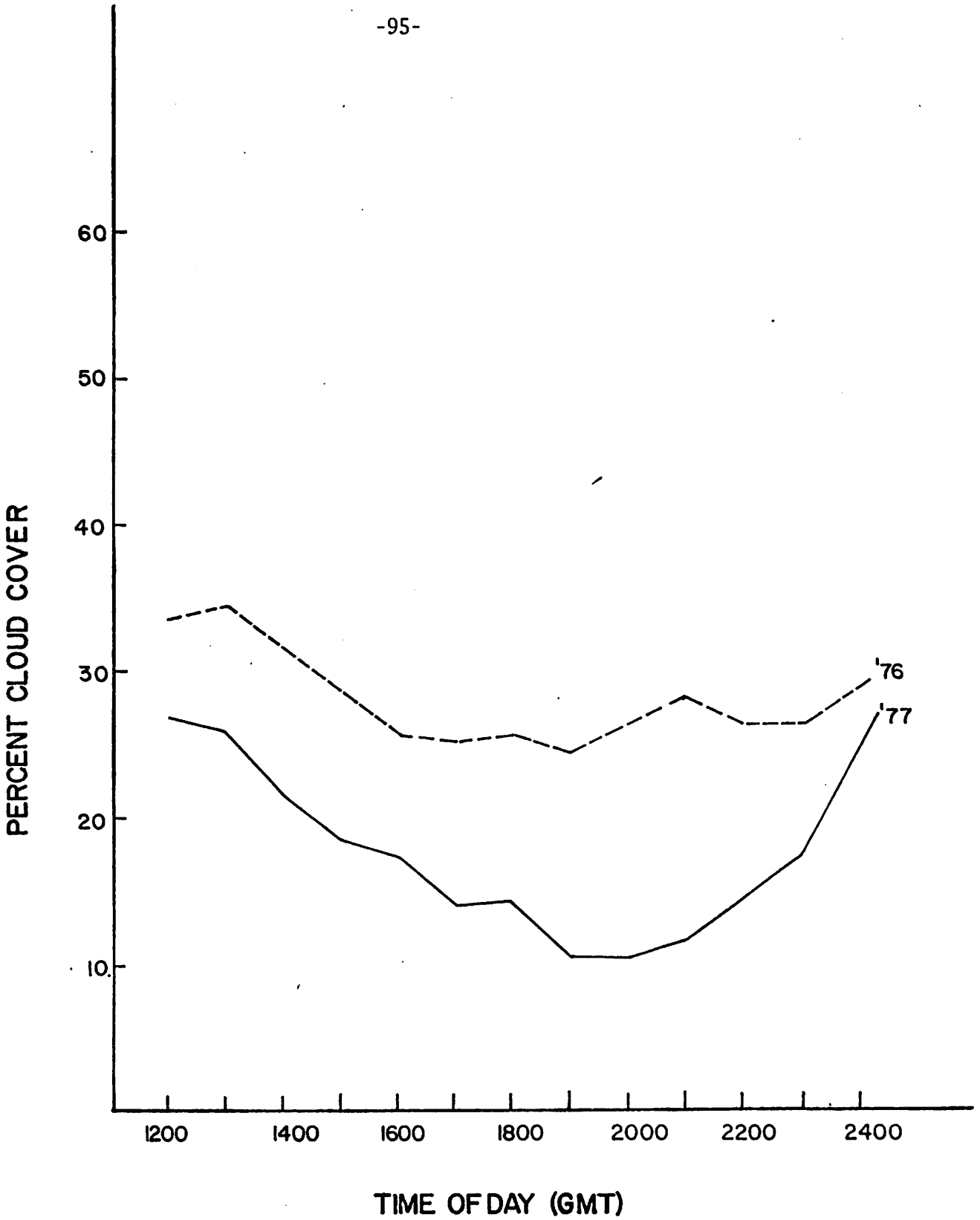

Figure 2. Diurnal variation of percent cloud cover during June for 1976 and 1977.

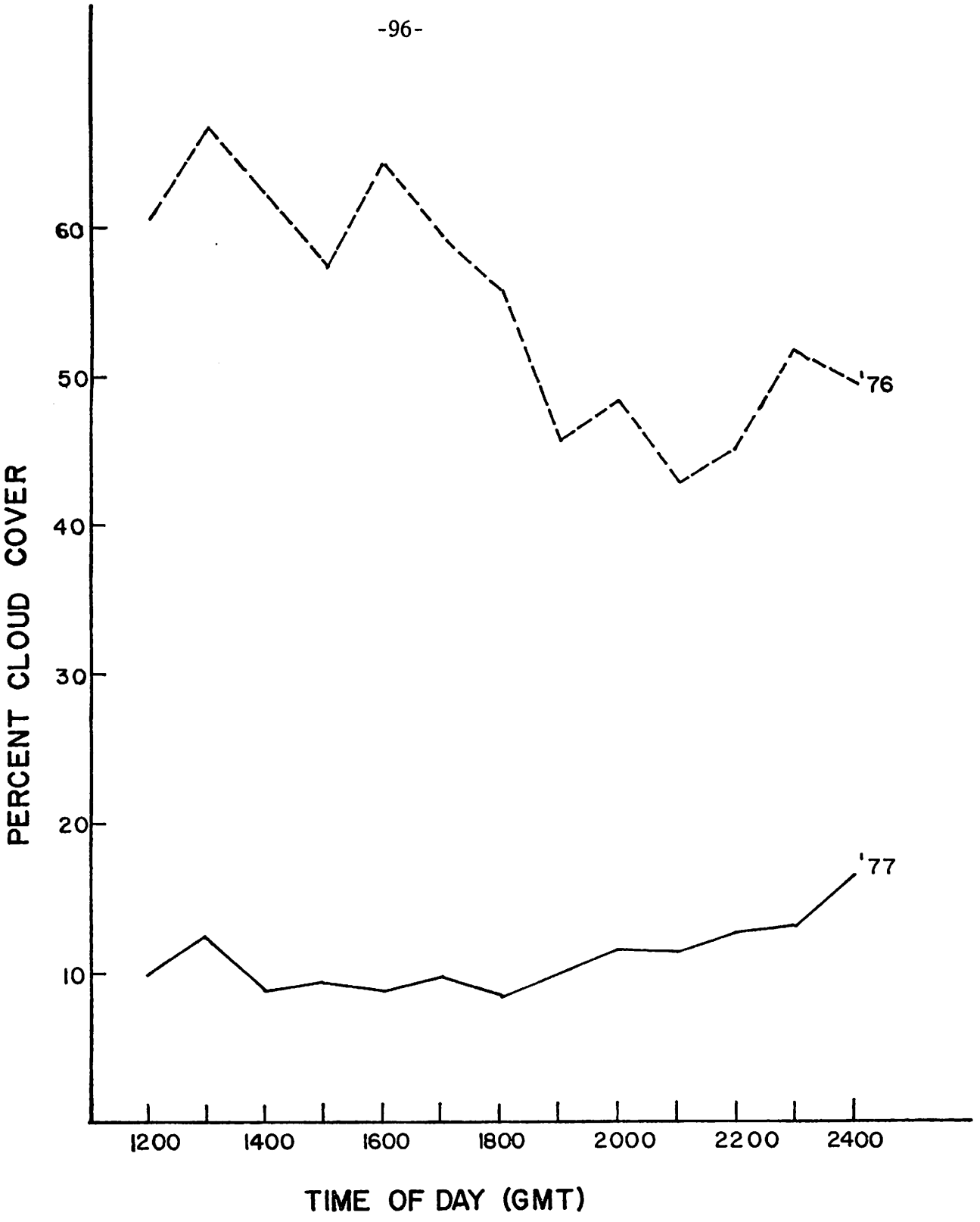

Figure 3. Diurnal variation of percent cloud cover during July for 1976 and 1977.

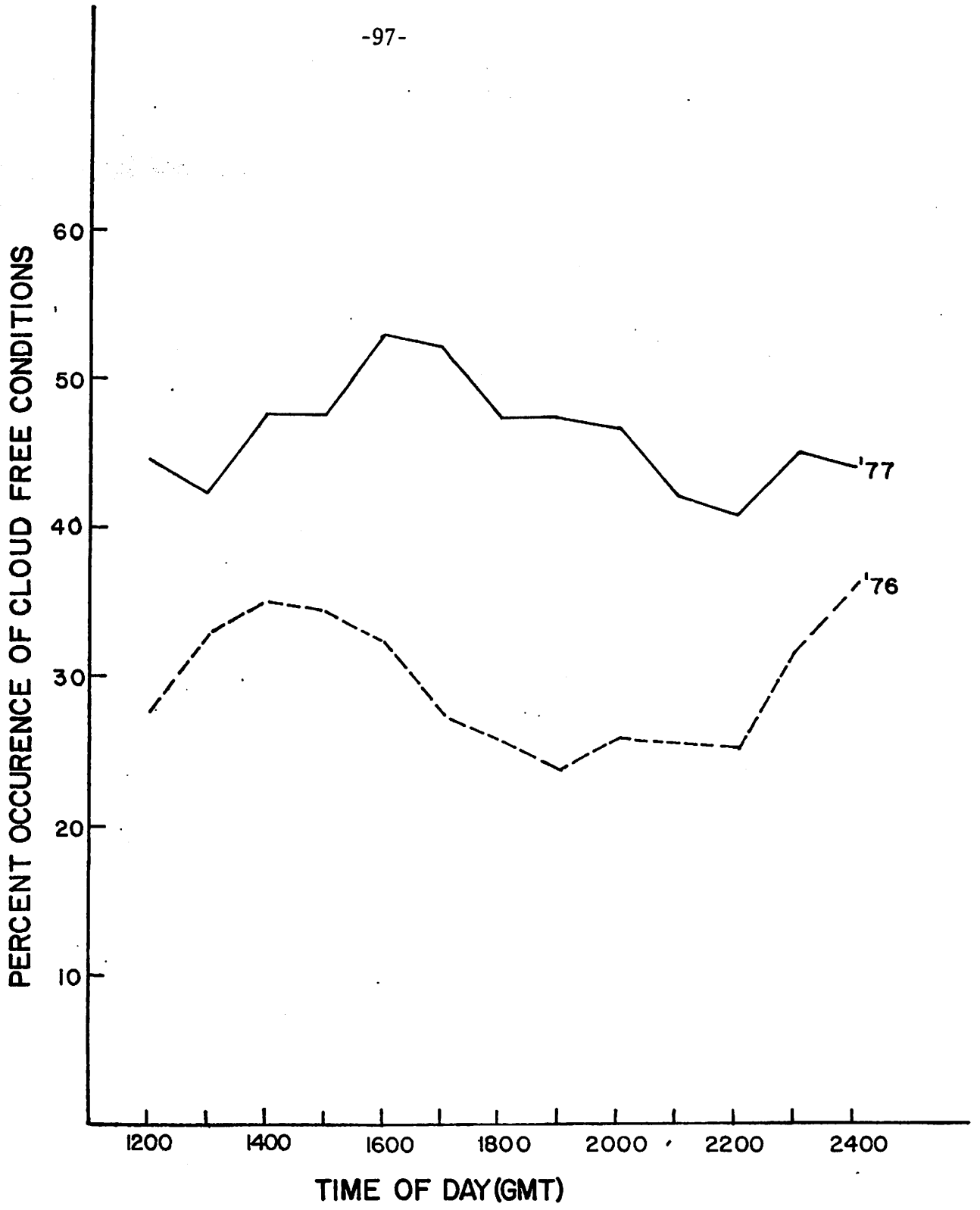

Figure 4. Diurnal variation of the frequency of occurrence of cloud free conditions during June for 1976 and 1977.

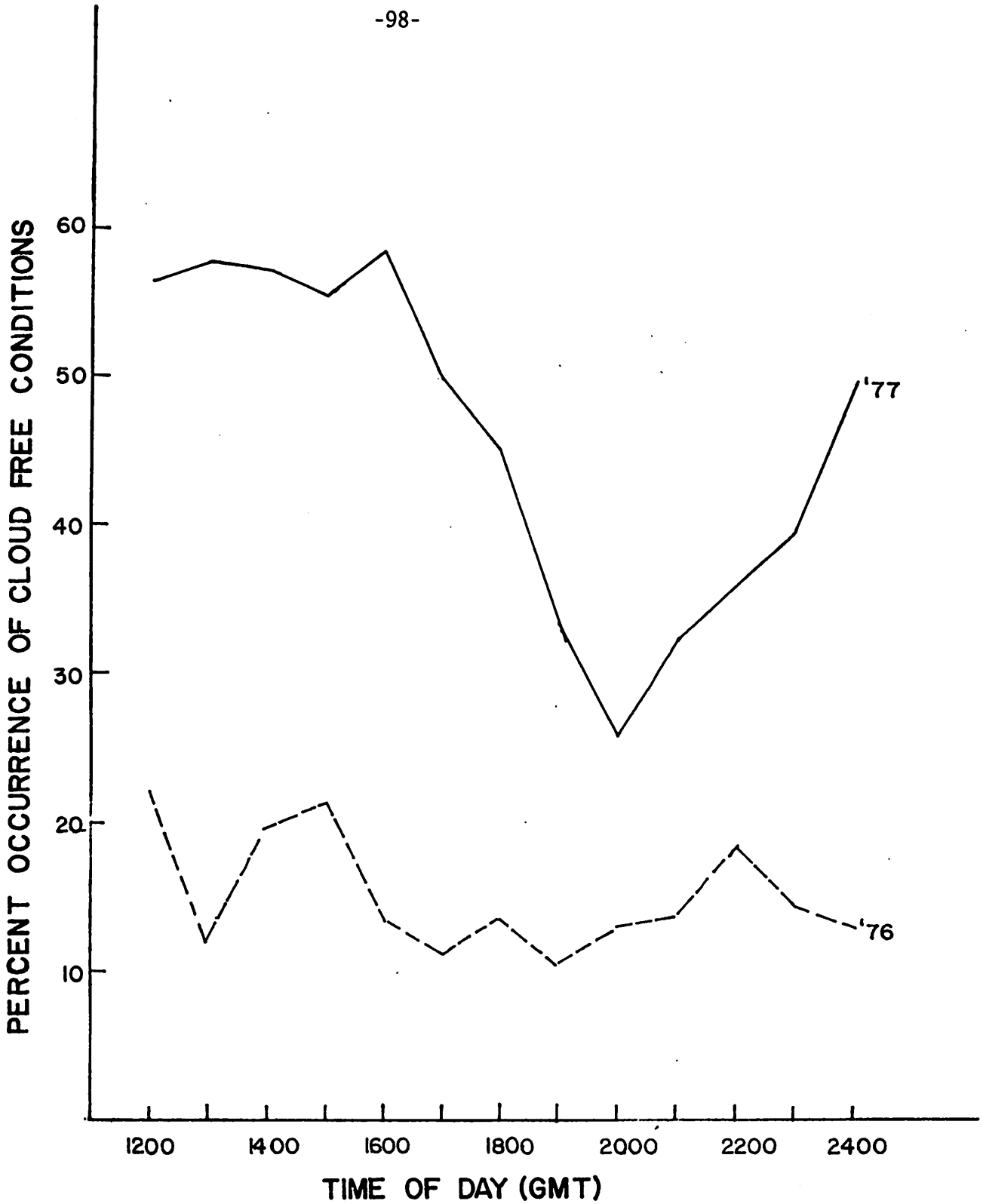

Figure 5. Diurnal variation of the frequency of occurrence of cloud free conditions during July for 1976 and 1977.

from 1976 to 1977 are seen to be much less in June than July. In Figure 4 we see that cloud free conditions are most frequent in the morning and decrease toward minimum values (absence of clear skies) in the late afternoon. Average values of the frequency of occurrence of clear skies during June daylight hours are 29% for 1976 and 46% for 1977.

Large differences exist between 1976 and 1977 in the frequency of occurrence of clear skies during July, as seen in Figure 5. In 1976 cloud free conditions occurred approximately 15% of the time, with diurnal variations being quite small. In contrast during 1977, clear skies were observed nearly 60% of the time during morning hours, with a rapid decrease to a minimum of 26% at 2000 GMT (3 p.m. CDT) followed by a return to 50% at 2400 GMT (7 p.m. CDT). The daytime average frequency of occurrence of cloud free conditions for July 1977 was 46%.

The number of isolated clouds observed in 1976 and 1977 are plotted for June and July in Figures 6 and 7, respectively. Greater counts occurred for 1977 in both months, the more dramatic difference being in July. Average values in 1976 were 2 and 1 isolated clouds within the study area for June and July, respectively. During 1977 the average number of isolated clouds was 5 for June and 14 for July. All four curves in Figures 6 and 7 display similar trends, with a morning minimum and an afternoon peak near 2000 GMT (3 p.m. CDT). However, the diurnal variation was much stronger in 1977, especially in July.

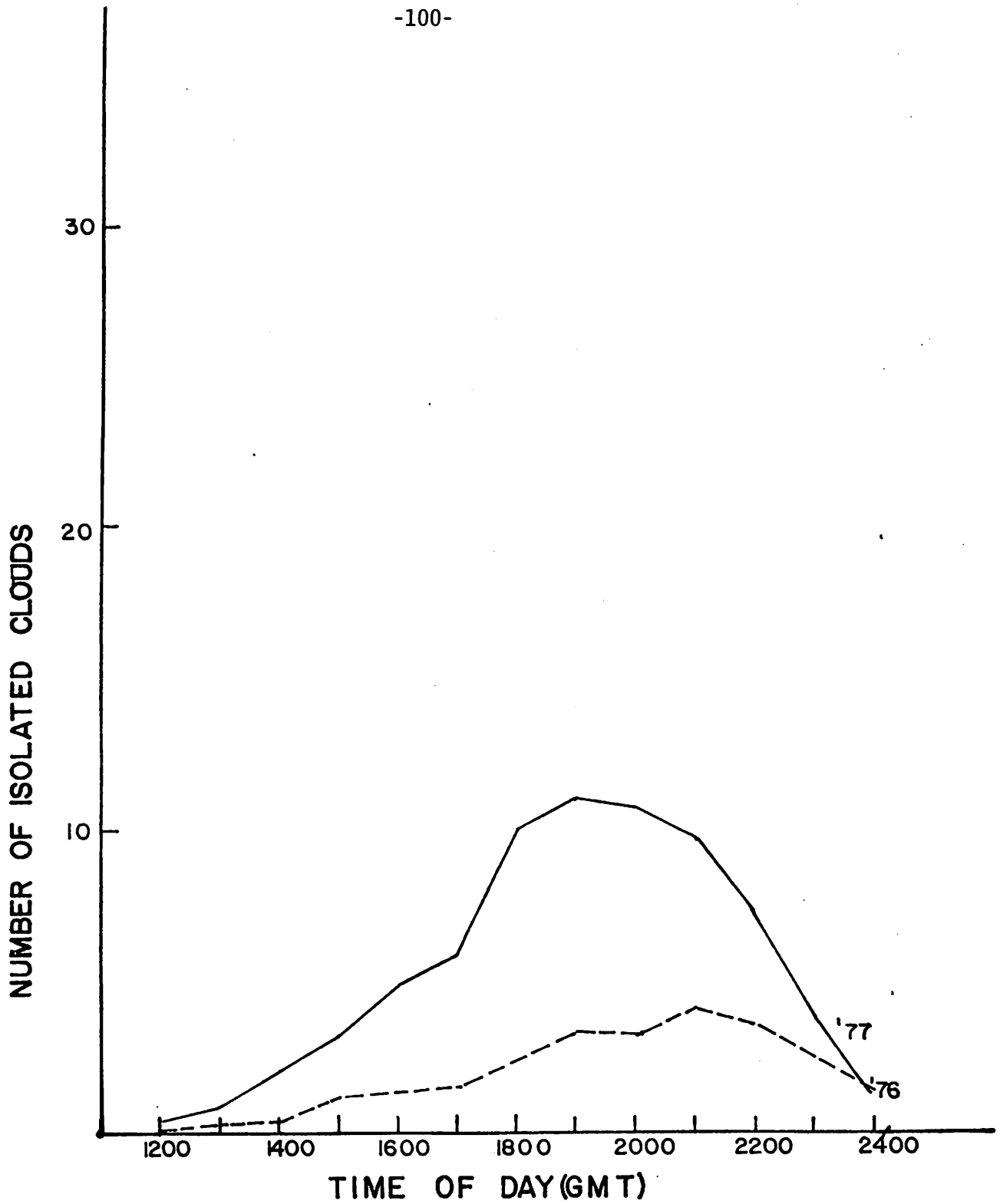

Figure 6. Diurnal variation of the number of isolated clouds during June for 1976 and 1977.

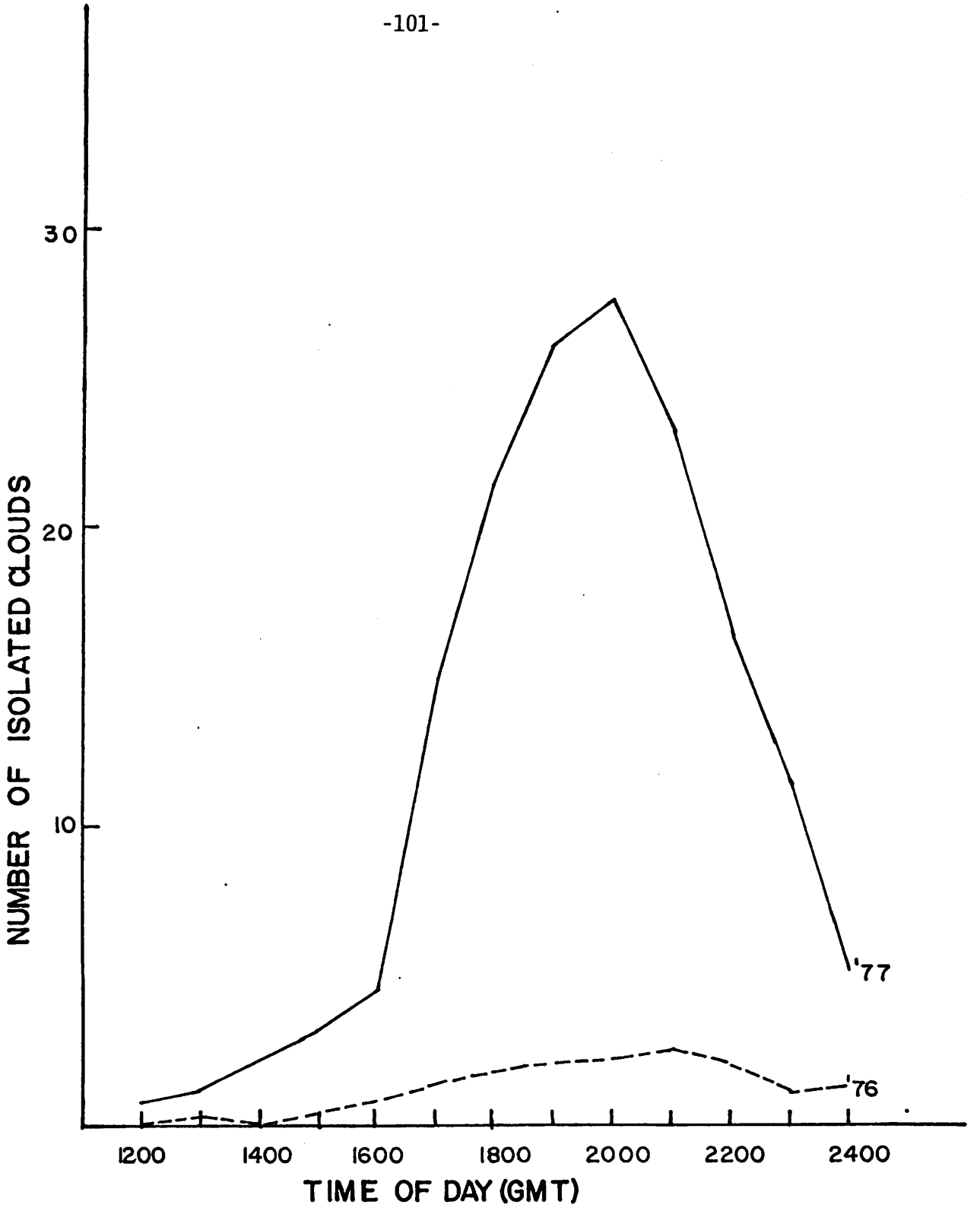

Figure 7. Diurnal variation of the number of isolated clouds during July for 1976 and 1977.

The interpretation of the results described above is taking place at the present time. In addition, data have been extracted from GOES imagery for the Texas HIPLEX 1978 summer field program and are being prepared for analysis at this time. The results for 1976, 1977 and 1978 will then be analysed as a unit and the results will be published as a technical report.

2.2 22 June 1976 Radiance Data Case Study

A major objective of the Texas HIPLEX satellite study is the development of techniques to extract quantitative information from the radiance data provided by the GOES observation systems. Radiance data have the advantage of eliminating the subjectivity involved in visually interpreting photographic imagery. A disadvantage of the radiance data is the huge amount of data which must be dealt with. A specific goal of the project is to determine efficient data processing methods which permit important cloud properties to be extracted from the data.

The date 22 June 1976 has been selected as an intensive case study. This case has been used for the development of analysis methods to treat the radiance data. Some examples are discussed here of an analysis technique to determine cloud amount, distribution, temperature, height and movement through the utilization of sets of simultaneous satellite visible (VIS) and infrared (IR) data and the corresponding radiosonde data.

To identify the cloud cover region, a brightness critical value to distinguish cloud from underlying non-cloud background is found as a primary factor in this study. Because the solar radiation is attenuated by scattering and absorption in proportion to the path length traveled through the atmosphere, Beer's law has been applied to obtain these critical values as they vary with solar zenith angle.

Using the brightness critical value as an input variable, a cloud summary computer program was utilized to obtain the following statistical results for this study:

1. Percentage of cloud cover and mean brightness of cloud and non-cloud for the entire region.
2. Size, maximum brightness, mean and standard deviation of brightness and location of brightness and geometric center of every individual cloud.
3. Tables of the frequency distribution of brightness of individual data points, the frequency distribution of mean brightness of clouds and the frequency distribution of cloud size.

All of these data sources are used to analyze the cloud properties and patterns and their variations with time.

The ability to deal with a visible representation of the data is very helpful when handling large quantities of data. A most valuable support to the effort has been provided by Colorado State University (CSU), which had made available to our project the video imaging system of the Department of Atmospheric Science. Both VIS and IR data

on June 22 were preprocessed and reformated from raw data tapes. Through the use of the CSU All Digital Video Imaging System for Atmospheric Research (ADVISAR), it was found that extremely bright or dark single data points or lines, which could be identified as bad data or bad data lines, existed in some of the VIS radiance data sets. They represented less than 0.5% of the data in the most of the data sets. At 2245 GMT of June 22 and 0045 GMT of June 23, the existence of several bad data lines increased the percentage of bad data to 1% of the data set. In order to correct these bad data values, every data point was compared with its surrounding data values. If the data value in question deviated by more than a prescribed amount from the surrounding points, it was replaced by their average. A bad data line was corrected using an interpolated value which was obtained from the data points in the lines above and below the bad line. In this manner, good VIS data sets were produced for subsequent analysis.

The VIS and IR digital data arrays for the 315 x 315 km target region are 216 x 216 and 27 x 54 arrays, respectively. The VIS and IR sensors of GOES simultaneously scan the earth in a west to east direction, then step down and scan again. However, there is a misalignment of the VISSR sensors that causes an east-west offset between the VIS and IR data.

In order to investigate the offset and accurately match VIS and IR data, two data sets of identical resolution are required. A 216 x 216 array was considered by dividing each IR data point into 32 new IR subareas. Although this method

would have kept all of the original VIS information, the extensive interpolation of IR data did not produce patterns consistent with the VIS data. In addition, use of the highly expanded IR data set would have greatly increased computation times for analysis. A 54 x 54 array size was also considered to produce an identical resolution for VIS and IR data sets. In this method, every new VIS data area would replace a 4 x 4 array of original VIS data points. This method was tested by producing computer-generated cloud patterns from the 54 x 54 VIS data array. However, it was found that many of the smaller clouds disappeared, indicating that the combination of this many data points resulted in too much smoothing. As a result of the testing, an array of 108 x 108 pixels (approximately 3 km resolution) was selected as the optimum array size. This resolution involves both compressing the VIS data and stretching the IR data. It was found that no cloud information was lost while compressing the VIS data to an 108 x 108 array. By utilizing the interpolation technique described below, the stretch 108 x 108 IR array was able to reproduce cloud patterns which agreed well with the higher resolution VIS data.

The corrected and coregistered sets of VIS and IR data were used to produce computer-generated plots of the cloud patterns in the study area. These are shown in Figure 8. Plotted are objectively determined contours of cloud top temperature derived from the IR data and albedo derived from the VIS data.

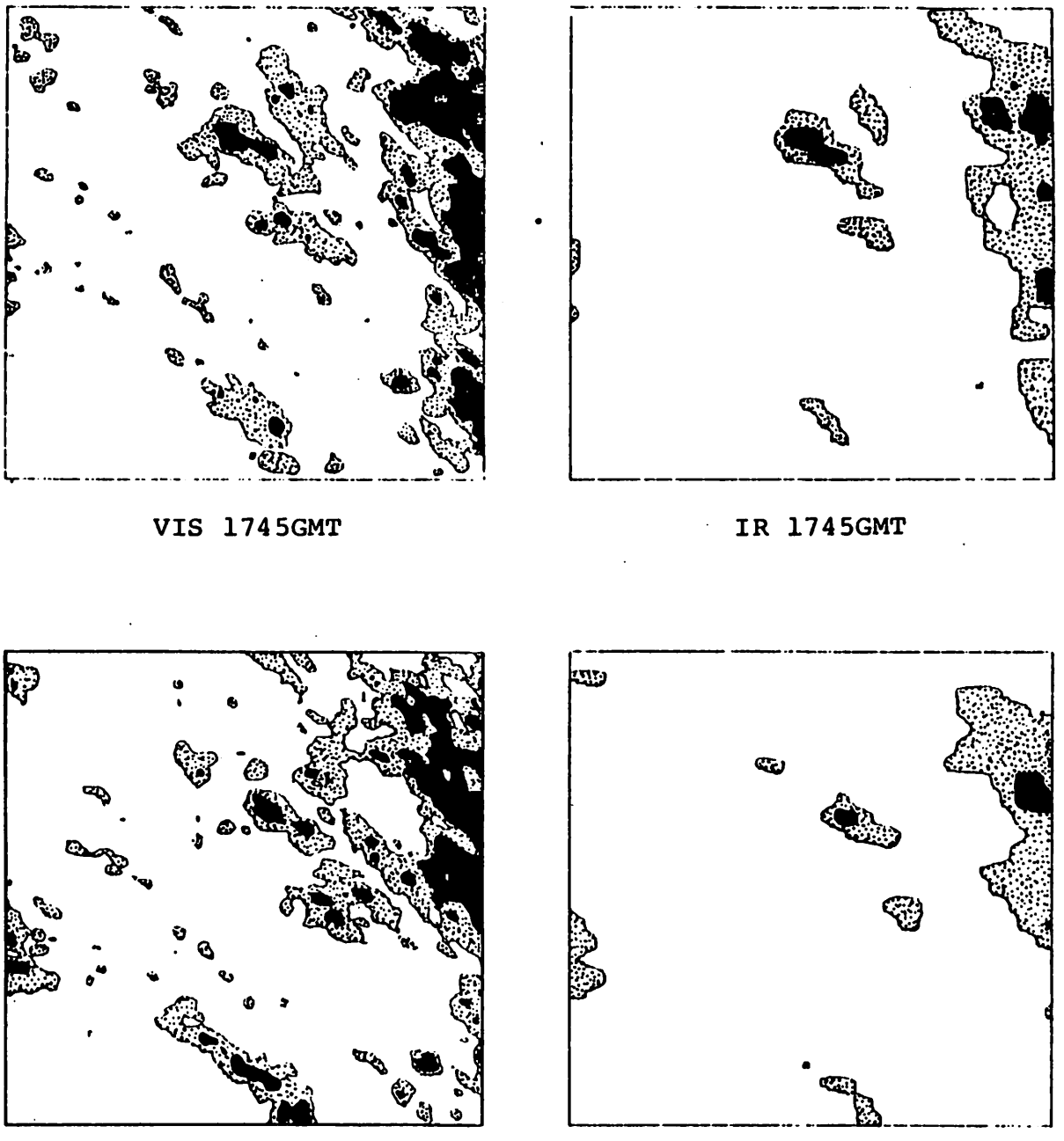

Figure 8. Computer-generated plots of visible and infrared radiance patterns from 1745 GMT on 22 June 1976 to 0115 GMT on 23 June,1976.

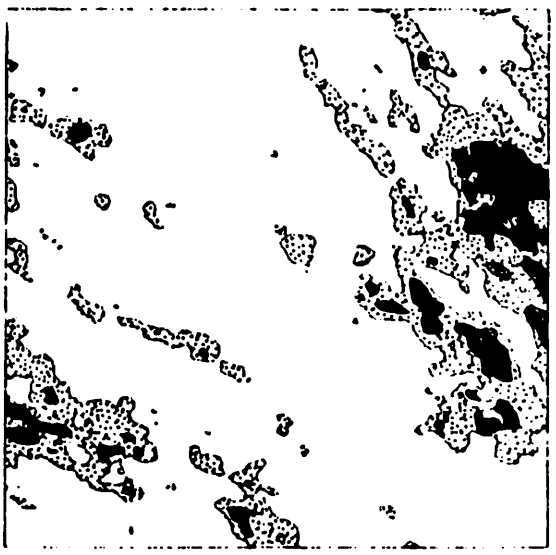

VIS 1845GMT

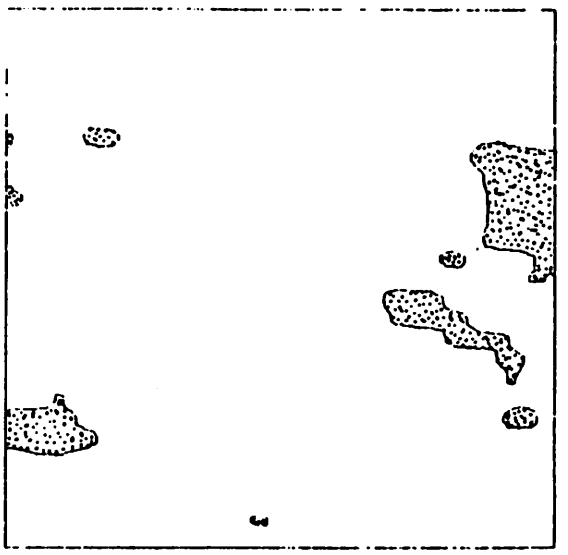

IR 1845GMT

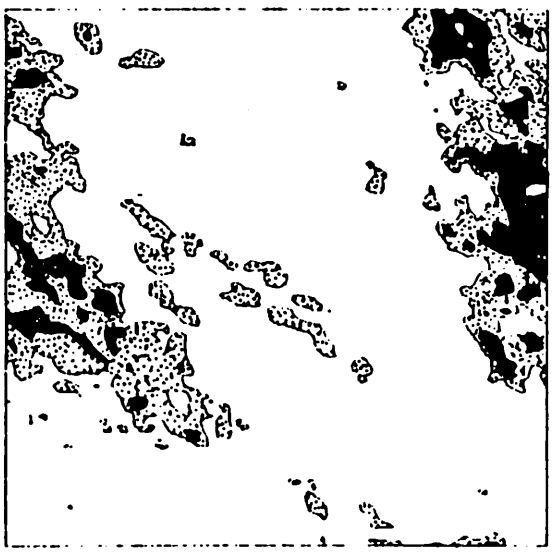

VIS 1945GMT

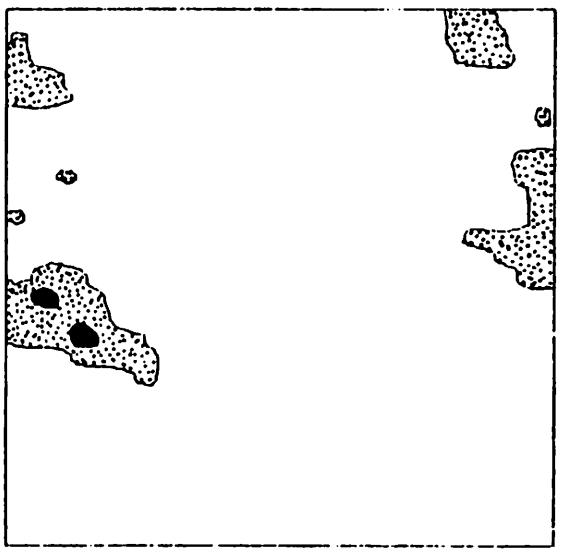

IR 1945GMT

Figure 8 continued.

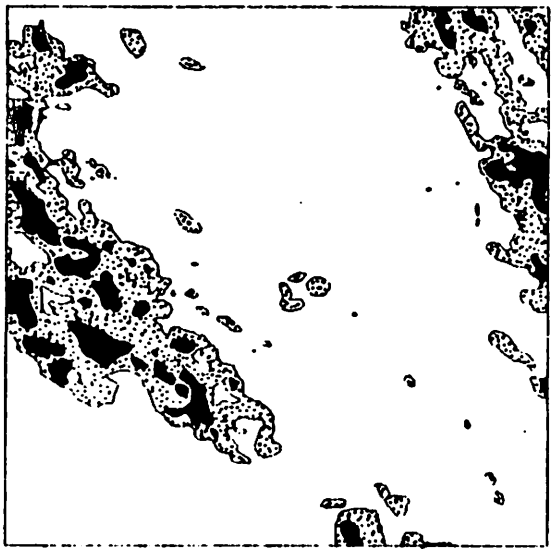

VIS 2015GMT

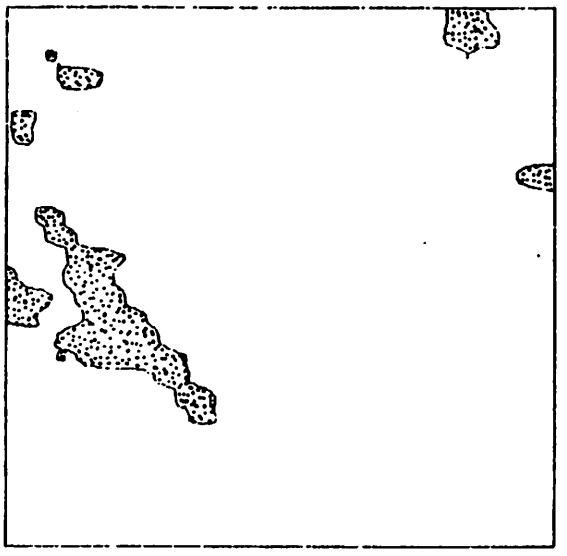

IR 2015GMT

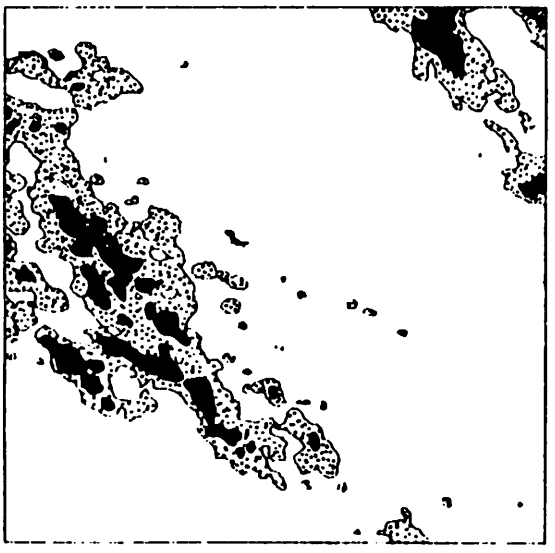

VIS 2045GMT

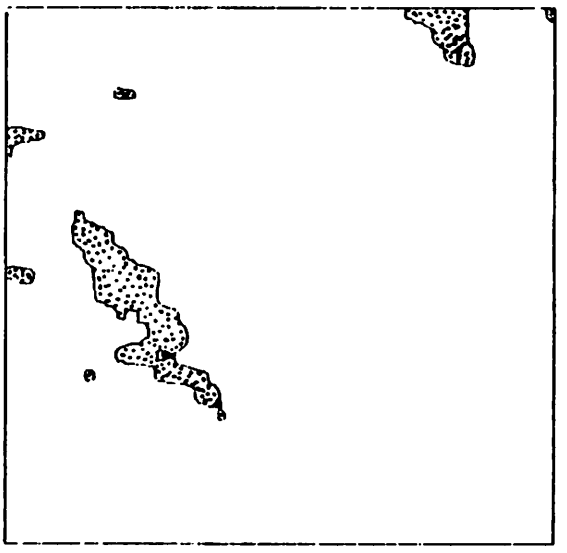

IR 2045GMT

Figure 8 continued.

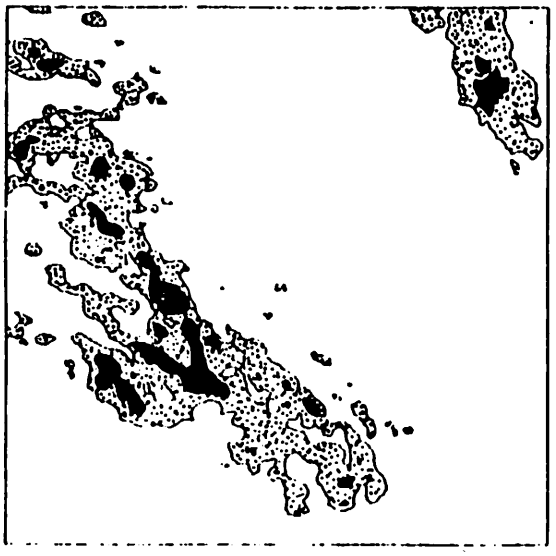

VIS 2115GMT

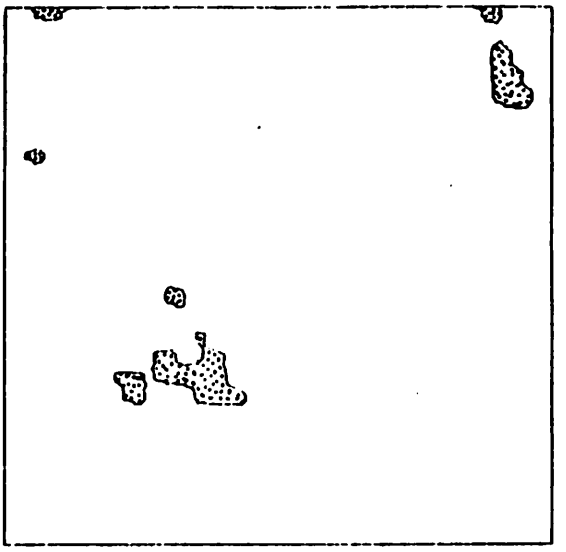

IR 2115GMT

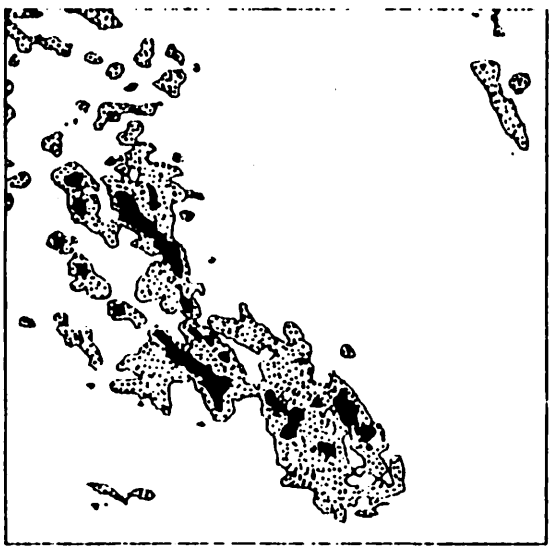

VIS 2145GMT

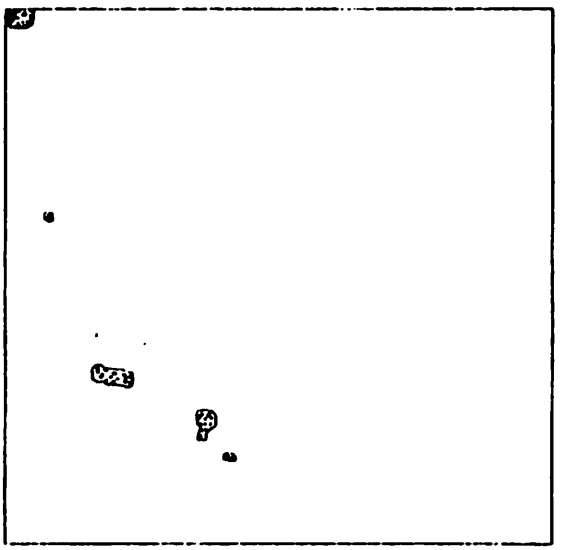

IR 2145GMT

Figure 8 continued.

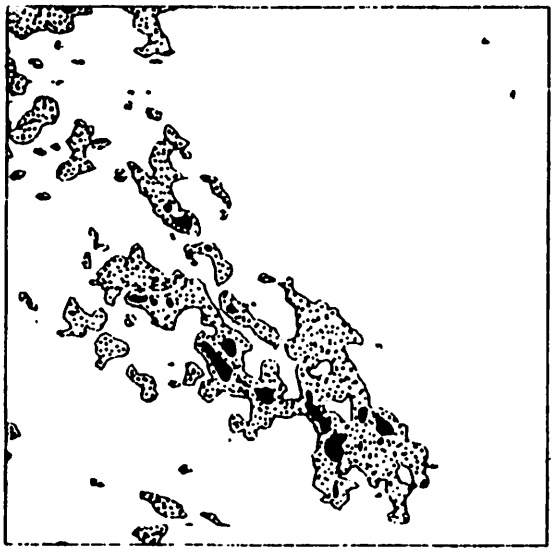

VIS 2215GMT

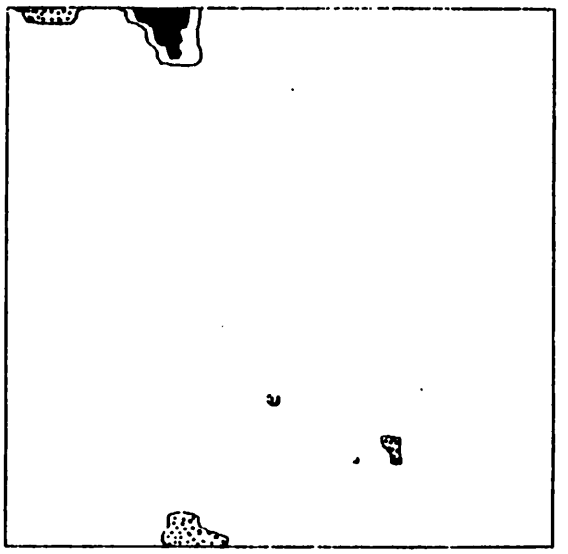

IR 2215 GMT

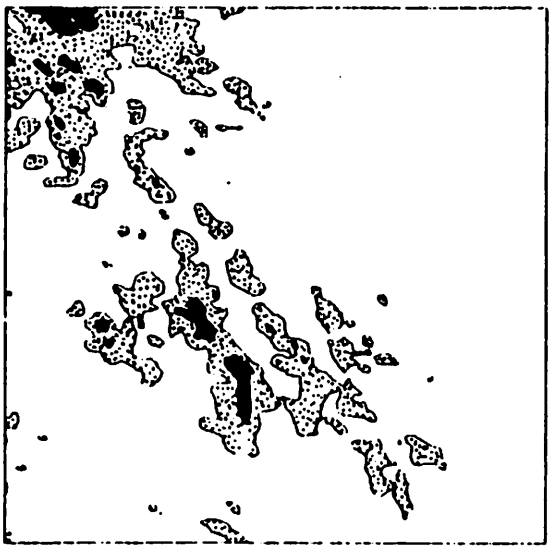

VIS 2245GMT

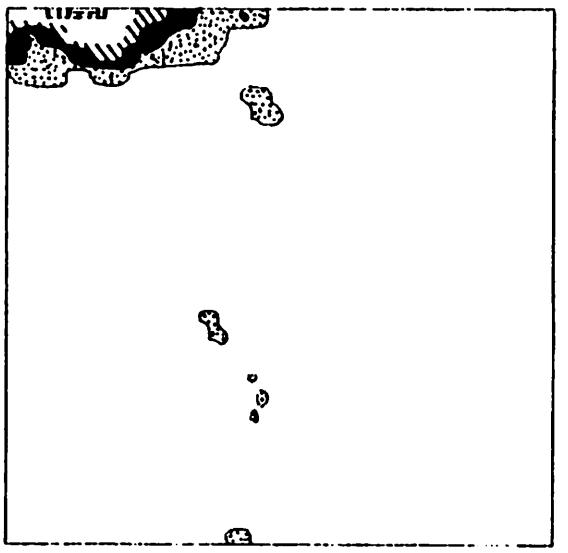

IR 2245GMT

Figure 8 continued.

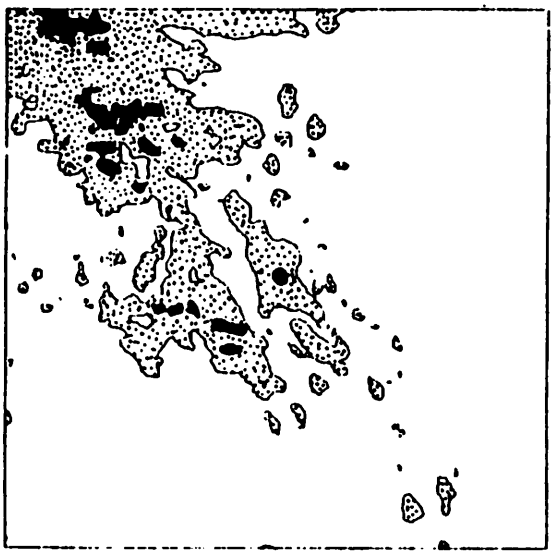

VIS 2315 GMT

IR 2315GMT

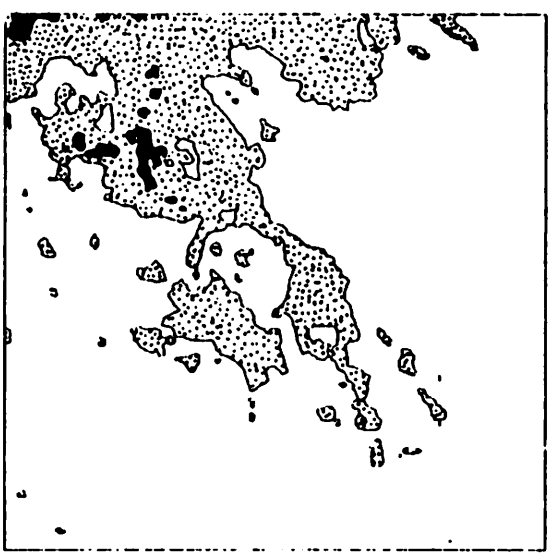

VIS 2345GMT

IR 2345GMT

Figure 8 continued.

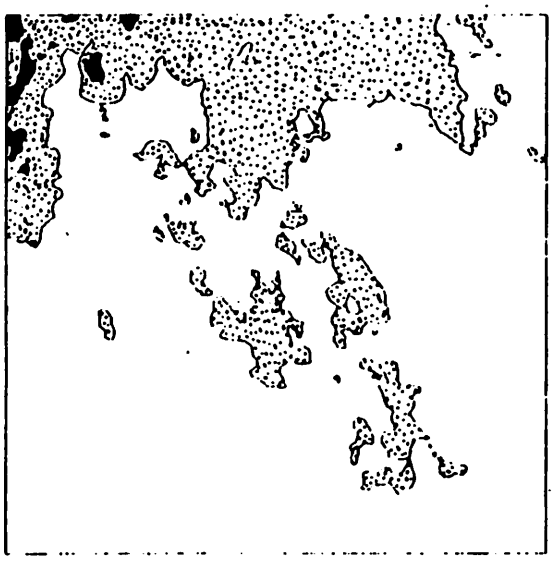

VIS 0015GMT

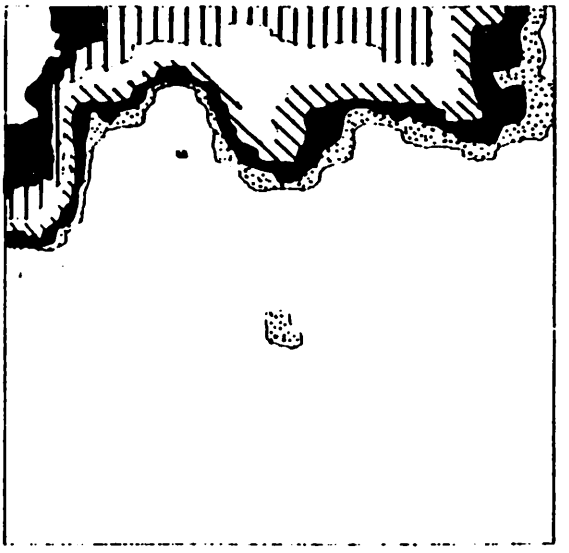

IR 0015GMT

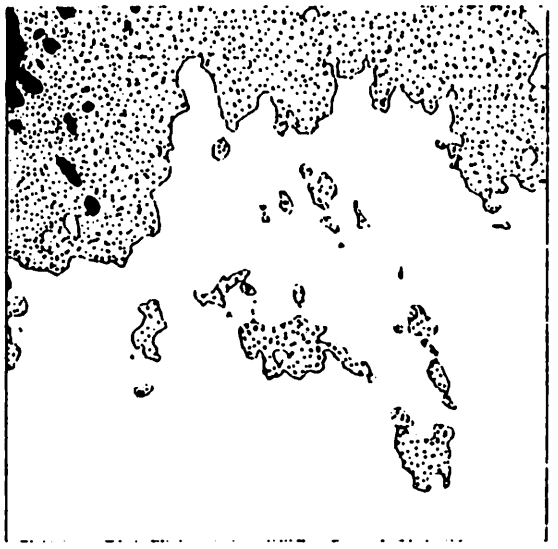

VIS 0045GMT

IR 0045GMT

Figure 8 continued.

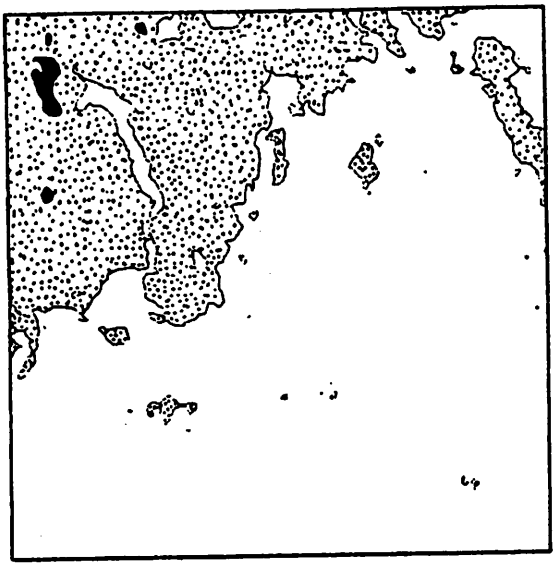

VIS 0115GMT

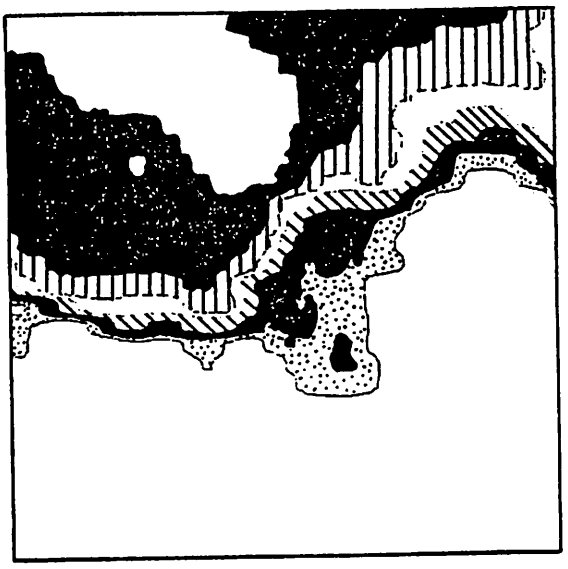

IR 0115GMT

VIS scale

Albedo

0.0 to 0.2

0.2 to 0.4

0.4 to 0.6

0.6 to 0.8

IR scale

Temperature (C)

T > 0

0 ≥ T > -10

-10 ≥ T > -20

-20 ≥ T > -30

-30 ≥ T > -40

-40 ≥ T > -50

-50 ≥ T > -60

-60 ≥ T

Figure 8 continued.

One item of interest is the extent of agreement between cloud parameters derived from the radiance data and those obtained by a visual inspection of the corresponding imagery. Comparisons of numbers of clouds and percentage of cloud cover obtained from satellite radiance data and from imagery are shown in Table 1. It shows a close agreement in cloud covereage detected from radiance data and imagery. Since the photographic imagery study area was divided into nine subareas, the percent cloud cover was observed for each subarea. Therefore, a more accurage estimate of percent cloud cover over the total area was obtained by averaging these nine values. The largest deviation of cloud coverage between radiance data and imagery, three percent difference, appears at 2100 GMT. At other times only one or two percent difference is observed. Table 1 also shows that the numbers of isolated and area clouds in radiance data study are close to that in imagery study at 1800 GMT and 1900 GMT. At 2000 GMT more isolated clouds were detected from the imagery. Through the ADVISAR display system, two large cluster-area clouds were found on each of the cloud pictures at 1945 GMT and 2015 GMT located in the eastern and western parts of the study area: one located from Hamlin to Robert Lee, the other located from Seminole to Midland. The size of these two cluster-area clouds are about 4,000 digital points, with an equivalent circular diameter of 100 kilometers. The computer cloud summary program will treat several small clouds as a large cluster-area cloud as long as those clouds are linked to-

Table 1. Comparison of numbers of clouds and percentage of cloud cover from satellite radiance data and imagery

Time	Total number of cloud		Number of medium isolated convective cloud		Number of large isolated and widespread cloud		Percentage of cloud cover (%)	
	Radiance Data	Imagery	Radiance Data	Imagery	Radiance Data	Imagery	Radiance Data	Imagery
1800	53	57	29	33	24	24	25	26
1900	46	45	26	25	20	20	25	27
2000	36	50	19	32	17	18	24	23
2100	34	29	24	15	10	14	20	23
2200	45	27	28	13	17	14	17	19

gether at even a few boundary points. However, in the imagery study these clouds will be separated as several isolated clouds. Therefore, more isolated clouds were detected from imagery at 2000 GMT. By 2200 GMT the solar zenith angle had increased to 45 degrees; the brightness of the scene was reduced and fewer small isolated clouds could be distinguished from the underlying surface in the photographic imagery. However, by adjusting the critical value to distinguish cloud from non-cloud the cloud summary program overcame this problem, leading to greater numbers of isolated clouds than cloud seen in the imagery.

The satellite IR radiance data can be utilized to determine features of cloud growth by relating temperature to height through rawinsonde data. The minimum temperature observed in the temperature plots for the different times can be used to show the highest cloud top in the entire data set at that time. The maximum temperature corresponding to the minimum IR data value, can represent the surface temperature for the data set. Both the maximum and minimum temperatures and the corresponding height of the maximum cloud top are shown in Table 2 throughout the study period. The minimum temperature at 1745 GMT corresponded to an extensive thunderstorm entering the study area (Figure 8). The thunderstorm rapidly moved southward from Lubbock into the study area. Meanwhile, the visible low clouds located in the west central portion of the area dissipated gradually. By 0045 GMT, the thunderstorm dominated most of the cloud cover region with a maximum

Table 2. Maximum and minimum temperatures, the height of the maximum cloud top and the corresponding maximum radar echo height in the study region.

Time (GMT)	Max. temp. (°C)	Min. temp (°C)	Max. cloud top (m)	(ft)	Radar echo top (ft)
June 22					
1745	37	-17	7,300	24,000	22,000
1815	36	-16	7,100	23,500	
1845	39	-10	6,200	20,500	20,000
1945	40	-13	6,700	22,000	*
2015	40	- 9	6,100	20,000	
2045	39	- 6	5,700	18,500	*
2115	39	-10	6,200	20,500	
2145	37	-16	7,100	23,500	*
2215	36	-18	7,400	24,500	
2245	34	-40	10,300	34,000	30,000
2315	34	-42	10,700	35,000	
2345	32	-51	12,000	39,500	42,000
June 23					
0015	32	-70	15,100	49,500	
0045	30	-70	15,100	49,500	46,000
0115	28	-68	14,700	48,000	

* no echo height was reported within this study region.

cloud top height of 15,100 m (49,500 ft.). The last column of Table 2 shows the maximum height of the radar precipitation echo obtained from NWS radar summary charts. No precipitation was indicated in this study area from 1945 GMT to 2145 GMT. At all other times the echo heights agree well with the satellite measurements. Since the satellite measurements are for the cloud top and radar detects the echo of the precipitation region, it is reasonable that satellite cloud top heights will be higher than the radar echo tops.

The complete analysis of results from this first case study is now being prepared for publication, and will appear as a separate technical report in the near future.

3. WORK PLANNED FOR THE NEXT REPORT PERIOD

The next report period extends from October 1978 to March 1979. Three primary tasks are planned for this time, and are briefly described below:

1. Completion of the satellite data report for the Texas HIPLEX 1978 summer field program. As mentioned above satellite imagery have been obtained for the 1978 field program. The imagery for each Mesoscale Operational Day will be compiled into a report documenting the observed cloud structure.
2. Completion of a 1976, 1977, 1978 comparative imagery study. Subsequent to the conversion of 1978 imagery into computer-compatible data, an analysis of cloud characteristics will be performed. The results from the three individual years will be combined and inter-annual comparisons will be made.
3. Analysis of 1977 Radiance Data. Two primary tasks will be pursued. The first consists of the development of an objective analysis technique to determine cloud movement from the translation of brightness centers within the cloud pattern. Secondly, time histories of individual cells will be constructed from coincident data sets of satellite, rainfall and radar measurements.

4. PERSONNEL

The following personnel worked on the project during the report period.

Jerry Jurica	Principal Investigator, Director of Project
Shih-Cheng Chao	Graduate Research Assistant, Imagery Data Analysis
Shwe-Yi Chi	Graduate Research Assistant, Radiance Data Analysis
Donald Williams	Research Associate, Computer Programming

TEXAS TECH UNIVERSITY
"RAINCELL CLIMATOLOGY FOR THE HIPLEX
SOUTHERN REGION"

The final report "Precipitation Climatology for the HIPLEX Southern Region," written by Dr. Donald R. Haragan, was submitted to the Department during the reporting period and concludes the work performed under contract 14-70029. The Department published the study as Technical Report LP-63 and transmitted thirty (30) copies of the report to the Bureau on August 1, 1978.

The following report entitled "Raincell Climatology For The HIPLEX Southern Region" was prepared by Dr. Haragan and concludes the work performed under contract 14-80050.

RAINCELL CLIMATOLOGY FOR THE HIPLEX SOUTHERN REGION

A Summary Report
for the period June 1, 1978 - August 31, 1978

by
Donald R. Haragan
Atmospheric Science Group
Texas Tech University
Lubbock, Texas 79409

Report prepared under

TDWR Contract No. 14-180000 IAC(78-79) 1336

Prepared for
Texas Department of Water Resources
Austin, Texas

Introduction

This report is a summary of work completed under TDWR Contract No. 14-80050. The nature of the research is such that the work is on-going. Technical reports will be issued as required by the contract at such time as individual research units are completed.

Much of the work performed under the present contract involved the development of data-processing soft-ware to be used in analyzing rainfall amounts. This report will summarize the work done but will not include all of the data which were reduced and analyzed. These data will be provided to users on request in any of the formats available.

Task 1

Task 1 involved the acquisition of all rainfall data (15-minute resolution) for the HIPLEX Southern region on magnetic tape from the Bureau of Reclamation. Data are now on hand for 1976, 1977 and 1978. Techniques have been developed which will present the rainfall data in the following formats:

1) tabulation of 15-minute rainfall amounts
2) tabulation of hourly rainfall amounts
3) tabulation of storm-total rainfall amounts
4) tabulation of daily rainfall amounts
5) network maps depicting any of the above.

Task 2

Task 2 required the identification of all periods when precipitation was recorded within the HIPLEX raingage network. These periods have been tabulated and are presented in Tables 1 and 2 for the 1976 and 1977 seasons respectively. It should be noted that not all periods exhibited significant

Table 1

BEGINNING AND ENDING TIMES OF RAINFALL PERIODS
FOR THE ENTIRE 1976 TEXAS HIPLEX RAINGAGE NETWORK

BEGINNING OF RAINFALL PERIOD	END OF RAINFALL PERIOD
MAY 1, 1976 - 9:15 P.M.	MAY 1, 1976 - 9:30 P.M.
MAY 2, 1976 - 4:00 P.M.	MAY 2, 1976 - 4:15 P.M.
MAY 3, 1976 - 5:15 P.M.	MAY 3, 1976 - 5:30 P.M.
MAY 4, 1976 - 1:00 P.M.	MAY 4, 1976 - 1:15 P.M.
MAY 5, 1976 - 4:45 A.M.	MAY 5, 1976 - 9:00 A.M.
MAY 5, 1976 - 11:00 A.M.	MAY 5, 1976 - 11:45 A.M.
MAY 5, 1976 - 12:30 P.M.	MAY 5, 1976 - 12:45 P.M.
MAY 5, 1976 - 2:15 P.M.	MAY 5, 1976 - 2:45 P.M.
MAY 6, 1976 - 10:45 A.M.	MAY 6, 1976 - 11:00 A.M.
MAY 6, 1976 - 3:00 P.M.	MAY 6, 1976 - 3:15 P.M.
MAY 7, 1976 - 6:15 A.M.	MAY 7, 1976 - 6:30 A.M.
MAY 7, 1976 - 6:45 A.M.	MAY 7, 1976 - 10:00 A.M.
MAY 7, 1976 - 10:45 A.M.	MAY 7, 1976 - 11:15 A.M.
MAY 7, 1976 - 12:30 P.M.	MAY 7, 1976 - 12:45 P.M.
MAY 7, 1976 - 4:15 P.M.	MAY 7, 1976 - 4:30 P.M.
MAY 7, 1976 - 9:30 P.M.	MAY 7, 1976 - 9:45 P.M.
MAY 9, 1976 - 1:30 P.M.	MAY 9, 1976 - 1:45 P.M.
MAY 9, 1976 - 4:30 P.M.	MAY 9, 1976 - 4:45 P.M.
MAY 10, 1976 - 2:15 P.M.	MAY 10, 1976 - 2:30 P.M.
MAY 10, 1976 - 2:45 P.M.	MAY 10, 1976 - 3:00 P.M.
MAY 10, 1976 - 4:00 P.M.	MAY 10, 1976 - 4:15 P.M.
MAY 11, 1976 - 2:30 P.M.	MAY 11, 1976 - 2:45 P.M.
MAY 12, 1976 - 8:30 A.M.	MAY 12, 1976 - 8:45 A.M.
MAY 12, 1976 - 11:00 A.M.	MAY 12, 1976 - 11:15 A.M.
MAY 12, 1976 - 4:00 P.M.	MAY 12, 1976 - 4:15 P.M.
MAY 14, 1976 - 3:30 P.M.	MAY 14, 1976 - 3:45 P.M.
MAY 16, 1976 - 8:30 A.M.	MAY 16, 1976 - 8:45 A.M.
MAY 20, 1976 - 6:00 A.M.	MAY 20, 1976 - 7:00 A.M.
MAY 20, 1976 - 10:15 A.M.	MAY 20, 1976 - 10:30 A.M.
MAY 20, 1976 - 3:00 P.M.	MAY 20, 1976 - 3:15 P.M.
MAY 20, 1976 - 5:15 P.M.	MAY 20, 1976 - 5:30 P.M.
MAY 20, 1976 - 7:30 P.M.	MAY 20, 1976 - 9:00 P.M.
MAY 20, 1976 - 10:00 P.M.	MAY 20, 1976 - 10:15 P.M.
MAY 20, 1976 - 11:30 P.M.	MAY 20, 1976 - 11:45 P.M.
MAY 21, 1976 - 2:00 P.M.	MAY 21, 1976 - 2:15 P.M.
MAY 21, 1976 - 5:45 P.M.	MAY 21, 1976 - 6:00 P.M.
MAY 22, 1976 - 8:30 A.M.	MAY 22, 1976 - 8:45 A.M.
MAY 23, 1976 - 4:30 P.M.	MAY 23, 1976 - 4:45 P.M.

MAY 24, 1976 - 7:30 P.M.	MAY 24, 1976 - 9:00 P.M.
MAY 25, 1976 - 2:45 P.M.	MAY 25, 1976 - 4:00 P.M.
MAY 25, 1976 - 4:15 P.M.	MAY 25, 1976 - 4:30 P.M.
MAY 25, 1976 - 5:00 P.M.	MAY 25, 1976 - 5:30 P.M.
MAY 26, 1976 - 10:45 A.M.	MAY 26, 1976 - 11:00 A.M.
JUNE 1, 1976 - 3:45 P.M.	JUNE 1, 1976 - 4:00 P.M.
JUNE 4, 1976 - 9:30 A.M.	JUNE 4, 1976 - 10:45 A.M.
JUNE 4, 1976 - 7:15 P.M.	JUNE 4, 1976 - 9:00 P.M.
JUNE 5, 1976 - 2:15 P.M.	JUNE 5, 1976 - 4:00 P.M.
JUNE 5, 1976 - 6:45 P.M.	JUNE 5, 1976 - 8:30 P.M.
JUNE 6, 1976 - 6:30 A.M.	JUNE 6, 1976 - 7:15 A.M.
JUNE 6, 1976 - 3:15 P.M.	JUNE 6, 1976 - 3:30 P.M.
JUNE 7, 1976 - 3:00 P.M.	JUNE 7, 1976 - 4:30 P.M.
JUNE 11, 1976 - 5:30 P.M.	JUNE 11, 1976 - 6:15 P.M.
JUNE 12, 1976 - 11:00 A.M.	JUNE 12, 1976 - 11:15 A.M.
JUNE 18, 1976 - 11:00 A.M.	JUNE 18, 1976 - 11:15 A.M.
JUNE 21, 1976 - 11:30 A.M.	JUNE 21, 1976 - 11:45 A.M.
JUNE 21, 1976 - 9:45 P.M.	JUNE 22, 1976 - 12:00 A.M.
JUNE 22, 1976 - 1:45 A.M.	JUNE 22, 1976 - 2:00 A.M.
JUNE 22, 1976 - 9:45 A.M.	JUNE 22, 1976 - 10:00 A.M.
JUNE 22, 1976 - 3:00 P.M.	JUNE 22, 1976 - 3:15 P.M.
JUNE 22, 1976 - 8:00 P.M.	JUNE 22, 1976 - 8:30 P.M.
JUNE 22, 1976 - 8:45 P.M.	JUNE 22, 1976 - 11:15 P.M.
JUNE 22, 1976 - 11:30 P.M.	JUNE 23, 1976 - 12:00 A.M.
JUNE 23, 1976 - 1:00 A.M.	JUNE 23, 1976 - 3:30 A.M.
JUNE 23, 1976 - 4:00 A.M.	JUNE 23, 1976 - 4:15 A.M.
JUNE 23, 1976 - 5:15 P.M.	JUNE 23, 1976 - 5:30 P.M.
JUNE 23, 1976 - 7:00 P.M.	JUNE 23, 1976 - 8:30 P.M.
JUNE 26, 1976 - 8:45 P.M.	JUNE 26, 1976 - 9:15 P.M.
JUNE 30, 1976 - 10:30 A.M.	JUNE 30, 1976 - 11:00 A.M.
JUNE 30, 1976 - 1:00 P.M.	JUNE 30, 1976 - 1:30 P.M.
JUNE 30, 1976 - 3:00 P.M.	JUNE 30, 1976 - 3:15 P.M.
JUNE 30, 1976 - 3:30 P.M.	JUNE 30, 1976 - 3:45 P.M.
JUNE 30, 1976 - 9:15 P.M.	JUNE 30, 1976 - 9:45 P.M.
JULY 2, 1976 - 8:00 P.M.	JULY 2, 1976 - 9:45 P.M.

JULY 2, 1976 - 10:00 P.M.
JULY 2, 1976 - 11:00 P.M.
JULY 3, 1976 - 2:45 A.M.
JULY 3, 1976 - 7:30 A.M.
JULY 3, 1976 - 8:15 A.M.
JULY 3, 1976 - 2:45 P.M.
JULY 3, 1976 - 4:15 P.M.
JULY 4, 1976 - 3:00 P.M.
JULY 4, 1976 - 7:30 P.M.
JULY 5, 1976 - 3:15 A.M.
JULY 5, 1976 - 7:45 A.M.
JULY 5, 1976 - 10:30 A.M.
JULY 5, 1976 - 11:45 A.M.
JULY 5, 1976 - 2:45 P.M.
JULY 7, 1976 - 3:15 P.M.
JULY 8, 1976 - 11:30 A.M.
JULY 9, 1976 - 11:00 A.M.
JULY 9, 1976 - 12:00 P.M.
JULY 9, 1976 - 1:15 P.M.
JULY 9, 1976 - 2:45 P.M.
JULY 10, 1976 - 4:30 A.M.
JULY 10, 1976 - 5:15 A.M.
JULY 10, 1976 - 9:45 A.M.
JULY 10, 1976 - 10:45 A.M.
JULY 10, 1976 - 11:45 A.M.
JULY 10, 1976 - 12:15 P.M.
JULY 10, 1976 - 1:15 P.M.
JULY 10, 1976 - 4:15 P.M.
JULY 10, 1976 - 11:00 P.M.
JULY 11, 1976 - 1:00 A.M.
JULY 11, 1976 - 1:45 A.M.
JULY 11, 1976 - 4:45 A.M.
JULY 11, 1976 - 2:45 P.M.
JULY 11, 1976 - 3:45 P.M.
JULY 11, 1976 - 4:45 P.M.
JULY 11, 1976 - 6:00 P.M.
JULY 11, 1976 - 8:30 P.M.
JULY 11, 1976 - 10:00 P.M.
JULY 11, 1976 - 11:15 P.M.

JULY 2, 1976 - 10:15 P.M.
JULY 3, 1976 - 1:00 A.M.
JULY 3, 1976 - 7:15 A.M.
JULY 3, 1976 - 7:45 A.M.
JULY 3, 1976 - 2:30 P.M.
JULY 3, 1976 - 4:00 P.M.
JULY 3, 1976 - 5:15 P.M.
JULY 4, 1976 - 3:15 P.M.
JULY 4, 1976 - 11:00 P.M.
JULY 5, 1976 - 3:30 A.M.
JULY 5, 1976 - 8:15 A.M.
JULY 5, 1976 - 10:45 A.M.
JULY 5, 1976 - 2:15 P.M.
JULY 5, 1976 - 3:00 P.M.
JULY 7, 1976 - 3:30 P.M.
JULY 8, 1976 - 11:45 A.M.
JULY 9, 1976 - 11:15 A.M.
JULY 9, 1976 - 1:00 P.M.
JULY 9, 1976 - 2:30 P.M.
JULY 9, 1976 - 3:00 P.M.
JULY 10, 1976 - 5:00 A.M.
JULY 10, 1976 - 6:00 A.M.
JULY 10, 1976 - 10:00 A.M.
JULY 10, 1976 - 11:00 A.M.
JULY 10, 1976 - 12:00 P.M.
JULY 10, 1976 - 12:45 P.M.
JULY 10, 1976 - 3:45 P.M.
JULY 10, 1976 - 8:00 P.M.
JULY 11, 1976 - 12:45 A.M.
JULY 11, 1976 - 1:15 A.M.
JULY 11, 1976 - 4:30 A.M.
JULY 11, 1976 - 2:15 P.M.
JULY 11, 1976 - 3:15 P.M.
JULY 11, 1976 - 4:30 P.M.
JULY 11, 1976 - 5:30 P.M.
JULY 11, 1976 - 6:30 P.M.
JULY 11, 1976 - 8:45 P.M.
JULY 11, 1976 - 10:15 P.M.
JULY 11, 1976 - 11:30 P.M.

JULY 12, 1976 - 12:15 A.M.
JULY 12, 1976 - 1:15 A.M.
JULY 12, 1976 - 10:30 A.M.
JULY 12, 1976 - 11:00 A.M.
JULY 12, 1976 - 12:45 P.M.
JULY 12, 1976 - 3:30 P.M.
JULY 13, 1976 - 1:30 A.M.
JULY 13, 1976 - 2:30 A.M.
JULY 13, 1976 - 9:30 A.M.
JULY 13, 1976 - 5:30 P.M.
JULY 14, 1976 - 1:45 A.M.
JULY 14, 1976 - 2:45 A.M.
JULY 14, 1976 - 5:00 A.M.
JULY 14, 1976 - 5:30 A.M.
JULY 14, 1976 - 6:30 A.M.
JULY 14, 1976 - 10:45 A.M.
JULY 14, 1976 - 12:15 P.M.
JULY 14, 1976 - 1:30 P.M.
JULY 14, 1976 - 8:45 P.M.
JULY 14, 1976 - 9:45 P.M.

JULY 15, 1976 - 1:15 A.M.
JULY 15, 1976 - 2:30 A.M.
JULY 15, 1976 - 4:15 A.M.
JULY 15, 1976 - 7:30 A.M.
JULY 15, 1976 - 10:15 A.M.
JULY 15, 1976 - 12:30 P.M.
JULY 15, 1976 - 1:00 P.M.
JULY 15, 1976 - 3:30 P.M.
JULY 15, 1976 - 5:45 P.M.
JULY 16, 1976 - 8:00 A.M.
JULY 16, 1976 - 11:15 A.M.
JULY 16, 1976 - 1:15 P.M.

JULY 12, 1976 - 12:30 A.M.
JULY 12, 1976 - 9:45 A.M.
JULY 12, 1976 - 10:45 A.M.
JULY 12, 1976 - 12:00 P.M.
JULY 12, 1976 - 1:00 P.M.
JULY 12, 1976 - 3:45 P.M.
JULY 13, 1976 - 2:15 A.M.
JULY 13, 1976 - 9:15 A.M.
JULY 13, 1976 - 4:00 P.M.
JULY 13, 1976 - 6:00 P.M.
JULY 14, 1976 - 2:00 A.M.
JULY 14, 1976 - 3:45 A.M.
JULY 14, 1976 - 5:15 A.M.
JULY 14, 1976 - 5:45 A.M.
JULY 14, 1976 - 10:00 A.M.
JULY 14, 1976 - 12:00 P.M.
JULY 14, 1976 - 12:30 P.M.
JULY 14, 1976 - 7:00 P.M.
JULY 14, 1976 - 9:15 P.M.
JULY 14, 1976 - 10:30 P.M.

JULY 15, 1976 - 1:30 A.M.
JULY 15, 1976 - 3:30 A.M.
JULY 15, 1976 - 4:30 A.M.
JULY 15, 1976 - 9:45 A.M.
JULY 15, 1976 - 12:00 P.M.
JULY 15, 1976 - 12:45 P.M.
JULY 15, 1976 - 2:45 P.M.
JULY 15, 1976 - 3:45 P.M.
JULY 15, 1976 - 6:15 P.M.
JULY 16, 1976 - 8:30 A.M.
JULY 16, 1976 - 12:30 P.M.
JULY 16, 1976 - 1:45 P.M.

JULY 16, 1976 - 2:00 P.M.
JULY 16, 1976 - 2:45 P.M.
JULY 16, 1976 - 7:30 P.M.
JULY 17, 1976 - 7:30 A.M.
JULY 17, 1976 - 8:30 A.M.
JULY 17, 1976 - 1:00 P.M.
JULY 17, 1976 - 1:30 P.M.
JULY 17, 1976 - 4:30 P.M.
JULY 17, 1976 - 5:15 P.M.
JULY 17, 1976 - 10:30 P.M.
JULY 18, 1976 - 10:45 A.M.
JULY 18, 1976 - 12:15 P.M.
JULY 18, 1976 - 1:00 P.M.
JULY 18, 1976 - 7:15 P.M.
JULY 21, 1976 - 11:30 A.M.
JULY 22, 1976 - 7:30 A.M.
JULY 22, 1976 - 11:15 A.M.
JULY 22, 1976 - 1:00 P.M.
JULY 22, 1976 - 6:30 P.M.
JULY 22, 1976 - 7:45 P.M.
JULY 22, 1976 - 10:00 P.M.
JULY 23, 1976 - 3:00 A.M.
JULY 23, 1976 - 5:00 A.M.
JULY 23, 1976 - 5:45 A.M.
JULY 23, 1976 - 11:45 A.M.
JULY 24, 1976 - 4:00 P.M.
JULY 26, 1976 - 6:00 P.M.
JULY 29, 1976 - 2:30 A.M.

JULY 16, 1976 - 2:15 P.M.
JULY 16, 1976 - 3:15 P.M.
JULY 16, 1976 - 7:45 P.M.
JULY 17, 1976 - 8:15 A.M.
JULY 17, 1976 - 8:45 A.M.
JULY 17, 1976 - 1:15 P.M.
JULY 17, 1976 - 2:00 P.M.
JULY 17, 1976 - 5:00 P.M.
JULY 17, 1976 - 7:30 P.M.
JULY 17, 1976 - 10:45 P.M.
JULY 18, 1976 - 11:00 A.M.
JULY 18, 1976 - 12:45 P.M.
JULY 18, 1976 - 1:15 P.M.
JULY 18, 1976 - 7:30 P.M.
JULY 21, 1976 - 11:45 A.M.
JULY 22, 1976 - 11:00 A.M.
JULY 22, 1976 - 12:15 P.M.
JULY 22, 1976 - 6:15 P.M.
JULY 22, 1976 - 6:45 P.M.
JULY 22, 1976 - 8:30 P.M.
JULY 23, 1976 - 12:45 A.M.
JULY 23, 1976 - 4:30 A.M.
JULY 23, 1976 - 5:15 A.M.
JULY 23, 1976 - 6:00 A.M.
JULY 23, 1976 - 1:00 P.M.
JULY 24, 1976 - 4:15 P.M.
JULY 26, 1976 - 6:15 P.M.
JULY 29, 1976 - 3:00 A.M.

Table 2

BEGINNING AND ENDING TIMES OF RAINFALL PERIODS
FOR THE ENTIRE 1977 TEXAS HIPLEX RAINGAGE NETWORK
APRIL 4, 1977 - SEPTEMBER 29, 1977

BEGINNING OF RAINFALL PERIOD	END OF RAINFALL PERIOD
APRIL 6, 1977 - 8:00 P.M.	APRIL 6, 1977 - 8:15 P.M.
APRIL 14, 1977 - 2:45 A.M.	APRIL 14, 1977 - 9:15 A.M.
APRIL 14, 1977 - 10:15 A.M.	APRIL 14, 1977 - 5:45 P.M.
APRIL 14, 1977 - 6:15 P.M.	APRIL 14, 1977 - 7:15 P.M.
APRIL 14, 1977 - 7:45 P.M.	APRIL 14, 1977 - 10:30 P.M.
APRIL 15, 1977 - 7:45 A.M.	APRIL 15, 1977 - 8:15 A.M.
APRIL 16, 1977 - 2:30 P.M.	APRIL 17, 1977 - 4:00 A.M.
APRIL 17, 1977 - 4:15 A.M.	APRIL 17, 1977 - 4:30 A.M.
APRIL 17, 1977 - 6:00 A.M.	APRIL 17, 1977 - 7:00 A.M.
APRIL 17, 1977 - 7:15 A.M.	APRIL 17, 1977 - 8:15 A.M.
APRIL 17, 1977 - 3:00 P.M.	APRIL 17, 1977 - 3:30 P.M.
APRIL 17, 1977 - 4:45 P.M.	APRIL 17, 1977 - 6:00 P.M.
APRIL 19, 1977 - 3:15 P.M.	APRIL 19, 1977 - 7:15 P.M.
APRIL 19, 1977 - 7:45 P.M.	APRIL 19, 1977 - 8:00 P.M.
APRIL 19, 1977 - 8:45 P.M.	APRIL 19, 1977 - 9:00 P.M.
APRIL 19, 1977 - 9:15 P.M.	APRIL 19, 1977 - 9:30 P.M.
APRIL 19, 1977 - 9:45 P.M.	APRIL 19, 1977 - 11:45 P.M.
APRIL 20, 1977 - 4:15 P.M.	APRIL 20, 1977 - 4:30 P.M.
APRIL 20, 1977 - 5:00 P.M.	APRIL 20, 1977 - 7:30 P.M.
APRIL 20, 1977 - 7:45 P.M.	APRIL 20, 1977 - 8:00 P.M.
APRIL 28, 1977 - 7:15 P.M.	APRIL 28, 1977 - 9:45 P.M.
APRIL 29, 1977 - 10:00 P.M.	APRIL 30, 1977 - 1:30 A.M.
APRIL 30, 1977 - 1:45 A.M.	APRIL 30, 1977 - 2:00 A.M.
APRIL 30, 1977 - 11:00 A.M.	APRIL 30, 1977 - 11:15 A.M.
MAY 4, 1977 - 5:45 P.M.	MAY 4, 1977 - 6:30 P.M.
MAY 5, 1977 - 1:30 P.M.	MAY 5, 1977 - 2:15 P.M.
MAY 5, 1977 - 3:30 P.M.	MAY 5, 1977 - 5:30 P.M.
MAY 5, 1977 - 6:00 P.M.	MAY 5, 1977 - 6:15 P.M.
MAY 5, 1977 - 7:00 P.M.	MAY 5, 1977 - 7:15 P.M.
MAY 8, 1977 - 10:15 P.M.	MAY 9, 1977 - 3:30 A.M.
MAY 9, 1977 - 4:30 A.M.	MAY 9, 1977 - 4:45 A.M.
MAY 9, 1977 - 9:15 P.M.	MAY 10, 1977 - 1:30 A.M.
MAY 10, 1977 - 6:15 P.M.	MAY 10, 1977 - 9:45 P.M.
MAY 10, 1977 - 10:15 P.M.	MAY 10, 1977 - 10:30 P.M.

MAY 10, 1977 - 11:15 P.M.	MAY 10, 1977 - 11:30 P.M.
MAY 11, 1977 - 1:30 P.M.	MAY 11, 1977 - 2:15 P.M.
MAY 13, 1977 - 8:30 A.M.	MAY 13, 1977 - 10:00 A.M.
MAY 19, 1977 - 3:45 P.M.	MAY 19, 1977 - 4:15 P.M.
MAY 19, 1977 - 7:15 P.M.	MAY 19, 1977 - 8:45 P.M.
MAY 20, 1977 - 3:15 P.M.	MAY 20, 1977 - 9:30 P.M.
MAY 21, 1977 - 3:00 A.M.	MAY 21, 1977 - 3:15 A.M.
MAY 21, 1977 - 4:00 A.M.	MAY 21, 1977 - 4:15 A.M.
MAY 24, 1977 - 4:30 A.M.	MAY 24, 1977 - 6:00 A.M.
MAY 26, 1977 - 10:15 A.M.	MAY 26, 1977 - 10:45 A.M.
MAY 28, 1977 - 10:00 P.M.	MAY 28, 1977 - 10:15 P.M.
MAY 29, 1977 - 8:15 P.M.	MAY 29, 1977 - 11:15 P.M.
MAY 30, 1977 - 6:00 P.M.	MAY 30, 1977 - 6:15 P.M.
MAY 30, 1977 - 6:45 P.M.	MAY 30, 1977 - 8:15 P.M.
MAY 30, 1977 - 8:30 P.M.	MAY 30, 1977 - 9:00 P.M.
MAY 30, 1977 - 9:15 P.M.	MAY 30, 1977 - 9:30 P.M.
JUNE 1, 1977 - 1:45 A.M.	JUNE 1, 1977 - 9:30 A.M.
JUNE 1, 1977 - 9:45 A.M.	JUNE 1, 1977 - 10:45 A.M.
JUNE 1, 1977 - 11:00 A.M.	JUNE 1, 1977 - 11:30 A.M.
JUNE 2, 1977 - 8:45 A.M.	JUNE 2, 1977 - 9:00 A.M.
JUNE 10, 1977 - 7:45 P.M.	JUNE 10, 1977 - 9:30 P.M.
JUNE 10, 1977 - 10:00 P.M.	JUNE 10, 1977 - 10:15 P.M.
JUNE 11, 1977 - 10:00 P.M.	JUNE 12, 1977 - 4:15 A.M.
JUNE 12, 1977 - 4:30 A.M.	JUNE 12, 1977 - 5:30 A.M.
JUNE 12, 1977 - 6:15 A.M.	JUNE 12, 1977 - 6:30 A.M.
JUNE 13, 1977 - 10:45 P.M.	JUNE 14, 1977 - 12:30 A.M.
JUNE 14, 1977 - 12:45 A.M.	JUNE 14, 1977 - 1:30 A.M.
JUNE 18, 1977 - 9:15 P.M.	JUNE 19, 1977 - 1:15 A.M.
JUNE 19, 1977 - 1:45 A.M.	JUNE 19, 1977 - 2:00 A.M.
JUNE 20, 1977 - 10:30 P.M.	JUNE 21, 1977 - 6:15 A.M.
JUNE 21, 1977 - 6:45 A.M.	JUNE 21, 1977 - 7:15 A.M.
JUNE 21, 1977 - 11:45 A.M.	JUNE 21, 1977 - 12:00 P.M.
JUNE 21, 1977 - 5:15 P.M.	JUNE 21, 1977 - 8:15 P.M.
JUNE 21, 1977 - 8:30 P.M.	JUNE 22, 1977 - 1:45 A.M.

JUNE 22, 1977 - 2:15 A.M.
JUNE 22, 1977 - 3:CC A.M.
JUNE 22, 1977 - 6:CO A.M.
JUNE 22, 1977 - 7:15 A.M.
JUNE 22, 1977 - 9:30 A.M.
JUNE 22, 1977 - 12:15 P.M.
JUNE 22, 1977 - 10:30 P.M.
JUNE 22, 1977 - 11:45 P.M.
JUNE 23, 1977 - 2:30 A.M.
JUNE 23, 1977 - 3:CO A.M.
JUNE 23, 1977 - 8:30 A.M.
JUNE 23, 1977 - 1C:CO A.M.
JUNE 23, 1977 - 1:30 P.M.
JUNE 23, 1977 - 8:45 P.M.
JUNE 23, 1977 - 9:15 P.M.
JUNE 23, 1977 - 10:15 P.M.
JUNE 24, 1977 - 12:15 A.M.
JUNE 24, 1977 - 2:3C A.M.
JUNE 24, 1977 - 6:CO A.M.
JUNE 24, 1977 - 6:45 A.M.
JUNE 24, 1977 - 7:15 A.M.
JUNE 24, 1977 - 9:CO A.M.
JUNE 24, 1977 - 11:15 A.M.
JUNE 24, 1977 - 12:15 P.M.
JUNE 24, 1977 - 1:15 P.M.
JUNE 24, 1977 - 2:15 P.M.
JUNE 24, 1977 - 5:CO P.M.
JUNE 24, 1977 - 8:CO P.M.
JUNE 25, 1977 - 12:45 A.M.
JUNE 25, 1977 - 8:45 A.M.
JUNE 25, 1977 - 12:15 P.M.

JUNE 22, 1977 - 2:3[illegible]
JUNE 22, 1977 - 3:[illegible]
JUNE 22, 1977 - 6:1[illegible]
JUNE 22, 1977 - 7:4[illegible]
JUNE 22, 1977 - 1C:C[illegible]
JUNE 22, 1977 - 1C:1[illegible]
JUNE 22, 1977 - 11:3[illegible]
JUNE 23, 1977 - 2:1[illegible]
JUNE 23, 1977 - 2:4[illegible]
JUNE 23, 1977 - 8:C[illegible]
JUNE 23, 1977 - 9:C[illegible]
JUNE 23, 1977 - 1C:3[illegible]
JUNE 23, 1977 - 8:3[illegible]
JUNE 23, 1977 - 9:C[illegible]
JUNE 23, 1977 - 9:3[illegible]
JUNE 24, 1977 - 12:C[illegible]
JUNE 24, 1977 - 12:3[illegible]
JUNE 24, 1977 - 5:3[illegible]
JUNE 24, 1977 - 6:1[illegible]
JUNE 24, 1977 - 7:C[illegible]
JUNE 24, 1977 - 7:3[illegible]
JUNE 24, 1977 - 11:C[illegible]
JUNE 24, 1977 - 11:3[illegible]
JUNE 24, 1977 - 12:3[illegible]
JUNE 24, 1977 - 1:3[illegible]
JUNE 24, 1977 - 4:4[illegible]
JUNE 24, 1977 - 5:4[illegible]
JUNE 25, 1977 - 12:3[illegible]
JUNE 25, 1977 - 1:C[illegible]
JUNE 25, 1977 - 12:C[illegible]
JUNE 25, 1977 - 1:1[illegible]

JUNE 25, 1977 - 1:30 P.M.
JUNE 25, 1977 - 10:00 P.M.
JUNE 26, 1977 - 1:45 A.M.
JUNE 26, 1977 - 3:30 A.M.
JUNE 26, 1977 - 4:00 A.M.
JUNE 26, 1977 - 4:15 P.M.
JUNE 26, 1977 - 5:00 P.M.
JUNE 26, 1977 - 9:30 P.M.
JUNE 26, 1977 - 10:00 P.M.
JUNE 26, 1977 - 10:30 P.M.
JUNE 27, 1977 - 10:45 A.M.
JUNE 28, 1977 - 4:45 A.M.
JUNE 28, 1977 - 1:15 P.M.
JUNE 28, 1977 - 1:45 P.M.
JUNE 28, 1977 - 3:45 P.M.
JULY 1, 1977 - 4:00 A.M.
JULY 1, 1977 - 4:30 P.M.
JULY 8, 1977 - 12:30 P.M.
JULY 8, 1977 - 8:00 P.M.
JULY 8, 1977 - 8:30 P.M.
JULY 8, 1977 - 9:15 P.M.
JULY 8, 1977 - 10:30 P.M.
JULY 8, 1977 - 11:45 P.M.
JULY 9, 1977 - 2:15 A.M.
JULY 9, 1977 - 3:15 A.M.
JULY 9, 1977 - 4:15 A.M.
JULY 9, 1977 - 4:45 A.M.
JULY 9, 1977 - 8:15 A.M.
JULY 9, 1977 - 3:00 P.M.
JULY 9, 1977 - 3:45 P.M.
JULY 9, 1977 - 8:00 P.M.

JUNE 25, 1977 - 9:45 P.M.
JUNE 26, 1977 - 1:15 A.M.
JUNE 26, 1977 - 2:00 A.M.
JUNE 26, 1977 - 3:45 A.M.
JUNE 26, 1977 - 4:30 A.M.
JUNE 26, 1977 - 4:45 P.M.
JUNE 26, 1977 - 5:15 P.M.
JUNE 26, 1977 - 9:45 P.M.
JUNE 26, 1977 - 10:15 P.M.
JUNE 26, 1977 - 10:45 P.M.
JUNE 27, 1977 - 11:00 A.M.
JUNE 28, 1977 - 5:00 A.M.
JUNE 28, 1977 - 1:30 P.M.
JUNE 28, 1977 - 2:00 P.M.
JUNE 28, 1977 - 4:15 P.M.
JULY 1, 1977 - 4:30 A.M.
JULY 1, 1977 - 5:00 P.M.
JULY 8, 1977 - 7:30 P.M.
JULY 8, 1977 - 8:15 P.M.
JULY 8, 1977 - 8:45 P.M.
JULY 8, 1977 - 9:30 P.M.
JULY 8, 1977 - 11:15 P.M.
JULY 9, 1977 - 12:15 A.M.
JULY 9, 1977 - 2:45 A.M.
JULY 9, 1977 - 3:45 A.M.
JULY 9, 1977 - 4:30 A.M.
JULY 9, 1977 - 8:00 A.M.
JULY 9, 1977 - 8:30 A.M.
JULY 9, 1977 - 3:15 P.M.
JULY 9, 1977 - 5:00 P.M.
JULY 9, 1977 - 8:30 P.M.

JULY 21, 1977 - 12:30 P.M.
JULY 21, 1977 - 1:15 P.M.
JULY 21, 1977 - 11:15 P.M.
JULY 22, 1977 - 1:00 A.M.
JULY 22, 1977 - 1:30 A.M.
JULY 22, 1977 - 2:30 A.M.
JULY 22, 1977 - 12:45 P.M.
JULY 22, 1977 - 1:45 P.M.
JULY 26, 1977 - 11:30 P.M.
JULY 27, 1977 - 1:15 A.M.
JULY 27, 1977 - 8:00 A.M.
JULY 27, 1977 - 3:15 P.M.
JULY 27, 1977 - 4:45 P.M.
JULY 27, 1977 - 7:15 P.M.
JULY 27, 1977 - 8:00 P.M.
JULY 28, 1977 - 1:45 A.M.
JULY 28, 1977 - 8:00 A.M.
JULY 28, 1977 - 9:00 A.M.
JULY 28, 1977 - 9:30 A.M.
JULY 28, 1977 - 1:45 P.M.
JULY 29, 1977 - 12:45 A.M.
JULY 29, 1977 - 2:30 A.M.
JULY 29, 1977 - 3:00 A.M.
JULY 29, 1977 - 8:15 A.M.
JULY 29, 1977 - 10:30 A.M.
JULY 29, 1977 - 2:45 P.M.
JULY 29, 1977 - 8:00 P.M.
JULY 29, 1977 - 9:00 P.M.
AUGUST 1, 1977 - 2:00 P.M.
AUGUST 1, 1977 - 3:30 P.M.
AUGUST 10, 1977 - 1:00 A.M.
AUGUST 10, 1977 - 3:00 A.M.
AUGUST 11, 1977 - 12:30 P.M.
AUGUST 11, 1977 - 1:00 P.M.
AUGUST 11, 1977 - 1:45 P.M.
AUGUST 11, 1977 - 7:30 P.M.

JULY 21, 1977 - 1:00 P.M.
JULY 21, 1977 - 10:30 P.M.
JULY 21, 1977 - 11:45 P.M.
JULY 22, 1977 - 1:15 A.M.
JULY 22, 1977 - 2:15 A.M.
JULY 22, 1977 - 12:30 P.M.
JULY 22, 1977 - 1:30 P.M.
JULY 22, 1977 - 2:45 P.M.
JULY 27, 1977 - 1:00 A.M.
JULY 27, 1977 - 1:45 A.M.
JULY 27, 1977 - 8:45 A.M.
JULY 27, 1977 - 4:30 P.M.
JULY 27, 1977 - 7:00 P.M.
JULY 27, 1977 - 7:30 P.M.
JULY 27, 1977 - 8:15 P.M.
JULY 28, 1977 - 2:45 A.M.
JULY 28, 1977 - 8:45 A.M.
JULY 28, 1977 - 9:15 A.M.
JULY 28, 1977 - 9:45 A.M.
JULY 28, 1977 - 5:15 P.M.
JULY 29, 1977 - 1:00 A.M.
JULY 29, 1977 - 2:45 A.M.
JULY 29, 1977 - 8:00 A.M.
JULY 29, 1977 - 9:15 A.M.
JULY 29, 1977 - 10:45 A.M.
JULY 29, 1977 - 7:45 P.M.
JULY 29, 1977 - 8:45 P.M.
JULY 29, 1977 - 9:15 P.M.
AUGUST 1, 1977 - 3:15 P.M.
AUGUST 1, 1977 - 4:15 P.M.
AUGUST 10, 1977 - 2:45 A.M.
AUGUST 10, 1977 - 3:15 A.M.
AUGUST 11, 1977 - 12:45 P.M.
AUGUST 11, 1977 - 1:30 P.M.
AUGUST 11, 1977 - 6:45 P.M.
AUGUST 11, 1977 - 7:45 P.M.

AUGUST 12, 1977 - 7:45 P.M.
AUGUST 12, 1977 - 9:30 P.M.
AUGUST 13, 1977 - 2:45 P.M.
AUGUST 13, 1977 - 3:45 P.M.
AUGUST 13, 1977 - 7:45 P.M.
AUGUST 14, 1977 - 2:15 P.M.
AUGUST 14, 1977 - 4:30 P.M.
AUGUST 14, 1977 - 7:00 P.M.
AUGUST 14, 1977 - 10:00 P.M.
AUGUST 15, 1977 - 2:15 P.M.
AUGUST 19, 1977 - 4:30 P.M.
AUGUST 19, 1977 - 7:45 P.M.
AUGUST 19, 1977 - 8:15 P.M.
AUGUST 20, 1977 - 2:45 A.M.
AUGUST 20, 1977 - 3:45 A.M.
AUGUST 20, 1977 - 4:15 A.M.
AUGUST 20, 1977 - 8:00 A.M.
AUGUST 20, 1977 - 9:15 A.M.
AUGUST 20, 1977 - 3:15 P.M.
AUGUST 20, 1977 - 8:00 P.M.
AUGUST 20, 1977 - 9:00 P.M.
AUGUST 21, 1977 - 3:00 A.M.
AUGUST 21, 1977 - 5:00 A.M.
AUGUST 21, 1977 - 6:00 A.M.
AUGUST 21, 1977 - 12:15 P.M.
AUGUST 22, 1977 - 2:15 A.M.
AUGUST 22, 1977 - 3:15 A.M.
AUGUST 22, 1977 - 4:00 A.M.
AUGUST 22, 1977 - 6:30 A.M.
AUGUST 22, 1977 - 8:00 A.M.
AUGUST 22, 1977 - 11:15 A.M.
AUGUST 23, 1977 - 4:15 P.M.
AUGUST 23, 1977 - 11:45 P.M.
AUGUST 24, 1977 - 2:15 A.M.

AUGUST 12, 1977 - 9:15 P.M.
AUGUST 12, 1977 - 9:45 P.M.
AUGUST 13, 1977 - 3:15 P.M.
AUGUST 13, 1977 - 7:30 P.M.
AUGUST 13, 1977 - 8:00 P.M.
AUGUST 14, 1977 - 4:15 P.M.
AUGUST 14, 1977 - 6:45 P.M.
AUGUST 14, 1977 - 9:45 P.M.
AUGUST 14, 1977 - 10:45 P.M.
AUGUST 15, 1977 - 2:30 P.M.
AUGUST 19, 1977 - 5:15 P.M.
AUGUST 19, 1977 - 8:00 P.M.
AUGUST 20, 1977 - 2:30 A.M.
AUGUST 20, 1977 - 3:00 A.M.
AUGUST 20, 1977 - 4:00 A.M.
AUGUST 20, 1977 - 4:30 A.M.
AUGUST 20, 1977 - 8:45 A.M.
AUGUST 20, 1977 - 3:00 P.M.
AUGUST 20, 1977 - 3:30 P.M.
AUGUST 20, 1977 - 8:30 P.M.
AUGUST 20, 1977 - 9:15 P.M.
AUGUST 21, 1977 - 3:45 A.M.
AUGUST 21, 1977 - 5:45 A.M.
AUGUST 21, 1977 - 11:45 A.M.
AUGUST 21, 1977 - 1:00 P.M.
AUGUST 22, 1977 - 2:45 A.M.
AUGUST 22, 1977 - 3:30 A.M.
AUGUST 22, 1977 - 6:15 A.M.
AUGUST 22, 1977 - 7:00 A.M.
AUGUST 22, 1977 - 11:00 A.M.
AUGUST 22, 1977 - 11:30 A.M.
AUGUST 23, 1977 - 10:00 P.M.
AUGUST 24, 1977 - 12:30 A.M.
AUGUST 24, 1977 - 2:30 A.M.

AUGUST 24, 1977 - 3:CO P.M.	ALGUST 24, 1977 - 4:CC PM.
AUGUST 27, 1977 - 5:30 P.M.	ALGUST 28, 1977 - 9:45 A.M.
AUGUST 28, 1977 - 10:30 A.M.	ALGUST 28, 1977 - 10:45 A.M.
AUGUST 28, 1977 - 11:15 A.M.	ALGUST 28, 1977 - 11:3C A.M.
AUGUST 28, 1977 - 12:30 P.M.	ALGUST 28, 1977 - 12:45 P.M.
AUGUST 28, 1977 - 2:30 P.M.	ALGUST 28, 1977 - 6:3C P.M.
AUGUST 28, 1977 - 7:CO P.M.	ALGUST 28, 1977 - 7:15 P.M.
AUGUST 28, 1977 - 7:45 P.M.	ALGUST 28, 1977 - 8:CC P.M.
AUGUST 29, 1977 - 12:45 A.M.	ALGUST 29, 1977 - 1:30 A.M.
SEPTEMBER 4, 1977 - 10:15 P.M.	SEPTEMBER 4, 1977 - 11:30 P.M.
SEPTEMBER 4, 1977 - 11:45 P.M.	SEPTEMBER 5, 1977 - 12:CC A.M.
SEPTEMBER 5, 1977 - 12:15 A.M.	SEPTEMBER 5, 1977 - 12:30 A.M.
SEPTEMBER 5, 1977 - 12:45 A.M.	SEPTEMBER 5, 1977 - 1:CC A.M.
SEPTEMBER 5, 1977 - 4:15 A.M.	SEPTEMBER 5, 1977 - 5:15 A.M.
SEPTEMBER 5, 1977 - 5:45 A.M.	SEPTEMBER 5, 1977 - 6:CC A.M.
SEPTEMBER 5, 1977 - 2:45 P.M.	SEPTEMBER 5, 1977 - 3:15 P.M.
SEPTEMBER 5, 1977 - 3:45 P.M.	SEPTEMBER 5, 1977 - 4:45 P.M.
SEPTEMBER 6, 1977 - 11:45 A.M.	SEPTEMBER 6, 1977 - 1:15 P.M.
SEPTEMBER 6, 1977 - 1:30 P.M.	SEPTEMBER 6, 1977 - 2:CC P.M.
SEPTEMBER 6, 1977 - 2:30 P.M.	SEPTEMBER 6, 1977 - 4:15 P.M.
SEPTEMBER 6, 1977 - 4:30 P.M.	SEPTEMBER 6, 1977 - 5:45 P.M.
SEPTEMBER 6, 1977 - 6:CO P.M.	SEPTEMBER 6, 1977 - 6:15 P.M.
SEPTEMBER 6, 1977 - 6:45 P.M.	SEPTEMBER 6, 1977 - 7:CC P.M.
SEPTEMBER 6, 1977 - 7:30 P.M.	SEPTEMBER 6, 1977 - 8:CC P.M.
SEPTEMBER 6, 1977 - 8:15 P.M.	SEPTEMBER 6, 1977 - 8:30 P.M.
SEPTEMBER 6, 1977 - 8:45 P.M.	SEPTEMBER 6, 1977 - 9:CC P.M.
SEPTEMBER 7, 1977 - 11:CO A.M.	SEPTEMBER 7, 1977 - 11:15 A.M.
SEPTEMBER 7, 1977 - 11:30 A.M.	SEPTEMBER 7, 1977 - 11:45 A.M.
SEPTEMBER 7, 1977 - 8:45 P.M.	SEPTEMBER 7, 1977 - 9:CO P.M.
SEPTEMBER 10, 1977 - 3:15 P.M.	SEPTEMBER 10, 1977 - 4:CC P.M.
SEPTEMBER 10, 1977 - 4:30 P.M.	SEPTEMBER 10, 1977 - 6:45 P.M.
SEPTEMBER 10, 1977 - 7:15 P.M.	SEPTEMBER 10, 1977 - 7:30 P.M.
SEPTEMBER 12, 1977 - 4:45 A.M.	SEPTEMBER 12, 1977 - 9:30 A.M.

SEPTEMBER 12, 1977 - 11:45 A.M.
SEPTEMBER 12, 1977 - 12:45 P.M.
SEPTEMBER 13, 1977 - 5:00 P.M.
SEPTEMBER 13, 1977 - 5:45 P.M.
SEPTEMBER 13, 1977 - 7:00 P.M.
SEPTEMBER 17, 1977 - 1:15 P.M.
SEPTEMBER 17, 1977 - 2:15 P.M.
SEPTEMBER 17, 1977 - 7:00 P.M.
SEPTEMBER 18, 1977 - 5:00 A.M.
SEPTEMBER 18, 1977 - 6:30 A.M.
SEPTEMBER 18, 1977 - 7:15 A.M.
SEPTEMBER 18, 1977 - 8:30 A.M.

SEPTEMBER 12, 1977 - 12:30 P.M.
SEPTEMBER 12, 1977 - 1:00 P.M.
SEPTEMBER 13, 1977 - 5:30 P.M.
SEPTEMBER 13, 1977 - 6:15 P.M.
SEPTEMBER 13, 1977 - 7:15 P.M.
SEPTEMBER 17, 1977 - 2:00 P.M.
SEPTEMBER 17, 1977 - 2:30 P.M.
SEPTEMBER 17, 1977 - 8:45 P.M.
SEPTEMBER 18, 1977 - 5:15 A.M.
SEPTEMBER 18, 1977 - 6:45 A.M.
SEPTEMBER 18, 1977 - 8:15 A.M.
SEPTEMBER 18, 1977 - 11:00 A.M.

rainfall amounts, since the only requirement for rain-period designation was that rain be reported somewhere within the network. Periods of significant precipitation have been selected and analyzed according to storm size, velocity, duration, intensity and meso-synoptic type. These data will be used for the climatology developed in Task 3 and for the individual case studies in Task 4.

Task 3

Task 3 was designed to formulate a rain-cell climatology based upon the data gathered in Task 2. Due to a scarcity of rainfall events during 1977, insufficient data are available in order to formulate a "climatology" at this time. Each storm that affected the network has been recorded and analyzed. This procedure was continued in 1978 and will be followed once again in 1979. At the completion of the 1979 field season, a climatology of rainfall events will be formulated and published as a separate technical report. In the meantime, complete data are available for all days selected as primary and secondary case study days. Tables 3 and 4 give the diurnal distribution of precipitation within the network for May and June of 1976 and 1977 respectively. The rainfall reported is simply the sum of all rainfall which was recorded by the gages during those months.

Task 4

Task 4 involved intensive case studies in conjunction with the parallel investigation utilizing radar, satellite and meso-network data. These case studies are underway, but completion has been delayed pending analysis of the radar data.

Figures 1 through 8 show examples of precipitation maps which have been prepared for each of the case-study periods. Each of these maps re-

Table 3

DIURNAL VARIATION OF RAINFALL
FOR THE ENTIRE TEXAS HIPLEX NETWORK
MAY AND JUNE 1975

PERIOD	RAINFALL (ALL GAGES SUMMED TOGETHER)
12:00 A.M. - 1:00 A.M.	0.10
1:00 A.M. - 2:00 A.M.	0.11
2:00 A.M. - 3:00 A.M.	0.43
3:00 A.M. - 4:00 A.M.	0.11
4:00 A.M. - 5:00 A.M.	0.61
5:00 A.M. - 6:00 A.M.	7.38
6:00 A.M. - 7:00 A.M.	5.08
7:00 A.M. - 8:00 A.M.	4.76
8:00 A.M. - 9:00 A.M.	4.61
9:00 A.M. - 10:00 A.M.	3.93
10:00 A.M. - 11:00 A.M.	0.41
11:00 A.M. - 12:00 P.M.	1.12
12:00 P.M. - 1:00 P.M.	0.20
1:00 P.M. - 2:00 P.M.	1.10
2:00 P.M. - 3:00 P.M.	1.17
3:00 P.M. - 4:00 P.M.	4.37
4:00 P.M. - 5:00 P.M.	1.31
5:00 P.M. - 6:00 P.M.	0.51
6:00 P.M. - 7:00 P.M.	0.20
7:00 P.M. - 8:00 P.M.	5.14
8:00 P.M. - 9:00 P.M.	3.62
9:00 P.M. - 10:00 P.M.	0.86
10:00 P.M. - 11:00 P.M.	1.01
11:00 P.M. - 12:00 A.M.	0.90

Table 4

DIURNAL VARIATION OF RAINFALL
FOR THE ENTIRE TEXAS HIPLEX NETWORK
MAY AND JUNE 1977

PERIOD	RAINFALL (ALL GAGES SUMMED TOGETHER)
12:00 A.M. - 1:00 A.M.	29.10
1:00 A.M. - 2:00 A.M.	23.84
2:00 A.M. - 3:00 A.M.	11.68
3:00 A.M. - 4:00 A.M.	5.20
4:00 A.M. - 5:00 A.M.	4.09
5:00 A.M. - 6:00 A.M.	7.37
6:00 A.M. - 7:00 A.M.	6.90
7:00 A.M. - 8:00 A.M.	4.57
8:00 A.M. - 9:00 A.M.	1.81
9:00 A.M. - 10:00 A.M.	0.85
10:00 A.M. - 11:00 A.M.	0.70
11:00 A.M. - 12:00 P.M.	0.41
12:00 P.M. - 1:00 P.M.	0.75
1:00 P.M. - 2:00 P.M.	3.54
2:00 P.M. - 3:00 P.M.	9.23
3:00 P.M. - 4:00 P.M.	13.61
4:00 P.M. - 5:00 P.M.	24.26
5:00 P.M. - 6:00 P.M.	15.07
6:00 P.M. - 7:00 P.M.	8.57
7:00 P.M. - 8:00 P.M.	9.99
8:00 P.M. - 9:00 P.M.	9.61
9:00 P.M. - 10:00 P.M.	8.23
10:00 P.M. - 11:00 P.M.	20.34
11:00 P.M. - 12:00 A.M.	36.63

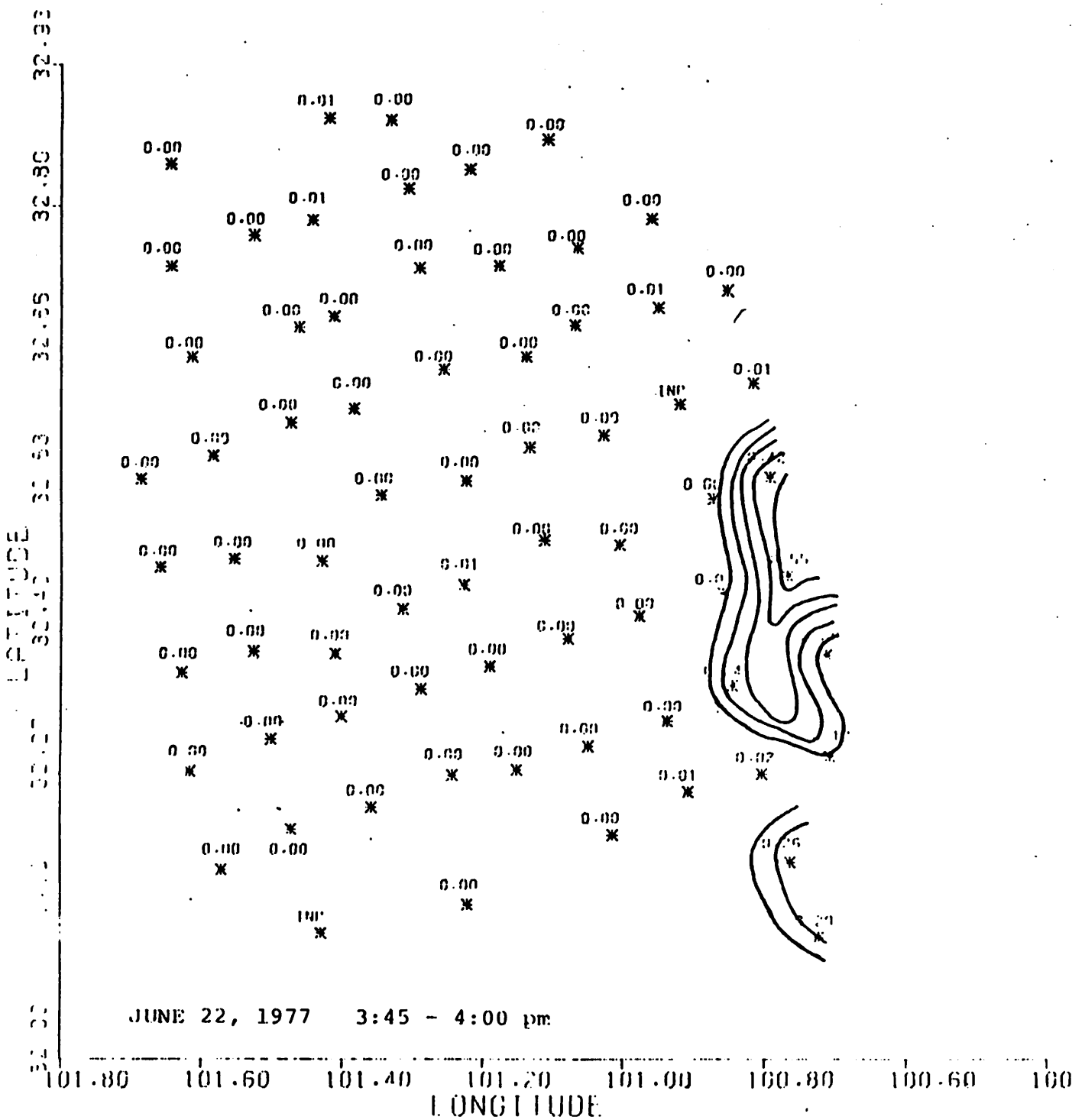

Rainfall in inches

Contours at 0.1 inch intervals

Figure 1

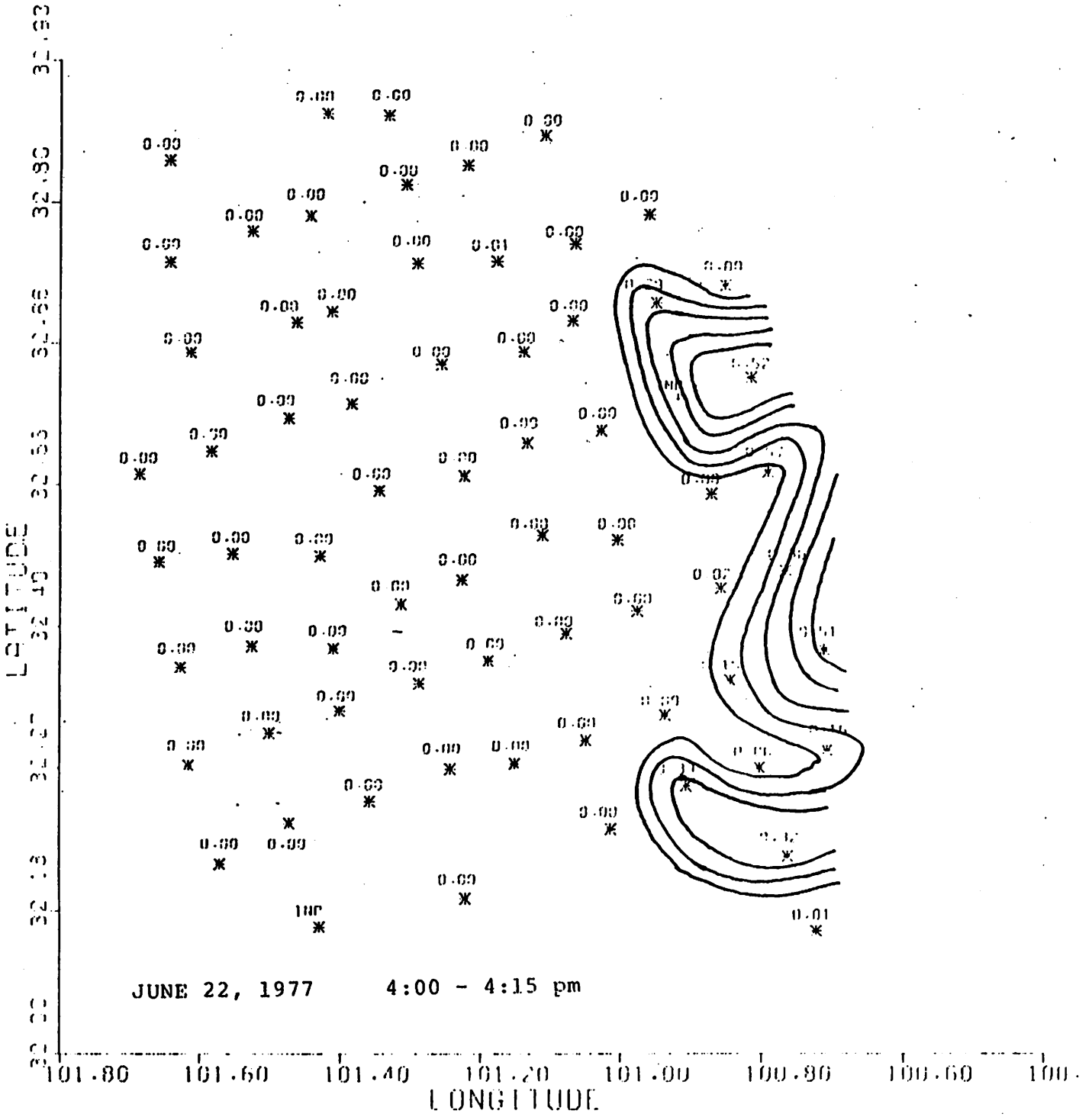
JUNE 22, 1977 4:00 - 4:15 pm
101.80
101.60
101.40
101.20
101.00
100.80
100.60
LONGITUDE

Figure 2

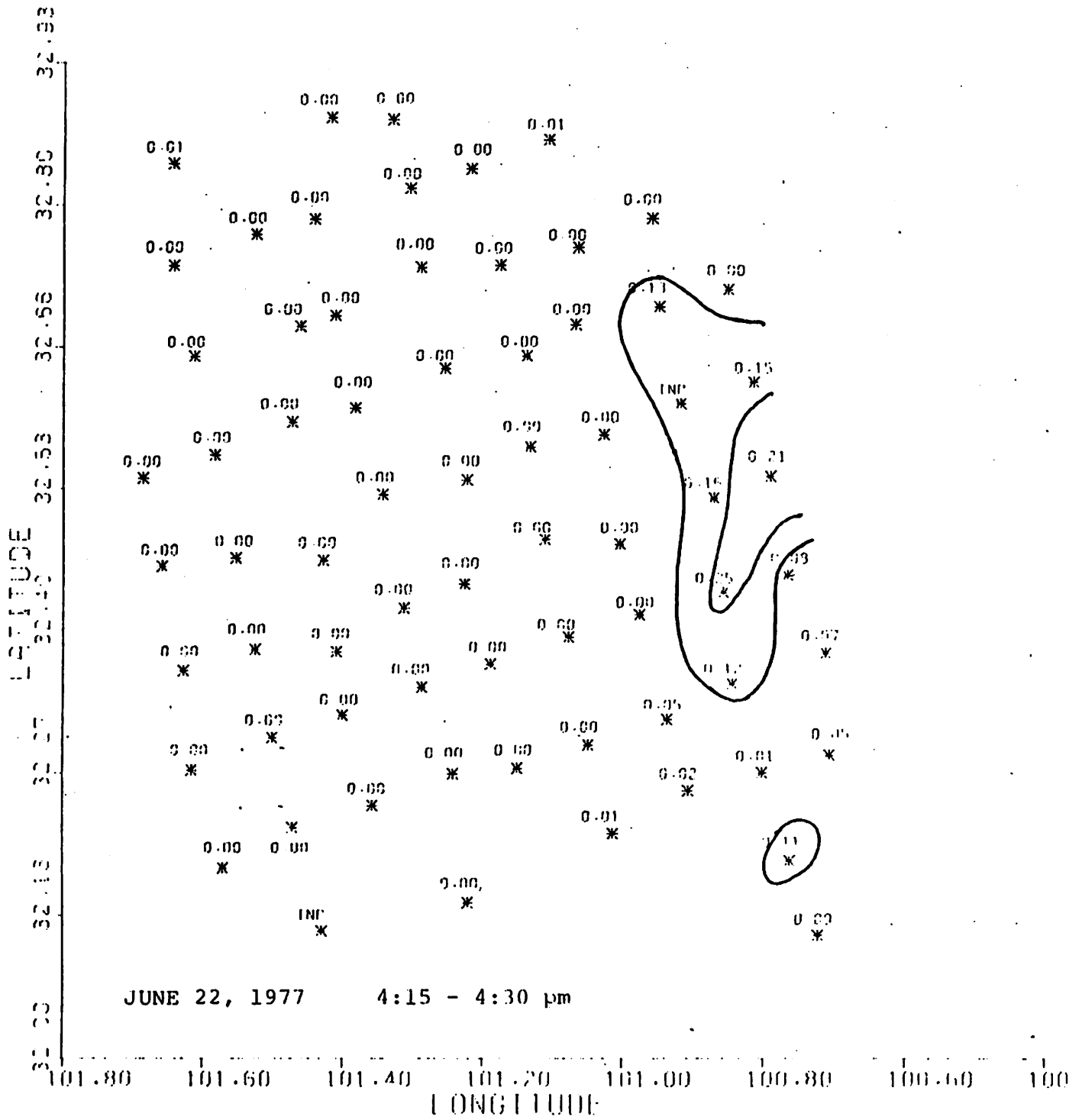
JUNE 22, 1977 4:15 - 4:30 pm
101.80
101.60
101.40
101.20
101.00
100.80
100.60
100
LONGITUDE

Figure 3

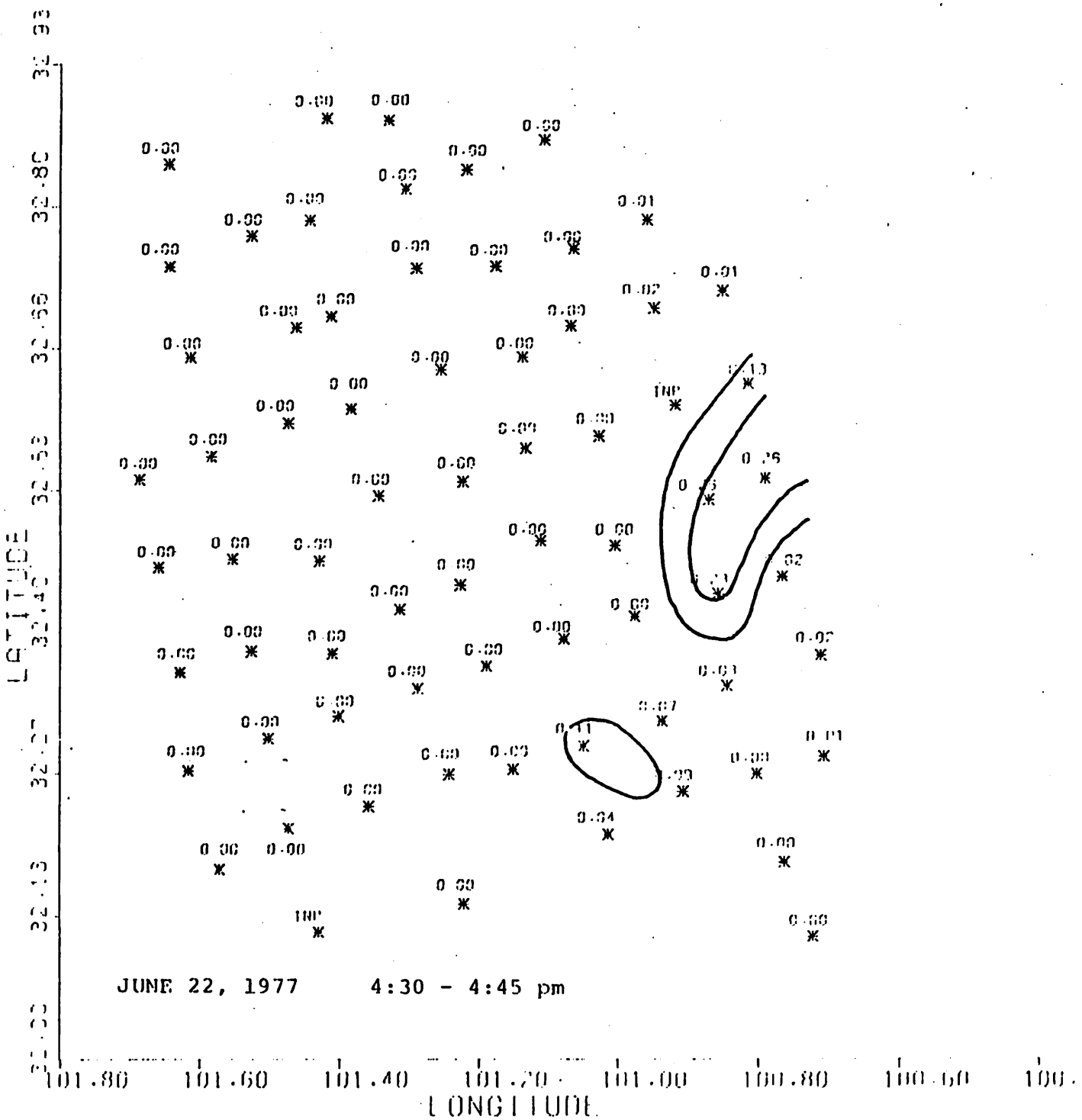
JUNE 22, 1977 4:30 - 4:45 pm
LONGITUDE
101.80
101.60
101.40
101.20
101.00
100.80
100.60
100.

Figure 4

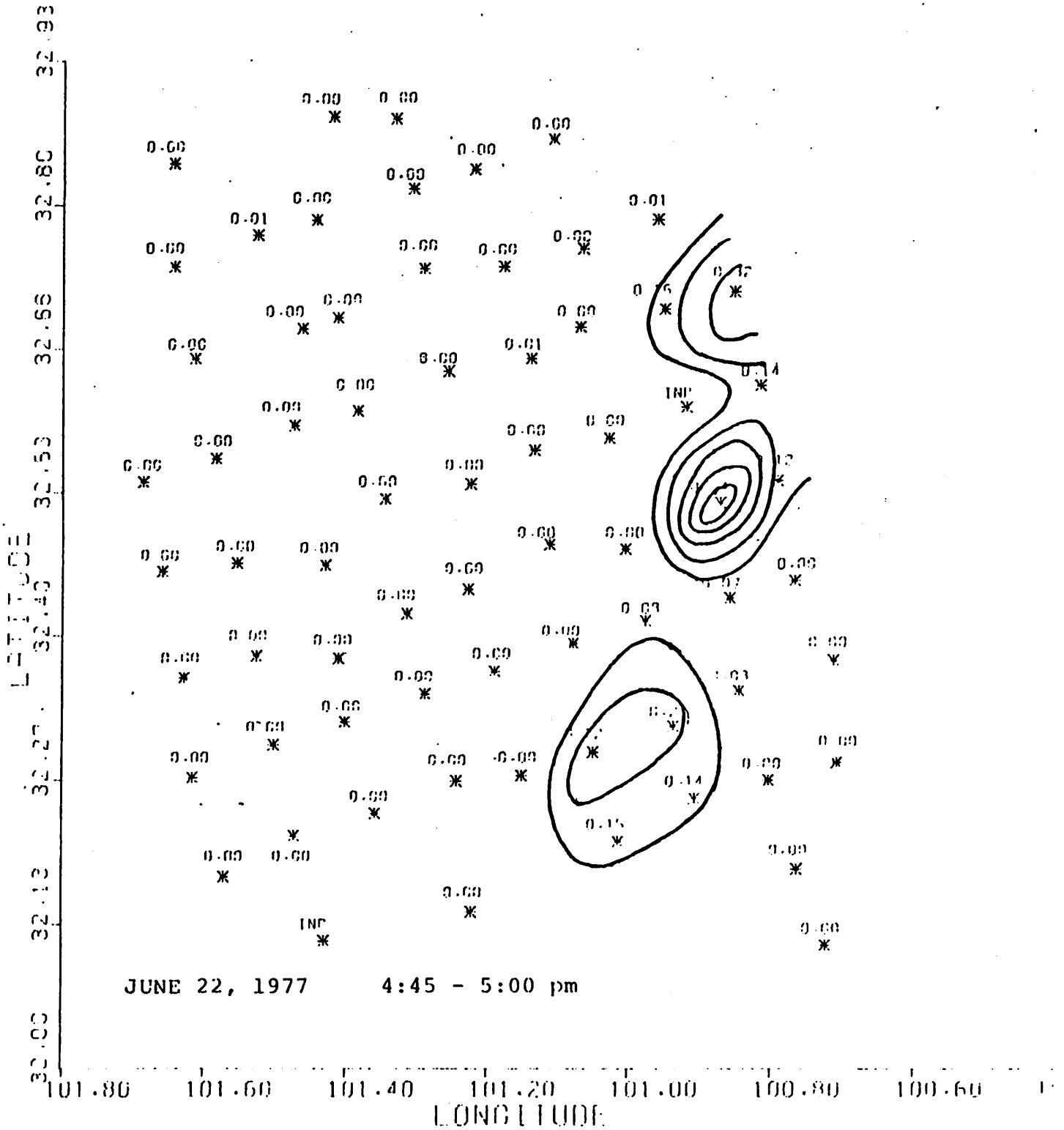
JUNE 22, 1977 4:45 - 5:00 pm
101.80
101.60
101.40
101.20
101.00
100.80
100.60
LONGITUDE

Figure 5

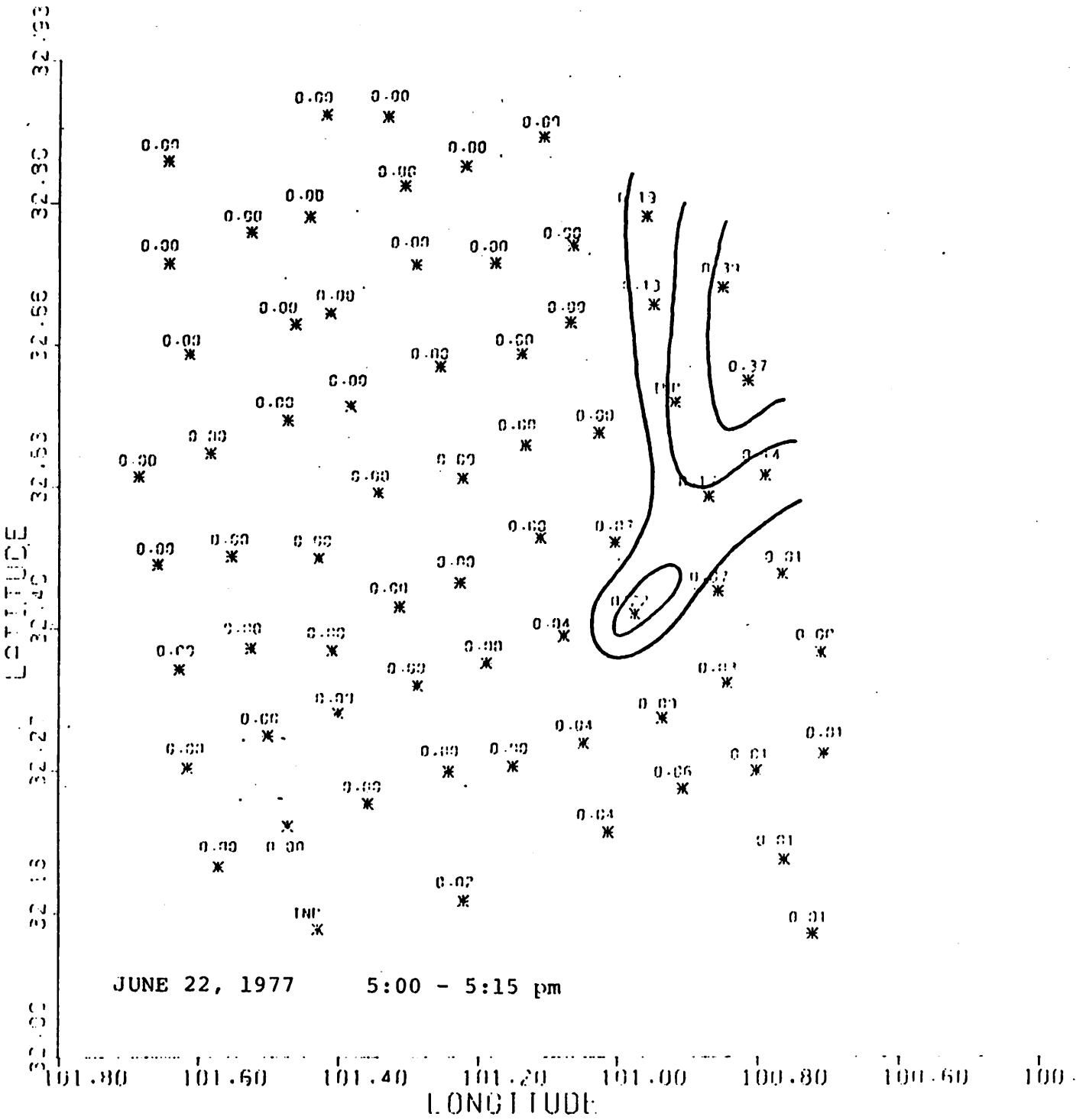
JUNE 22, 1977 5:00 - 5:15 pm
LONGITUDE
101.80
101.60
101.40
101.20
101.00
100.80
100.60

Figure 6

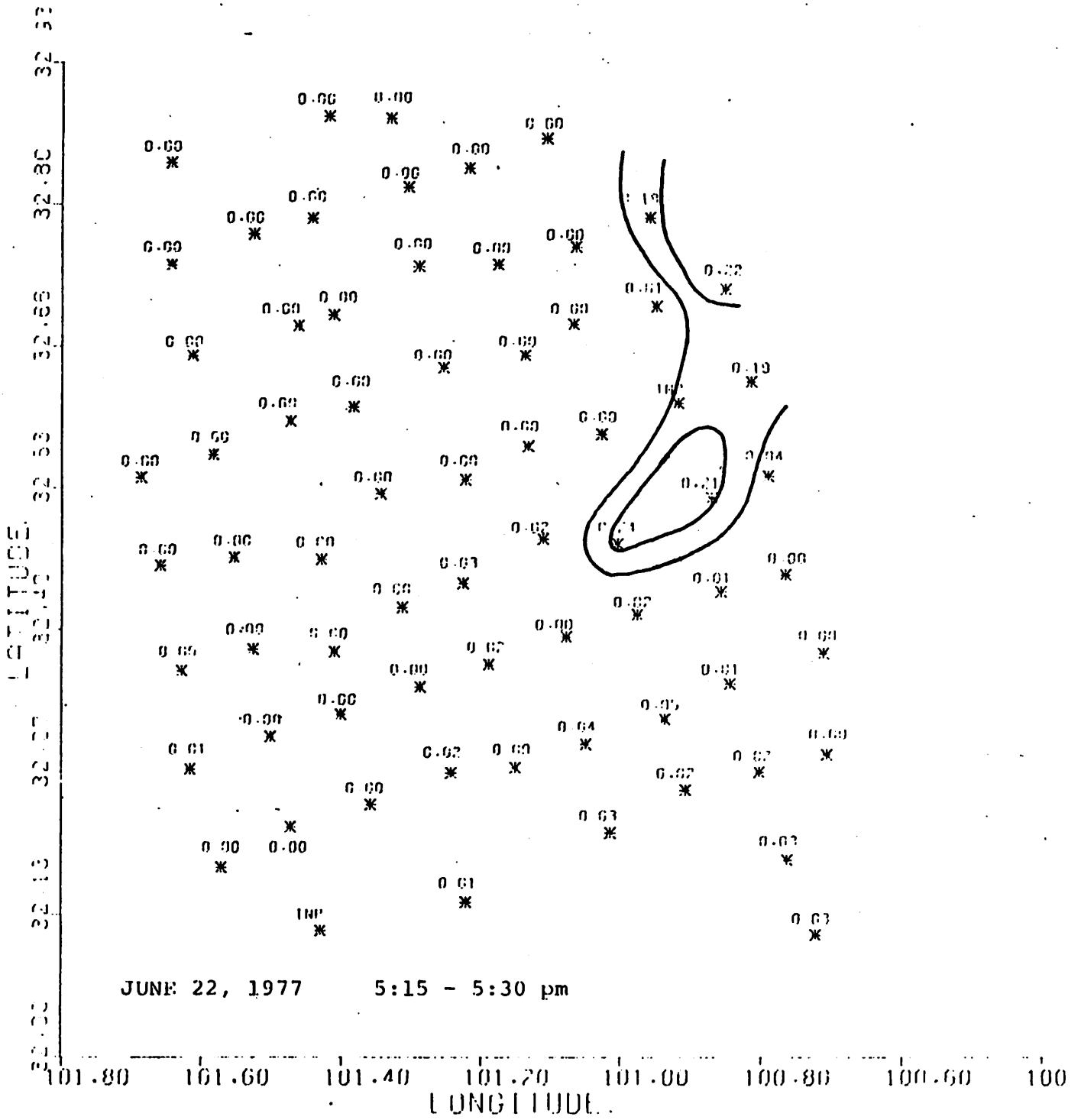
JUNE 22, 1977 5:15 - 5:30 pm
101.80
101.60
101.40
101.20
101.00
100.80
100.60
100
LONGITUDE

Figure 7

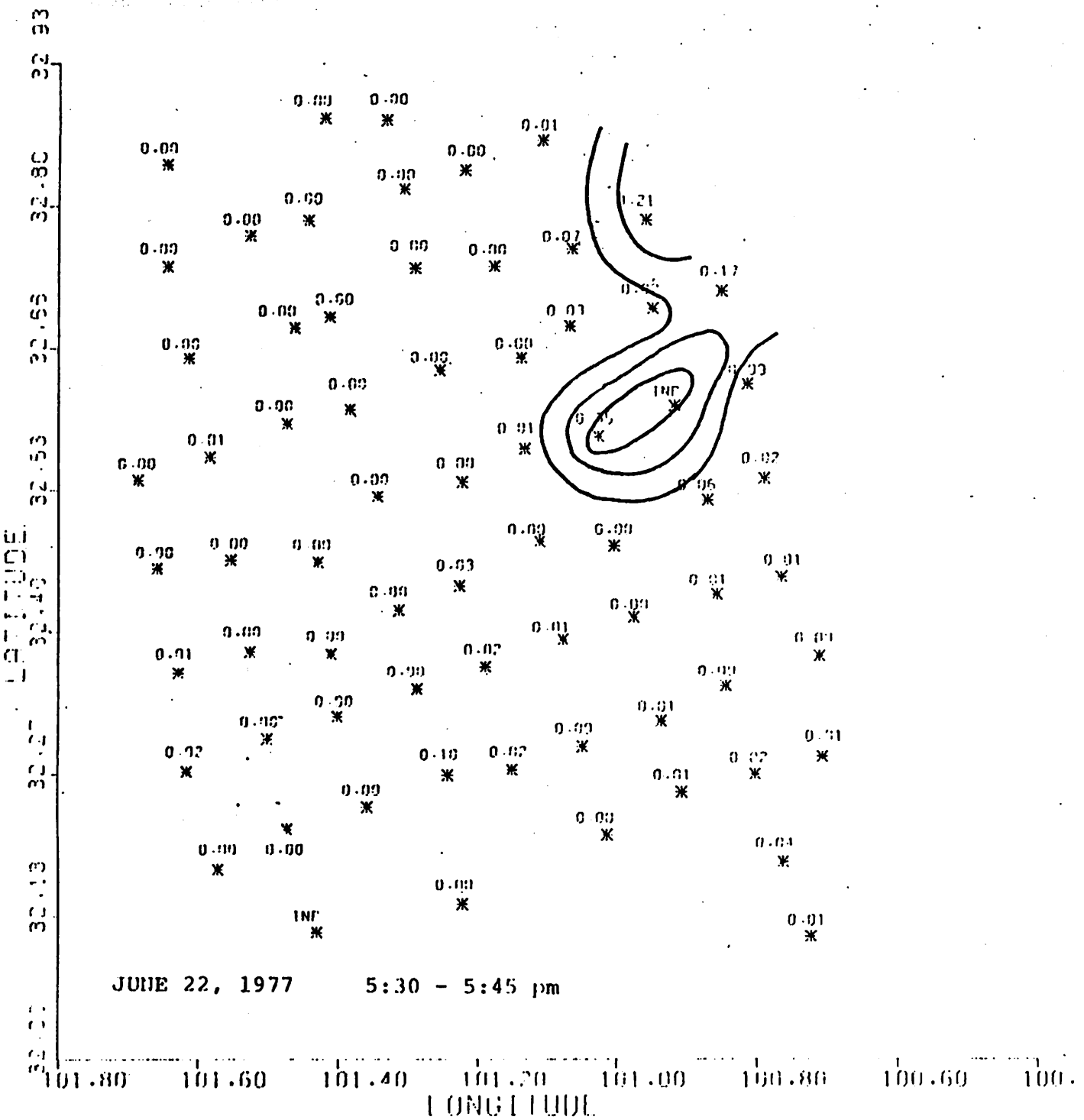
JUNE 22, 1977 5:30 - 5:45 pm
101.80
101.60
101.40
101.20
101.00
100.80
100.60
LONGITUDE

Figure 8

presents 15-minute precipitation during the period from 3:45 pm to 5:45 pm on June 22, 1977. Most of the precipitation recorded during this period occurred in the eastern portion of the network. Rainfall resulted from a line of convective activity which developed in eastern New Mexico and moved into the study area during the late afternoon. Computer-generated analyses of cloud albedo and cloud top temperatures permitted the movement and growth of the system to be followed with time. It was found that satellite-derived cloud top heights and observed radar echo tops agreed well.

Another date which is receiving primary emphasis is July 8, 1977. Rainfall intensities as high as 3.5 inches per hour were recorded as the storm moved through the HIPLEX network. Streamline analyses of surface winds have been prepared at hourly intervals. These analyses will be used in conjunction with the precipitation and radar analyses to identify relationships between distinctive features in the wind and precipitation patterns. For example, the surface wind field shows a distinctive cyclonic curvature in the vicinity of the line of observed precipitation. Completion of the radar analysis will provide a three-dimensional picture of the precipitation pattern.

Case studies will be provided for each of the primary and secondary days identified for 1977 and 1978. Internal reports will be distributed as the analyses are completed.

COLORADO RIVER MUNICIPAL WATER DISTRICT

INTERIM PROGRESS REPORT
1 APRIL - 30 SEPTEMBER 1978

The following report was prepared by the Colorado River Municipal Water District and submitted to the Department as an interim progress report for the period 1 April - 30 September 1978.

The TABLE OF CONTENTS provided below is supplemental information to the report added by the Department for ease of reference purposes.

TABLE OF CONTENTS

LIST OF TABLES

COLORADO RIVER MUNICIPAL WATER DISTRICT

Interim Progress Report
1 April - 30 September 1978

Prepared for:

United States Department of the Interior
Bureau of Reclamation
Division of Atmospheric Water Resources Management

Contract No. 14-06-D-7587

By:

Colorado River Municipal Water District
Post Office Box 869
Big Spring, Texas 79720

October 1978

The following report briefly outlines those services performed by the Colorado River Municipal Water District during the 1978 Texas-HIPLEX interim period 1 April - 30 September.

During this period the CRMWD maintained and operated an extensive network of recording and non-recording raingages, provided the services of a rawinsonde operator and a radar meteorologist. In addition to these services, the CRMWD also contracted to the HIPLEX program two multi-engine aircraft for the purpose of performing cloud seeding and cloud sampling flights.

RAINGAGE NETWORK

CRMWD personnel placed 81 fence post raingages in operation and serviced the 81 Belfort recording gages, placing them in an operational mode during late March and early April 1978. All raingages were located at sites used during the 1977 program.

Rainfall readings were recorded during April from the fence post gages and chart recorded data from the Belfort gages began May 1, 1978.

Data from the recording gages were extracted from the charts at 15-minute intervals and forwarded to Texas A&M University, and the original charts forwarded to Miles City for key punching and processing.

Rainfall data from both recording and non-recording gages were entered on forms prepared by the District. These forms indicated the rainfall amounts on a daily basis for each month. Following each month, these forms were forwarded to Texas Department of Water Resources, Texas Tech University and The Bureau of Reclamation.

Except for minor acts of vandalism, the Belfort gages performed well. Clocks generally operated within $\pm$ 10 minutes per week. Some clocks failed due to rainfall entering the clock case as the result of vandalism. One gage was badly damaged by an automobile and another damaged by a bullet resulting in a seven-day loss of rainfall data from these gages. Aside from this, the raingage network functioned routinely and without many mechanical difficulties.

RAWINSONDE OPERATIONS

A total of 106 rawinsondes were launched during this interim reporting period. Eighty-one of these rawinsondes were launched in support of the Texas A&M mesoscale and Texas HIPLEX program. The remaining 25 were launched on an "as needed" basis in support of the local CRMWD cloud seeding program.

When not actively engaged in launching rawinsondes or the processing of that data, Mr. Hancock, the rawinsonde operator, performed intrasite and interstate data analysis using those atmospheric profiles collected during the 1976 and 1977 HIPLEX field programs. Comparisons of various

ISOTHERM HEIGHTS 1976

TABLE 1

-15° C

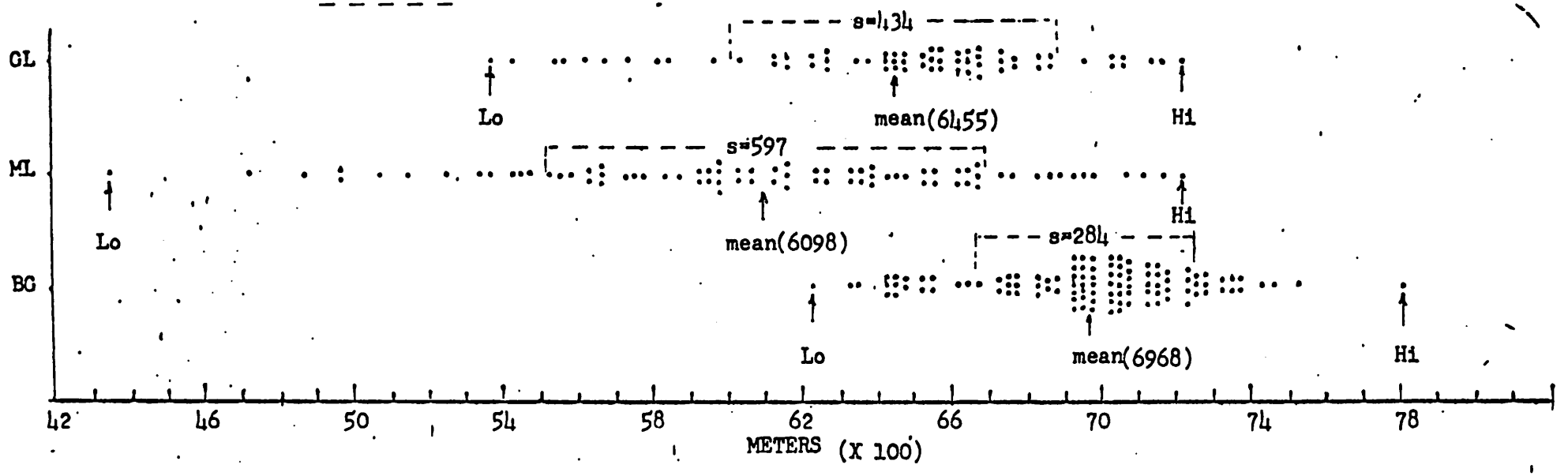

GOODLAND KS 72

M	#	M	#	M	#	M	#
5382	1	6240	1	6544	1	6781	1
5403	1	6267	1	6565	1	6790	1
5542	1	6295	1	6570	1	6832	1
5553	1	6350	1	6579	1	6838	1
5601	1	6368	1	6610	1	6847	1
5681	1	6418	1	6620	1	6873	1
5737	1	6420	1	6635	1	6971	1
5802	1	6443	2	6637	1	7025	1
5827	1	6451	1	6644	1	7065	1
5975	1	6453	1	6655	1	7086	1
6027	1	6482	1	6657	1	7090	1
6115	1	6497	1	6681	1	7158	1
6168	1	6499	1	6682	1	7177	1
6185	1	6500	1	6698	1	7202	1
6196	1	6504	1	6717	1		
6208	1	6507	1	6737	1		
6237	1	6521	1	6768	1		

MILES CITY MT 81

M	#	M	#	M	#	M	#
4340	1	5711	1	6168	1	6600	1
4717	1	5733	1	6197	1	6609	1
4870	1	5792	1	6210	1	6621	1
4973	2	5813	1	6231	1	6622	1
5091	1	5894	1	6262	1	6627	1
5140	1	5904	1	6285	1	6656	1
5255	1	5907	1	6300	1	6677	1
5374	1	5938	1	6301	1	6771	1
5381	1	5944	1	6311	1	6794	1
5411	1	5948	1	6366	1	6854	1
5416	1	5949	1	6367	1	6869	1
5455	1	5953	1	6371	1	6876	1
5505	1	5991	1	6399	1	6937	1
5544	1	6021	1	6409	1	6957	1
5595	1	6038	1	6451	1	6966	1
5615	1	6045	1	6465	1	7091	1
5641	1	6060	1	6505	1	7118	1
5648	1	6107	1	6530	1	7191	1
5683	1	6151	1	6555	1	7222	1
5685	1	6167	1	6581	1		

BIG SPRING TX 108

M	#	M	#	M	#	M	#	M	#
6233	1	6747	1	6946	1	7085	1	7222	1
6354	1	6774	1	6953	1	7088	1	7226	1
6359	1	6789	1	6959	1	7090	1	7247	1
6401	1	6794	1	6961	1	7095	1	7251	1
6442	1	6796	1	6964	1	7097	2	7261	1
6445	1	6813	1	6984	1	7100	1	7276	1
6455	1	6816	1	6989	1	7107	1	7279	1
6458	1	6817	1	6991	1	7108	1	7282	1
6472	1	6818	1	6994	1	7115	1	7329	1
6479	1	6838	1	6996	1	7119	1	7340	1
6498	1	6858	1	6998	1	7149	1	7350	1
6544	1	6888	1	7004	1	7153	1	7368	1
6558	1	6902	1	7007	1	7161	1	7376	1
6585	1	6907	1	7014	3	7177	1	7381	1
6591	1	6909	1	7035	1	7179	1	7423	1
6601	1	6912	1	7037	2	7180	1	7487	1
6603	1	6917	1	7049	1	7185	1	7506	1
6648	1	6919	1	7053	2	7192	1	7804	1
6713	1	6930	2	7065	1	7193	1		
6714	1	6933	1	7068	1	7202	1		
6723	1	6943	1	7082	1	7210	1		

TABLE 2

MEANS and STANDARD DEVIATIONS 1977

		GL		ML		RG	
	MBS	$\bar{x}$	s	$\bar{x}$	s	$\bar{x}$	s
Temperature Distribution	850	21.1	4.24	16.6	4.28	21.7	2.83
	700	11.4	2.64	5.5	3.70	10.3	1.77
	500	- 9.4	1.44	-12.0	2.41	- 7.2	1.36
Geopotential Heights	850	1497	30.59	1491	39.35	1530	17.03
	700	3152	25.38	3113	35.77	3183	15.78
	500	5856	27.89	5776	49.34	5892	22.35
Dew Point Depression	850	11.5	5.27	13.1	6.66	10.0	5.48
	700	13.2	5.57	10.2	6.64	10.6	7.11
	500	13.5	8.52	16.1	9.83	17.1	9.82
THETA	850	308.3	4.45	303.5	4.47	308.8	2.97
	700	315.1	2.93	308.5	4.10	313.9	1.96
	500	321.6	1.76	318.5	2.94	324.3	1.66
THETE	850	334.8	7.91	321.5	7.82	339.4	6.08
	700	330.6	4.15	321.3	6.56	331.8	5.98
	500	326.6	3.34	322.4	4.99	329.2	4.12
Wind Speed	850	8.5	3.79	7.6	4.15	7.1	3.77
	700	6.3	3.45	10.4	4.87	5.8	3.43
	500	8.5	4.16	17.7	7.79	7.7	4.47
THETE 700 - 850		- 4.3	7.16	- 0.3	6.77	- 7.7	6.26
500 - 700		- 4.0	3.79	0.7	4.27	- 2.9	5.83
Wind Speed 700 - 850		- 2.1	4.07	2.8	5.04	- 1.4	5.32
500 - 700		2.3	4.39	7.3	6.25	2.0	4.56
Precipitable Water	Sfc - 850	0.39	0.07	0.48	0.14	0.92	0.18
	Sfc - 700	1.45	0.29	1.29	0.36	2.17	0.43
	Sfc - 500	2.10	0.43	1.82	0.51	2.83	0.61
	Total	2.25	0.49	1.92	0.54	2.99	0.72

TABLE 3

MEANS and STANDARD DEVIATIONS 1977

	GL		ML		BG	
	$\bar{x}$	s	$\bar{x}$	s	$\bar{x}$	s
Isotherm Heights 0^{o}	4585	230	3882	495	4715	227
-5^{o}	5232	203	4673	416	5512	219
-10^{o}	5944	253	5457	413	6372	236
-15^{o}	6682	260	6215	391	7155	241
Mean Mixing Ratio Lowest 100 MBS	8.82	1.73	6.47	2.03	11.44	2.17
Lifted Index 100 MB Layer Adiabatic	1.81	3.16	2.72	3.48	- 1.89	2.22
Lifted Index 50 MB Layer Mean Values	0.26	3.81	3.74	3.45	- 1.83	2.40
Total - Totals	49.48	5.87	44.13	5.87	47.74	3.87
K Index	26.93	7.45	21.98	7.88	29.96	8.75
SWEAT Index	211.84	89.96	127.75	68.79	204.14	67.12

meteorological parameters were made for establishing correlations. Scatter diagrams and normalized data points diagrams were also prepared using data from the three intrastate Texas sites. Shown in Tables 1, 2 & 3 are samples of the data compilation. A report on these findings will be available in mid-1979.

AIRCRAFT OPERATION

In addition to the services performed by the Water District in support of the Texas HIPLEX program, the District, during this same period, independently sponsored a rain enhancement program to supplement surface water runoff into its own reservoirs. Shown in Tables 4 and 5 are all flights conducted by the sub-cloud base aircraft and presented in Tables 6 and 7 are the flights conducted by the on-top seeding aircraft. Table 5 lists only those flights made in direct support of the HIPLEX activities, while Table 4 shows all flights made indirectly supporting the HIPLEX program and also flights made in direct support of the CRMWD weather modification program. Provided in Tables 6 and 7 are those flights which were conducted by the P-Navajo aircraft. Separate tables were prepared to show those flights which directly supported HIPLEX as opposed to those flights made indirectly supporting it as well as those flights supporting the Water District's program.

On each flight, the District's pilots recorded data

T A B L E 4

AZTEC SUPPLEMENTAL FLIGHT SUMMARY

1 APRIL - 30 SEPTEMBER 1978

DATE	PURPOSE	FLIGHT TIME	AgI
4-7-78	CRMWD Seeding Flight	2.6	240
4-9-78	CRMWD Seeding Flight	2.3	460
4-30-78	Denver A/c Mod.	3.3	
5-4-78	Acceptance Flight	.4	
5-6-78	Return from Denver	3.2	
5-9-78	TDWR Photo Mission	1.6	
5-2-78	CRMWD Seeding Flight	1.7	20
5-10-78	CRMWD Seeding Flight	2.3	200
5-10-78	CRMWD Seeding Flight	1.0	20
5-11-78	CRMWD Seeding Flight	.8	20
5-15-78	CRMWD Seeding Flight	1.0	20
5-18-78	CRMWD Seeding Flight	1.6	220
5-25-78	CRMWD Seeding Flight	1.2	160
5-28-78	CRMWD Seeding Flight	.9	80
5-28-78	CRMWD Seeding Flight	1.6	300
5-28-78	CRMWD Seeding Flight	1.5	220
5-29-78	CRMWD Observation	.6	
5-31-78	CRMWD Seeding Flight	2.4	460
6-5-78	CRMWD Seeding Flight		480
6-6-78	CRMWD Seeding Flight		200
6-16-78	Parts Pick-up MAF	.7	
6-17-78	Cld. Physics Pack. @ Snyder	1.2	
6-28-78	Cld. Physics Flt. Test	3.2	
7-25-78	Parts Pick-up(LBB.RBT-LEE MAF)	3.0	
8-10-78	LBB Annual Inspection	1.0	
8-26-78	CRMWD Seeding Flight	1.1	200
8-27-78	CRMWD Observation	.8	
8-28-78	CRMWD Seeding Flight	1.0	40
8-29-78	CRMWD Seeding Flight	.8	160
9-4-78	CRMWD Seeding Flight	2.4	80
TOTAL:		45.2 HRS.	3580 GM.

TABLE 5

AZTEC HIPLEX WEATHER MODIFICATION
FLIGHT SUMMARY

1 JUNE - 31 JULY 1978

DATE	MISSION	FLIGHT TIME	AgI
6-2-78	Observation	1.0	
6-2-78	Observation	.9	
6-5-78	Seeding	2.1	240
6-13-78	Seeding	4.0	400
6-29-78	Sampling	2.2	
6-30-78	Seeding	2.8	180
7-1-78	Sampling	2.3	
7-2-78	Sampling	2.1	
7-3-78	Seeding	3.6	320
7-20-78	Sampling	2.9	
7-22-78	Sampling	3.0	
7-23-78	Sampling	2.5	
7-24-78	Sampling	2.9	
7-26-78	Sampling	1.5	
7-27-78	Instr. Calibration	2.5	
TOTAL:		36.3 HRS.	1140 GM.

T A B L E 6

P-NAVAJO SUPPLEMENTAL FLIGHT SUMMARY

12 MARCH - 30 SEPTEMBER 1978

DATE	PURPOSE	FLIGHT TIME	AgI
3-12-78	Flare Racks-Denver	2.0	
3-16-78	Return Trip from Denver	2.4	
5-2-78	CRMWD Test Flight	1.7	30
6-6-78	HIPLEX Test Flight	.4	
6-21-78	HIPLEX Test Flight	1.0	
6-22-78	Maint. to MAF VOR/DME	1.7	
6-28-78	Dr. Grubb to Snyder	1.0	
6-30-78	Maint. to MAF	1.4	
7-1-78	Equip. Pick-up/Wave Guide	1.1	
7-5-78	Maint. Flt. to LBB-Turbo	1.6	
7-12-78	Maint. Flt. Oil Change	.4	
8-3-78	CRMWD Seeding Flight	1.8	210
9-1-78	CRMWD Observation	1.6	
9-4-78	CRMWD Observation	1.0	
9-11-78	Annual Inspection-LBB	1.3	
9-20-78	CRMWD Observation	1.3	
TOTAL:		21.7 HRS.	240 GM.

T A B L E 7

P-NAVAJO HIPLEX WEATHER MODIFICATION FLIGHT SUMMARY

15 MAY - 15 AUGUST 1978

DATE	MISSION	FLIGHT TIME	AgI
6-6-78	Seeding	3.3	520
6-29-78	Observation	1.1	
7-1-78	Seeding	1.9	150
7-2-78	Observation	2.1	
7-3-78	Seeding	.8	960
7-3-78	Observation	.5	
7-3-78	Seeding	1.8	320
7-20-78	Seeding	2.2	300
7-22-78	Observation	2.2	
7-23-78	Seeding	2.3	2790
7-24-78	Observation	2.4	
7-26-78	Observation	1.4	
7-27-78	Instr. Calibration	2.2	
8-15-78	Seeding	2.6	810
TOTAL:		26.8 HRS.	5850 GM.

on cloud base heights and temperatures, updraft sizes and their magnitudes, and vertical temperature profiles of the atmosphere were recorded during ascents and descents. In addition, a brief written description of each flight was prepared for all District flights. Individual flight summaries can be obtained by request from the Texas Department of Water Resources.

RADAR OPERATIONS

Cloud census data were collected by the District's radar meteorologist and Mr. Robert Riggio using the FPS-77V Radar System located at Big Spring airport. Routine survey scans were made at approximate 2-minute time intervals with RHI, PPI and A/R-Scope interpretations being physically recorded during this period. Attempts were made to document information on those cells being seeded; however, because of the difficulty in locating the seeded clouds, only a limited amount of data were collected. Data collection was also hampered by the loss of an RHI Video Drive Motor which resulted in the loss of cloud top data throughout the HIPLEX period. Generally the radar system operated in a search mode assisting the aircraft crews in determining which block of the operations area to fly and also locating prime areas of cloud development with respect to the parent cloud.

SECTION II

WORK PLANNED FOR THE PERIOD

OCTOBER 1, 1978 - MARCH 31, 1979

Texas Department of Water Resources: Management of the Texas HIPLEX Program and Support Studies

Among the activities related to the Texas HIPLEX Program which are planned for the next reporting period (October 1, 1978 - March 31, 1979) by the Department staff are:

Administration of the 1974 Agreement between the Bureau and the Department including the review of proposals, negotiation and execution of contracts between the Department and the participant organizations of the Texas HIPLEX Program;

Distribution of the funds to support the various subcontractor services, including the $100,000 appropriation by the 65th Texas Legislature for the Texas HIPLEX Program and monies obligated to the Texas program during Federal Fiscal Year 1979 by the Bureau;

Coordination of data analysis activities which include the examination by subcontracting organizations of mesoscale data for 1977-78, radar echo occurrence vs. synoptic features, satellite-derived cloud characteristics, precipitation-storm cell characteristics, and, M-33 radar and cloud physics data;

Planning and coordination with the Bureau in developing the 1979 HIPLEX Operations Plan for the field experiments conducted at Big Spring;

Sponsorship of and participation in meetings and planning sessions with the Chief Scientist and HIPLEX participants and the Department's Weather Modification Advisory Committee;

Evaluation of forecasting performance during 1978; refinement of the objective forecast-decision tree; further investigations to refine the thunderstorm prediction model;

Analysis of the 1978 ice-nuclei data, analysis of 1976-78 rawinsonde data for all HIPLEX sites; census of severe storm watch-warning occurrences; continuation of a Federal-State cost-sharing study of the economic effects of weather modification activities in the Big Spring HIPLEX area; and

Preparation of the Texas HIPLEX monthly and interim progress reports to the Bureau.

Other HIPLEX-related work planned for the next six month period, which is traditionally performed through contract assignments, is contingent upon the amount of Federal monies to be made available for the conduct of the 1979 program. A comprehensive preliminary proposal will be submitted to the Bureau in November and more explicit work plans will be developed at a later date. These will define the nature of the work to be accomplished and will be a function of the funds allocated by the Bureau and the State of Texas. The 1979 contract-assigned work topics for consideration include: the collection and analysis of M-33 radar data; the collection and analysis of the mesoscale field data; a radar-echo climatology; a satellite derived cloud climatology; a precipitation climatology; and, the field provisions for the seeding aircraft, rawinsonde operations and the rain-gage network.

Meteorology Research, Incorporated

The expiration date of Department Contract 14-80038 with MRI is October 31, 1978. Remaining work due includes two technical reports which were reported to be in draft form during September. These reports include: a climatological summary which provides a classification of radar patterns into categories that could be associated with sub-synoptic weather types; and, a mesoscale pattern analysis which discusses six case studies of M-33 radar patterns from the 1976-77 seasons. The organization of patterns is discussed with their relation to sub-synoptic weather conditions. Attempts to relate similarities in these analyses to theoretical descriptions of mesoscale organization found in meteorological literature are made. See page 58 of this report for MRI's detailed outline of these reports.

SECTION III

PERSONNEL

Management of the Texas-HIPLEX Program and Support Studies (TDWR)

John T. Carr, Jr.	Director, TDWR Weather Modification & Technology Section
Robert Riggio	Meteorologist
George Bomar	Meteorologist
William Alexander	Resident Forecaster at Big Spring
Thomas Larkin	Meteorologist
William Hanshaw	Rain-Gage Technician
Keith Topham	Computer Program Analyst
Mike Kengla	Economist

Snyder Radar-Data-Collection Program and Data Analysis (MRI)

T.B. Smith	Supervisor
Robert Anderson	Project Manager at Snyder
Robert Schaff	Radar Technician
Mike Merritt	Radar Technician
Ed Huber	Radar Technician
John Lawton	Radar Technician
L. Boardman	Radar Technician

Mesoscale Field Program and Data Analysis (TAMU)

- Big Spring -

James R. Scoggins	Chief Scientist
Gordon Grant	Surface Network
Gary Petti	Surface Network
Steven Williams	Surface Network
Pete Reynolds	Rawinsonde Site
Robert Soptei	Rawinsonde Site
Steven Bishkin	Rawinsonde Site
Jerry Guynes	Electronics Technician

- College Station -

Betty Seymour	Data Specialist (part time)
Jackie Wilson	Data Specialist (part time)
Myron Gerhard	Data Specialist (part time)

Radar-Echo Climatology for the Southern HIPLEX Region (TAMU)

Dennis M. Driscoll	Principal Investigator
Judson W. Ladd	Graduate Research Assistant

Precipitation Climatology for the Southern HIPLEX Region (TTU)

Donald R. Haragan	Principal Investigator, Director of Project
James Holman	Research Associate
Debbie Kerr	Research Assistant and Secretary II

HIPLEX Rain-Gage and Rawinsonde Support Programs (CRMWD)

Owen H. Ivie	General Manager, Colorado River Municipal Water District
R.A. Schooling	Coordinator and Supervisor
John Girdzus	Radar Meteorologist
Alan Giacomelli	Cloud-Seeding Aircraft Pilot
Chuck Henry	Cloud-Seeding Aircraft Pilot
Harold Hancock	Rawinsonde Technician
Jill Odom	Assistant to the Rawinsonde Technician
Bruce Campbell	Observer in Seeding Aircraft
Humberto Padillo	Rain-gage Technician
Richard Halfmann	Rain-gage Technician

Satellite-Derived Cloud Climatology for the Southern HIPLEX Region (TTU).

The list of Texas Tech personnel is provided on page 120 of this report as submitted with Dr. Jurica's interim progress report.

APPENDIX

FORECASTING THE 1978 TEXAS HIPLEX PROGRAM: A SUMMARY

Prepared by:

William O. Alexander

Texas Department of Water Resources

Big Spring, Texas

October 1978

TABLE OF CONTENTS

LIST OF FIGURES

LIST OF TABLES

APPENDIX TABLES

INTRODUCTION

The conduct of the 1978 Texas HIPLEX program at Big Spring, Texas marks the third season in which Texas Department of Water Resources staff have provided the weather forecasting support services for the program. This is also the first season in which an organized forecast decision tree was used in the decision making process to develop a daily forecast. Derivation of the Texas HIPLEX Forecast Decision Tree (FDT) was based upon statistical evaluations of 1976-77 Texas HIPLEX forecast input and verification data.[1]

The 1978 Texas HIPLEX operational area (Op Area) was defined to be the area within a sixty nautical mile radius from Snyder, Texas excluding the areas east of Highway 84, north of 33.2°N and east of 100.5°W (Figure 1). The Op Area was well within the range of the radar systems based at the Big Spring, Texas Airport, Winston Field at Snyder and the National Weather Service (NWS) at Midland, Texas Air Terminal (MAF). Most convective clouds which developed over the Op Area were identifiable by sight from the Texas HIPLEX meteorological facility at Big Spring Airport.

The scope of this report is to: (1) examine the forecast performance issued in support of the 1978 Texas HIPLEX season; (2) provide a summary of forecasts and observations, including pre- and poststratification of all forecast days; and, (3) examine the performance of the FDT in the prestratification of each forecast day.

FORECAST PROCEDURE

The Texas HIPLEX Operations Plan[2] defines an operational day as one

---

1 Alexander, W.O. and Riggio, R.F.; "A Texas HIPLEX Forecast Decision Tree." Texas Department of Water Resources, July, 1978.

2 "HIPLEX 1977-78 Operations Plan--Big Spring-Snyder, Texas." Texas Department of Water Resources, March, 1977.

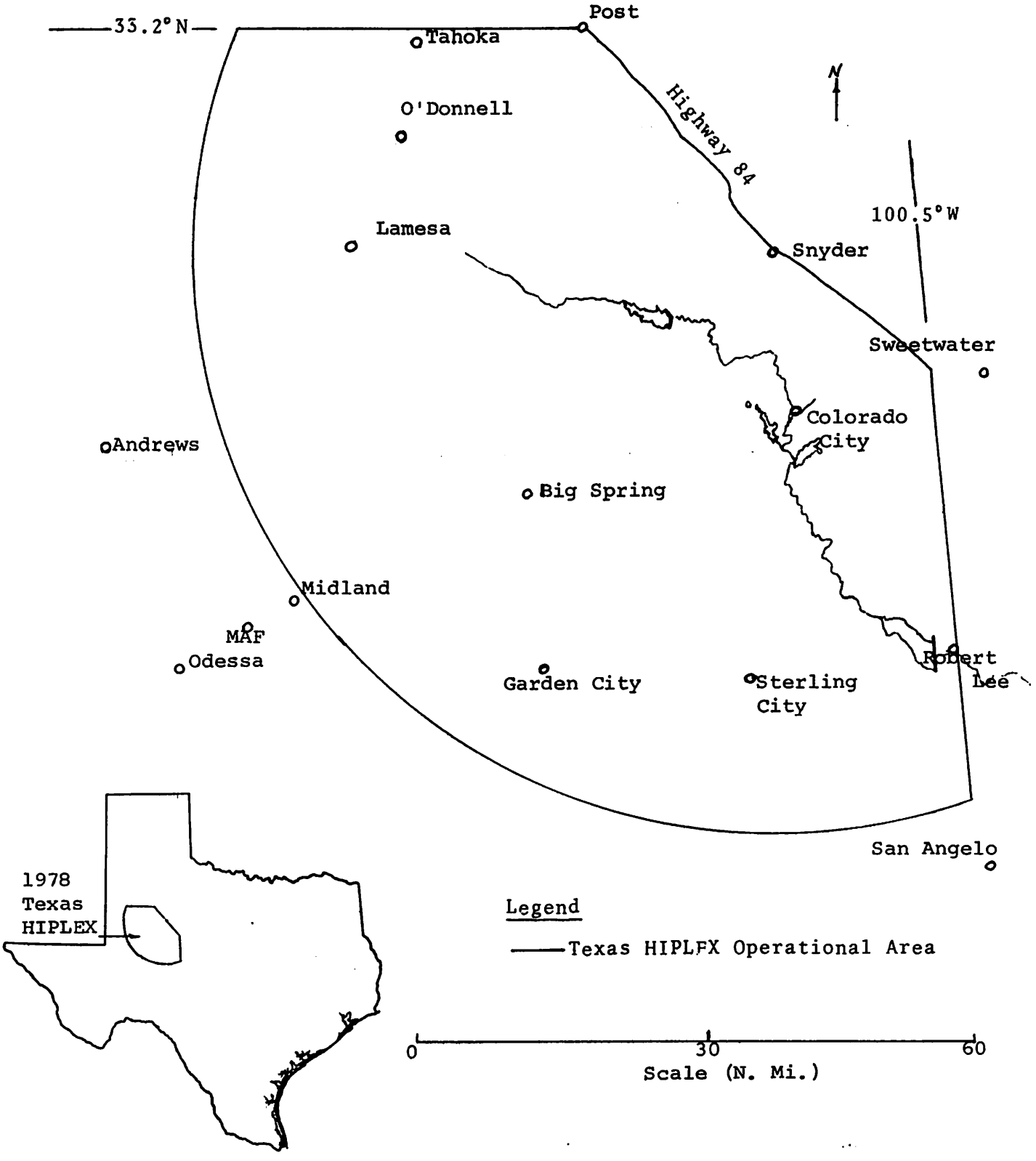

Figure 1. The 1978 Texas HIPLEX Operational Area Headquartered at Big Spring, Texas.

in which convective clouds are forecast to exist in the Op Area having vertical depths of at least 7,000 feet and bases at or below 12,000 feet above ground level and a cloud-top temperature colder than -5°C. These forecast parameters were essentially the same for the two previous Texas HIPLEX field seasons.

Development of the FDT was based on criteria used to define an operational day. The FDT relies heavily on the forecaster's ability to recognize potential atmospheric forcing, or non-forcing, situations for each forecast period, i.e., a dry line, a convergence line, surface trough, short wave, cold air advection aloft, or a closed upper-air low.

The presence of a forcing mechanism is the initital branch point in the FDT, followed by a moisture variable as the next branching point (Figure 2). From that branch point, close scrutiny is required of the individual sounding characteristics for the day, i.e., the presence of inversions, height of the lifting condensation level, vertical wind/moisture profile, and vorticity advection. Consequently, the FDT prestratifies each day not only as potentially operational or non-operational, but also according to anticipated convective development as defined by the convective index (CI) shown in Table 1.

The FDT was fully utilized and tested for the first time during the 1978 HIPLEX season. Using the FDT the forecaster prestratified each forecast period according to the convective indices listed in Table 1.

The FDT proved to be an effective method of logically organizing atmospheric data in a manner best suited for West Texas summertime atmospheric conditions. It has proven to be a valuable indicator in forecast preparation; however, since it is not completely objective--particularly in determining the existence of synoptic forcing, additional

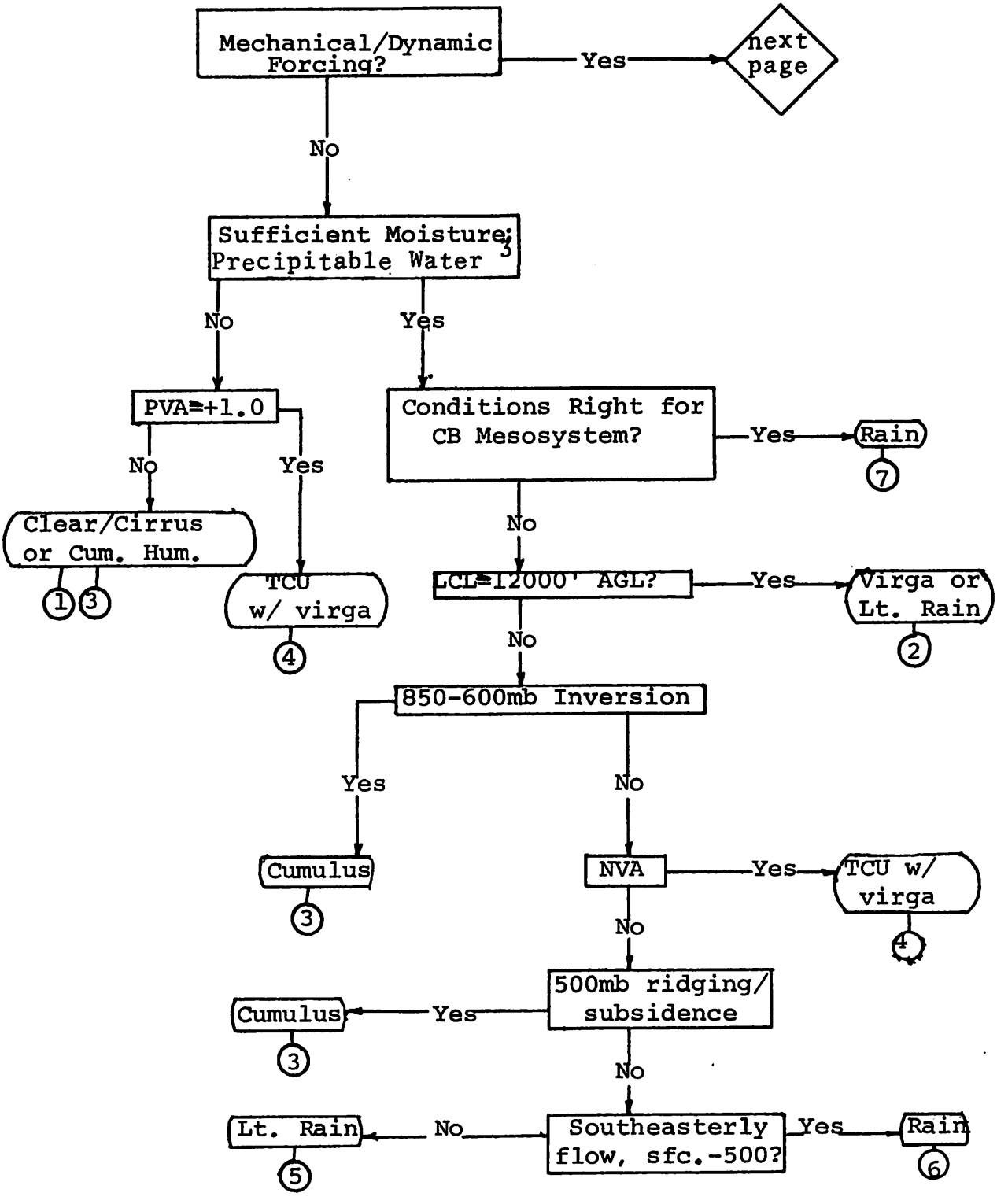

Figure 2. The 1978 Texas HIPLFX Forecast Decision Tree (FDT).

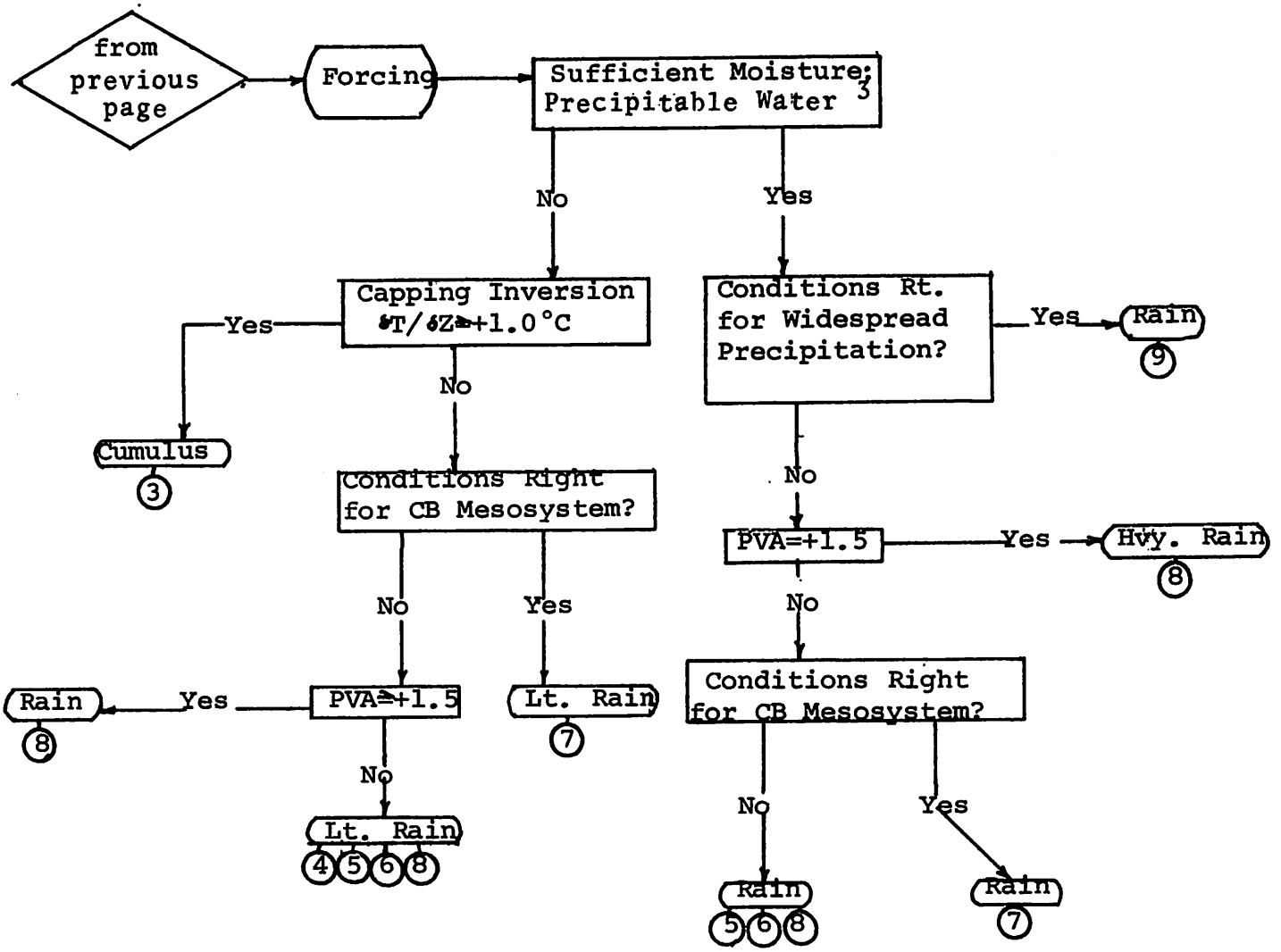

Figure 2. Continued.

---

3 Alexander et al, 1978.

Table 1. Class Definitions of the Convective Index (CI) Number.

Class No.	Definition
1	Clear or cirrus and non-precipitating mid-level altocumulus or altostratus
2	Mid-level clouds with virga or RW-; no low level clouds
3	Non-precipitating low level convective clouds (i.e. stratocumulus to small congestus)
4	Towering cumulus with virga but no rain reaching ground
5	Towering cumulus with light rainshowers which developed within the operational area either randomly or in lines; no cumulonimbus observed
6	Similar to Class 5 with cumulonimbus and thunderstorms which developed within operational area in addition to towering cumulus
7	Mesoscale cumulonimbus system which developed W-SW of operational area due to upslope and/or dry line-sfc trough and moved across operational area as line of thunderstorms or rainshowers
8	Mesoscale cumulonimbus system developed along synoptic feature (i.e. front or short wave aloft) and moved into operational area as line of thunderstorms or rainshowers
9	Widespread precipitation from overcast nimbostratus with embedded cumulonimbus

information is often desirable. Therefore, a computerized thunderstorm prediction model was developed to supplement the FDT.

The thunderstorm model, described in a report prepared by Riggio and Topham[4], is programmed in the Department's computer in Austin. Its data base was extracted from synoptic upper air rawinsonde data from the Midland, Del Rio, and Amarillo reporting stations for the 3-year period, 1972-1974. The model delineates the probability for thunderstorm development by "groups." A "group 1" day indicates thunderstorms are anticipated within a 50-mile area of Big Spring; a "group 2" day indicates development of thunderstorms within sight but outside the 50 mile area; and a "group 3" day indicates that no thunderstorms are to be expected within sight of the station.

SURFACE WEATHER OBSERVATIONS AND FORECAST VERIFICATIONS

Hourly weather observations were recorded at the Big Spring meteorological facility during each HIPLEX day by the on-site meteorologist. The observations included measurements of air temperature, precipitation, and wind speed and direction, while amount of cloud cover and cloud type were noted visually. Occasionally, pressure and dewpoint calculations were recorded. These data are archived at the Big Spring weather facility.

Forecast verification includes the use of the data previously enumerated, radar summaries from Big Spring, Snyder, and Midland, and HIPLEX pilot reports when available. These data define verified operational and non-operational days and also help define the CI number for each of the days. Forecast verification analyses were

---

4. Riggio, R.F. and Topham, K.L.; "Using Discriminant Analysis to Predict Rainshower Occurrence in the Texas HIPLEX Area." Texas Department of Water Resources, May, 1978.

performed for the 1978 Texas program on the basis of these input parameters.

FORECAST PERFORMANCE

Forecasting support for the 1978 Texas HIPLEX program began on May 15 and terminated July 31; however, HIPLEX-type forecasting continued through September. Statistically, the implementation of the FDT exhibited a gradual month-by-month improvement of the "Go"/"No Go" operational forecast. Operational forecast performance for May verified 78.6% and steadily improved to 83.3% during June and to 90.3% for July. Appendix Table 2 provides details on these statistics. The improved forecasts are attributed to familiarization with the FDT and refinements which were implemented during early June. Additionally, it may be noted that, similar to previous seasons, non-operational day forecasts were superior to operational day forecasts as documented in Appendix Tables 3 and 4.

Forecasts made during August and September have also been included in these tables. Note that both August and September indicate a continuing trend in forecast improvement. Forcing mechanisms were more easily identified (i.e., remains of tropical disturbances, strong surface front, etc.) than earlier in the HIPLEX season and forcing and non-forcing branches were more easily selected. Therefore, the FDT performed better in August and September in the forecasting of operational and non-operational days.

ACCURACY OF THE FDT

In addition to forecasting a Texas HIPLEX operational day, the FDT was designed to prestratify HIPLEX days according to the Texas HIPLEX CI number. Each Texas HIPLEX forecast day except two[5] is

[5] July 14 and July 16. Sounding data incomplete; FDT could not be used.

listed in Appendix Table 5 with the corresponding columns which identify prestratified CI (CIps) and verified CI (CIv) days.

Table 6 provides an indication of the accuracy in prestratification of the daily CI. It is important to note the CF (Correct Forecasts) column in Appendix Table 6. The CF column denotes the ratio CIv/CIps. Approximately, 67.1% of all prestratifications were correct.

SUMMARY AND CONCLUSIONS

Successful implementation of the first generation Forecast Decision Tree, supported by the thunderstorm model, is the single most significant accomplishment of the 1978 Texas HIPLEX forecasting support. While forecasts in May were substandard, refinements made to the FDT during early June--and gradual familiarization with its use--account for the steady improvement shown throughout the balance of the season.

The overall performance of the FDT encourages further development. The FDT performed considerably more reliable than anticipated--67.1% of all CI prestratifications were correct. Further refinement of the FDT will be performed during the winter months.

APPENDIX TABLES

Appendix Table 2. Summary of 1978 Texas HIPLEX Forecasts.

Month	Hit	Miss	%	Total Fcsts	
May	11	3	78.6	14	
June	25	5	83.3	30	HIPLEX: 85.3%
July	28	3	90.3	31	
August	22	2	91.7	24	
Sept.	25	1	96.2	26	
Overall	111	14	88.8	125	

Appendix Table 3. Summary of 1978 Texas HIPLEX Verified Operational Days.

Month	Hit	Miss	%	Total Fcsts	
May	8	3	72.7	11	
June	8	2	80.0	10	HIPLEX: 79.4%
July	11	2	84.6	13	
August	11	0	100.0	11	
Sept.	19	0	100.0	19	
Overall	57	7	89.1	64	

Appendix Table 4. Summary of 1978 Texas HIPLEX Verified Non-Op Days.

Month	Hit	Miss	%	Total Fcsts	
May	3	0	100.0	3	
June	17	3	85.0	20	HIPLEX: 90.2%
July	17	1	94.4	18	
August	11	2	84.6	13	
Sept.	6	1	85.7	7	
Overall	54	7	88.5	61	

Appendix Table 5. Convective Indices, 1978 Texas HIPLEX Program.

Date	May		June		July	
	CIps	CIv	CIps	CIv	CIps	CIv
1			6	3	6	6
2			6	6	6	5
3			3	4	5	6
4			8	3	-	-
5			6	6	3	3
6			6	6	3	1
7			6	6	1	1
8			3	3	1	1
9			3	1	1	1
10			3	1	3	3
11			1	1	3	3
12			6	3	1	3
13			6	6	3	3
14			3	3	3	3
15	3	6	1	1	3	6
16	1	1	1	1	-	-
17	3	3	1	1	2	3
18	6	6	3	3	2	3
19	6	6	3	3	3	3
20	6	6	2	6	3	5
21	4	4	1	1	5	3
22	6	6	1	1	5	6
23	7	7	1	1	6	6
24	7	7	1	1	6	6
25	8	7	1	1	3	3
26	8	8	1	1	6	6
27	-	-	3	3	6	6
28	-	-	5	5	4	4
29	-	-	8	5	6	5
30	3	5	6	6	6	6
31	3	8			5	6

Appendix Table 6. Error Analysis of the 1978 Convective Index Prestratification.

Month	N	CF	%CF
May	14	10	71.4
June	30	22	73.3
July	29	17	58.6
Total	73	49	67.1

N = number of prestratified days
CF = correct forecasts
%CR = percent of correct forecasts